The early cellular events that control mechano-inflammatory signalling after cartilage injury

Chris Chan

St Hilda's College, University of Oxford

Supervisor:

Professor Tonia Vincent

Kennedy Institute of Rheumatology

Nuffield Department of Orthopaedics, Rheumatology and Musculoskeletal Sciences University of Oxford

Thesis submitted in fulfilment of the requirements for the degree of Master of Science (MSc) in Molecular and Cellular Medicine

Trinity Term 2023

Word count: 28968

TABLE OF CONTENTS

ABSTRACT

Osteoarthritis (OA) is a degenerative joint disease that has no disease-modifying drug licenced for its treatment. Mechanical injury of cartilage is a principal risk factor in osteoarthritis (OA). Recent insights arising from our group demonstrate that mechano-sensitive intracellular signalling drives disease pathways. Cartilage injury is known to activate inflammatory signalling that leads to production of matrix-degrading proteases and consequent cartilage breakdown – a process our group has called mechanoflammation. Cartilage injury induces activation of transforming growth factor-β activated kinase 1 (TAK1), that further activates downstream extracellular signal regulated kinase (ERK), p38 and Jun N terminal kinase (JNK) mitogen-activated protein kinases (MAPKs). Our group has previously identified the role of apoptosis signal regulating kinase 1 (ASK1) and reactive oxygen species as key drivers of MAPKs on cartilage injury and downstream inflammatory gene regulation. My project sought to identify the role of ASK1 in the cartilage injury response. ASK1 was phosphorylated rapidly after cartilage injury, leading to the accumulation of ASK1 protein in the cell. Inhibition of ASK1 phosphorylation suppressed ASK1 accumulation, suggesting that phosphorylation was responsible for stabilising ASK1, most likely, by preventing its degradation. Degradation was through a proteosome-dependent mechanism as stabilisation of non-phosphorylated protein could be induced by pre-incubation with a proteosome inhibitor. IL1 and H_2O_2 stimulation of isolated primary chondrocytes activated MAPKs and NF-κB but did not appear to involve ASK1, although this needs repeating. Attempting to inhibit ASK1 in murine OA did not suppress cartilage degradation nor osteophyte formation. Giving mice a modified diet of oxidation-resistant compounds appeared to reduce injury-induced inflammatory gene regulation

in vitro but increased cartilage damage in murine OA. My findings provide further insight into the role of ASK1 and other mechano-inflammatory pathways in articular cartilage and highlight the challenges of inhibiting them in vivo.

ACKNOWLEDGEMENTS

I would like to thank my supervisor, Professor Tonia Vincent, for her continued guidance throughout my MRes. She has helped to develop my critical thinking and helped me overcome many obstacles throughout my studies. I would like to further thank the members of the Vincent group and Oxford Centre for Osteoarthritis Pathogenesis, who have aided me on a scientific and personal basis. From them, I have gained important skills and techniques to utilise in my research. The supportive and inclusive atmosphere in the Vincent group has made it a pleasure to work in the lab. Finally, thank you of course to my family for their love and support every step of the way.

LIST OF FIGURES

LIST OF TABLES

LIST OF ABBREVIATIONS

ADAMTS	A disintegrin and metalloproteinase with thrombospondin motifs
AKT	Serine/threonine kinase 1
ALDH1A2	Aldehyde dehydrogenase 1 family member A2
ALK	Anaplastic lymphoma kinase
AP1	Activator protein 1
ASK1	Apoptosis signal-regulating kinase 1
ATRA	All-trans retinoic acid
BMP	Bone morphogenetic protein
C/EBP	CCAAT-enhancer-binding proteins
cDNA	Complementary DNA
COL10A1	Collagen type X alpha 1 chain
COQ	Coenzyme Q
COX	Cyclooxygenase
CRABP	Cellular retinoic acid-binding protein
CTGF	Connective tissue growth factor
CXCL	Chemokine (C-X-C motif) ligand 1
CYP26	Cytochrome P450 family 26
DAMP	Damage-associated molecular pattern
ECM	Extracellular matrix
EGF	Epidermal growth factor
ELF	E74-like factor 3
ELK	ETS domain-containing protein-1
ERK	Extracellular signal-regulated kinase
ETS	E-twenty-six
FGF	Fibroblast growth factor
FGFR	Fibroblast growth factor receptor

FOX	Forkhead box protein
GAG	Glycosaminoglycan
GCPR	G-protein-coupled receptors
GSH	Glutathione
H2O2	Hydrogen peroxide
HDGF	Heparin binding growth factor
HIF	Hypoxia-inducible factor
IKB	Inhibitor of NF-κB
IKK	Iκb kinase
IL	Interleukin
IL1R	Interleukin-1 receptor
IRAK	Interleukin-1 receptor-associated kinase
JNK	C-Jun N-terminal kinase
LATS	Large tumour suppressor kinase
LTBP	Latent TGFβ binding proteins
MAPK	Mitogen-activated protein kinase
MEK/MKK	Mitogen-activated protein kinase kinase
MKP	MAPK phosphatases
MMP	Matrix metalloproteinase
MSC	Mesenchymal stem cell
MST	Mammalian ste20-like kinases
MYD88	Myeloid differentiation primary response 88
NADPH	Nicotinamide adenine dinucleotide phosphate
NASH	Non-alcoholic Steatohepatitis
NEMO	NF-kappa-B essential modulator
NF-kB	Nuclear factor kappa-light-chain-enhancer of activated B cells
NGF	Nerve growth factor

NO	Nitric oxide
NOS	Nitric oxide synthase
OA	Osteoarthritis
OPN	Osteopontin
PCM	Pericellular matrix
PDGF	Platelet-derived growth factor
PGE2	Prostaglandin E2
PI3K	Phosphoinositide 3-kinase
RAGE	Receptor for advanced glycation end products
RALDH	Retinal dehydrogenase
RAR	Retinoic acid receptor
RDH	Retinol dehydrogenase
ROS	Reactive oxygen species
RUNX2	Runt-related transcription factor 2
siRNA	Small interfering RNA
SMAD	Suppressor of Mothers against Decapentaplegic
SOD	Superoxide dismutase
SRC	Proto-oncogene tyrosine-protein kinase
TAB	TAK1-binding protein
TAK1	Transforming growth factor-β -activated kinase 1
TAZ	Transcriptional coactivator with PDZ-binding motif
TEAD	TEA domain family member
TGFβ	Transforming growth factor-β
TNF	Tumour necrosis factor
TOLLIP	Toll interacting protein
TRAF	TNF receptor associated factor
TRX	Thioredoxin
UBC13	Ubiquitin-conjugating enzyme 13

UEV1A	Ubiquitin conjugating enzyme variant 1A
VEGF	Vascular endothelial growth factor
WNT	Wingless/integrated pathway
XO	Xanthine oxidase
YAP	Yes-associated protein
4-HNE	4-hydroxynoneal
5Z-7	5z-7 oxozeanol

CHAPTER 1: INTRODUCTION

1.1 Osteoarthritis

Osteoarthritis (OA) is a prevalent degenerative joint disease that affects diarthrodial joints. The onset of symptoms in OA is subtle but progresses with disease advancement. Initial symptoms include joint stiffness, that eventually worsens to pain on prolonged joint movement (Martel-Pelletier., et al 2016). Pain can be temporarily relieved with rest although some patients with severe disease experience pain even at rest. Degree of symptoms vary depending on the type of affected joint and severity of disease. However, in some cases, the extent of deformity of the joint does not always correlate with increased pain. According to a patient study conducted in the US from the years 1991 to 2000, 40% of patients with the worst radiographic classification for OA are pain free (Rettig et al., 2008). Other musculoskeletal symptoms include muscle spasms, and tendon and capsular contractures (Swagerty D et al., 2001).

Diagnosis of osteoarthritis is often suggested upon physical examination. Patients with osteoarthritic joints commonly display physical findings such as bony enlargement, crepitus and limited range of motion around the joint (Berenbaum F et al., 2013). Further assessment of the osteoarthritic joint using imaging methods can further reveal radiographic manifestations, including joint space loss, osteophyte formation, cyst formation and subchondral sclerosis (increased bone density) (Berenbaum F et al., 2013). Radiographic assessment can be achieved using imaging modalities such as

computerised tomography (CT) scan and magnetic resonance imaging (MRI) (Swagerty D et al., 2001). Radiographic markers also provide information on the severity of disease progression in OA. For example, the development of an osteophyte is usually indicative of an advanced stage of OA (Swagerty D et al., 2001).

The aetiological nature of OA is multifactorial, consisting of genetic, biological, and biomechanical factors (Martel-Pelletier., et al 2016). There are many factors that are associated with increased risk of developing OA. Aging is the greatest contributing factor to OA. A study in the UK population estimates ~12.5% of patients aged 45 years or above to be affected by OA (Chen A et al., 2014). Sex is another risk factor. Women, especially those aged 50 or above (usually post-menopausal women) correlate with higher chance of developing OA, but the reason for this sex difference is still unclear (Hame S et al., 2013). Obesity induces greater loading stress on weight-bearing joints and adipose tissue produces pro-inflammatory mediators that can aggravate the joint environment. Abnormal or excessive mechanical trauma such as joint injuries or repetitive stress can damage the cartilage tissue, causing abnormal biomechanics and malignment of the joint, and consequent cartilage destruction (Goldring M., 2012). OA also appears to involve a strong genetic component and inheritance of OA is likely related to alterations in multiple genes (Fernandez M et al., 2008). Lastly, other health predispositions such bone deformities and metabolic diseases may also contribute to the early onset of OA (Heidari B et al., 2011).

To date, there are no effective clinical interventions to treat or decelerate OA progression besides total joint replacement surgery. Instead, current treatments aim to relieve symptoms such as to alleviate pain, maintain musculoskeletal functionality and to improve quality of life. Examples of common therapies include the pharmacological intake of nonsteroidal anti-inflammatory drugs (NSAIDs) to temporarily relieve pain, physical therapy modalities to improve overall musculoskeletal dynamics and dietary alterations to aid in weight loss (Pelletier J et al., 2016). When non-surgical therapies are inadequate, surgical interventions usually implemented as a last resort. The most common surgical intervention is joint replacement surgery, which involves the replacement of parts or the whole damaged joint with a prosthesis (Lamplot J et al., 2018). Other surgical methods include autologous chondrocyte implantation (ACI) - the implantation of healthy chondrocytes harvested from the patient back into the affected joint; and microfracture – perforation of the subchondral bone to stimulate formation of a new articular surface (Minas T et al., 2010; Yen Y et al., 2008). Overall, treatment development has been slow and challenging in OA, due to the complex mechanopathological nature of OA that involves both biochemical and biomechanical aspects. Additionally, the correlation of pain relief and structural improvement in OA is often not linear. Many clinical trials over the years have been unsuccessful due to inability to resolve all the multifaceted aspects that are associated with OA. As an example, some clinical trials were deemed unsuccessful because although they were effective in pain relief, they did not induce structure-modifying improvements (Rashad S et al., 1989).

The socio-economic cost of OA is high. Patients who suffer from OA are commonly burdened by costs for treatment, the need to adapt their homes and lives to the disease, and decreased work productivity (Roy D et al., 2010). As a result, OA can have a profound effect on the quality of life for those who suffer from it, by negatively impacting their physical and psychological parameters (Roy D et al., 2010).

The progression of OA has conventionally been described as the wear and tear of articular cartilage (the smooth connective tissue that articulates the end of bones). This concept has now evolved, and OA is now considered an active biologically driven disease which has impacts on the entire joint.

The joint tissues are highly mechanosensitive in nature and can respond to mechanical and biochemical signals, which play a role in maintaining cartilage homeostasis as well as in OA development. Cartilage injury is known to activate downstream inflammatory signaling that leads to production of matrix-degrading proteases and consequent cartilage breakdown. This process has been termed by our group as ‘mechanoflammation’ (Vincent T., 2013; Vincent T., 2019). Anabolic processes in cartilage are involved in repair, regeneration, and chondroprotection. These anabolic pathways are in part driven by the release of sequestered growth factors from the cartilage matrix upon injury. These new insights have helped shift the perspective of OA to a disease where there is a lack of repair-promoting responses and chronic

mechanoflammation driven by biochemical and mechanical stresses. Current target discovery approaches in OA are focused on suppressing mechanoflammation to inhibit matrix turnover and pain, whilst also promoting intrinsic repair signalling pathways. (Vincent T., et al 2019).

The road to developing of a disease modifying drug for OA has been challenging, and there are currently no approved and licensed therapeutics for OA. This is due to distinct nature of inflammation in osteoarthritis that differs from other inflammatory arthritides, such as rheumatoid arthritis (Vincent T., et al 2021). Osteoarthritis prevalence is increasing in developed societies where obesity and longevity increase, as are the socioeconomic costs for the treatment and management of OA (Hunter D., et al 2014; Kim H., et al 2022). Given the increasing prevalence of OA, there is a need to develop therapeutic agents for OA that can prevent structural deterioration, restore joint function, and improve symptoms.

1.2 Cartilage biology

Cartilage is a strong, flexible and semi-rigid connective tissue. It provides the supporting framework for the development of organs and long bones. In the musculoskeletal system, cartilage covers the surfaces of bones at joint articulations. There are three types of cartilage, which differ in the type of fibers they contain: hyaline, fibrocartilage and elastic cartilage. Hyaline cartilage is the most abundant cartilage type in the body, found in structures like the trachea, nose, epiphyseal growth plate and sternum. Hyaline cartilage is primarily composed of type II collagen and proteoglycans. It

provides a smooth and resilient surface that can resist compressive forces and wear-tear at articulation sites (Chang L., 2022). Fibrocartilage is mainly made up of type I collagen and contains much less proteoglycan than hyaline cartilage. Its tough and inflexible physical properties allow it to resist high degrees of tension and compression (Chang L., 2022). Elastic cartilage is histologically similar to hyaline cartilage but also contains elastic fibers, making it more flexible than hyaline cartilage (Chang L., 2022).

1.2.1 Articular cartilage

Articular cartilage is made of hyaline cartilage and provides cushioning of the joint on loading and a smooth lubricated surface for articulation. Cartilage is paucicellular, made of a sparse distribution of specialised cells (chondrocytes) surrounded by a dense extracellular matrix (ECM). It is also avascular and aneural (devoid of blood vessels and nerves), and is often subject to chemical and mechanical stresses.

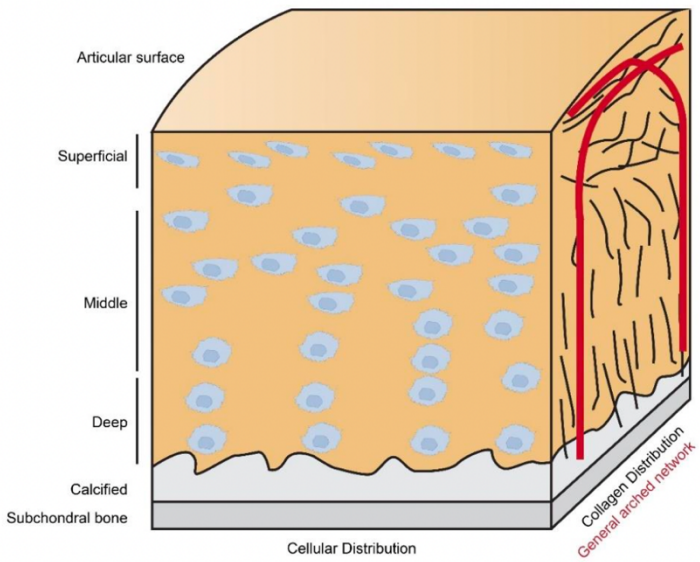

Figure 1.1: Structure of articular cartilage
Zonal distribution, cellular distribution and collagen distribution throughout articular cartilage. Deep chondrocytes appear a rounded, while superficial chondrocytes

appear flattened. Collagen is aligned parallel to the articular surface in the superficial zone, aligned obliquely in the middle zone and perpendicularly in the deep zone, creating in an overall arching of collagen ultrastructure. Adapted from Keppie S., 2021.

The structure of articular cartilage can be subdivided into 4 zones based on chondrocyte morphology and collagen fiber alignment: the superficial zone, the middle/transitional zone, the deep zone, and the calcified zone (Buckwalter J et al., 1998) (Figure 1.1). The superficial zone makes up the top 10-20% of articular cartilage thickness and serves to produce lubricants and protect deeper layers from shear stresses. The chondrocytes and collagen fibers in this zone (primarily type II and IX collagen) are aligned parallel to the articular surface (Eyre D et al., 2006). In the middle/transitional zone, chondrocytes appear rounded and are distributed throughout the matrix (Decker R et al., 2015). Collagen fibrils in this zone are thicker than the superficial zone, organized in an oblique manner. This zone makes up 40-60% of articular cartilage thickness and functions as the first resistor of compressive forces (Sophia Fox A et al., 2009). Chondrocytes in this middle zone are mainly responsible for producing and depositing type II collagen, aggrecan and other matrix molecules (Decker R et al., 2015). The deep zone provides the greatest resistance to compressive forces, given the perpendicular arrangement of collagen fibers to the articular surface (Sophia Fox A et al., 2009). In this zone, chondrocytes are hypertrophic and collagen fibers are thickest. The ECM has the highest proteoglycan abundance but lowest water content (Bashir A et al., 1997). The deep zone represents 30% of the cartilage thickness and is responsible for providing resistance to compressive forces (Sophia Fox A et al., 2009). Some chondrocytes and

collagen fibers seep into the deepest calcified region, a thin layer that connects the articular cartilage with the subchondral bone (Sophia Fox A et al., 2009).

1.2.2 Chondrocytes

Chondrocytes are the only cell type in articular cartilage, that, in human tissue, constitute about 2-5% of the total volume of articular cartilage (Muir H., 1995). Chondrocytes are cytoplasmically isolated from their neighboring cells and thus do not rely on cell-to-cell contact for communication (Muir H., 1995). Chondrocytes do respond to biomechanical stresses such as growth factors, mechanical loads, and hydrostatic pressures (Sophia Fox A et al., 2009). The functions of chondrocytes depend on the cell's location. Historically, the primary function of chondrocytes in articular cartilage has always thought to have been to synthesize and maintain ECM in order to withstand physical deformation. However, chondrocytes are highly sensitive to mechanical stress, which influence tissue homeostasis response, termed mechanoadaptation (Vincent T et al., 2019) and repair. Several mechanisms by which chondrocytes sense mechanical stress have been reported. These include cell surface integrins, stretch and cation-sensitive ion channels and the primary cilium, as well as by the release of growth factors (Drexler S et al., 2014; Keppie et al., 2021; Lee W et al., 2014; O'Conor C et al., 2014; Ross T et al., 2013; Wann A et al., 2012). Since articular cartilage is avascular, chondrocytes rely on passive diffusion of nutrients, oxygen, and metabolites from the articular surface (Archer C et al., 2003). Thus, chondrocytes reside in a relatively hypoxic environment, and favor glycolysis

as the primary means of energy production (Archer C et al., 2003, Falchuk K et al., 1970). Thus, chondrocytes possess low numbers of mitochondria (Akkiraju H et al., 2015).

1.2.3 Extracellular matrix (ECM)

Hyaline cartilage contains type II collagen as the most abundant component and other collagen types in lesser amounts (e.g., VI, IX, X, XI) (Eyre D et al., 2006). These minor collagens cross-link with type II collagen to be arranged into a fibrillar network that entraps proteoglycans, glycoproteins, and water (Correa D et al., 2017). Proteoglycans are the second most abundant group of macromolecules in the ECM. They are glycosylated protein monomers that possess high affinity to water, thus acquiring swelling properties that enable cartilage to resist compression forces (Akkiraju H et al., 2015) as well as assisting growth factor release on tissue compression (Keppie et al., 2021; Vincent T et al., 2002; Vincent T et al., 2006). Examples of proteoglycans include aggrecan, decorin, biglycan and fibromodulin (Akkiraju H et al., 2015; Vincent T et al., 2007). Aggrecan is the largest and most abundant proteoglycan present in articular cartilage. Aggrecan has negatively charged glycosaminoglycan (GAG) chains, that are chondroitin sulfate and keratin sulfate (Roughley P et al., 2014). Aggrecan monomers form proteoglycan aggregates with hyaluronan via link protein to provide macromolecular structures with high osmotic properties (Roughley P et al., 2014). Decorin and fibromodulin interact with the type II collagen fibers to facilitate fibrillogenesis and inter-fiber interactions (Hedbom E et al., 1993).

1.2.4 Pericellular matrix (PCM)

The pericellular matrix is a 2-4μm layer surrounding each chondrocyte. It contains proteoglycans, glycoproteins and non-collagenous proteins (Sophia Fox A et al., 2009). The chondrocyte and pericellular matrix together make up the chondron (Vincent T et al., 2019) (Figure 1.2).

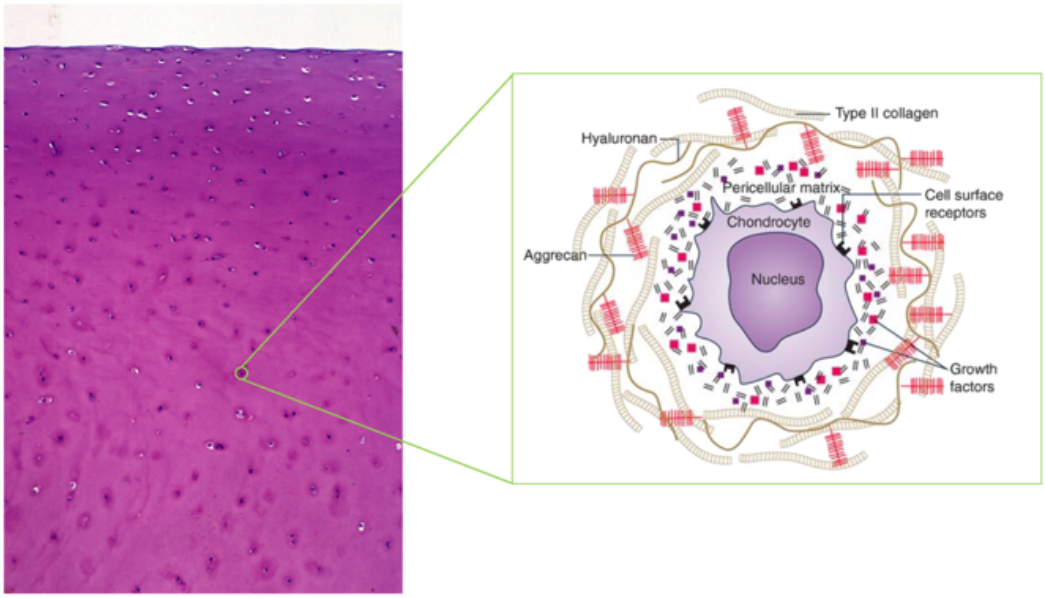

Figure 1.2: Articular cartilage, the chondrocyte and the surrounding matrix
Articular cartilage is paucicellular, with a sparse distribution of chondrocytes, the only cell type (left). The chondrocyte is surrounded by the pericellular matrix (PCM), together known as the chondron (right). The further removed matrix constitutes the extracellular matrix. Adapted from Vincent et al., 2019 (Figure reuse license number - 5632681383796).

The PCM is primarily composed of type IV collagen, fibronectin, and the proteoglycans perlecan and biglycan (Wang Q et al., 2008; Vincent T et al., 2007). Biochemical and mechanical signals perceived by the chondrocyte can be modulated by the PCM. The PCM affects chondrocyte signaling by regulating cell-matrix ligand binding, growth factor and enzyme sequestration, transport, assembly and activation (Guilak F et al., 2018). Our

group has highlighted in a review the importance of growth factor sequestration in chondrocyte signaling after cartilage injury, namely growth factors FGF2, HDGF and CTGF (Vincent T et al., 2019). Disruption of the PCM structure, by mechanical injury or proteolytic activity, can release these sequestered proteins, allowing them to signal to chondrocytes in an autocrine or paracrine manner (Wilusz R et al., 2014). For example, several growth factors, including FGF2 and TGFβ, are bound to the heparan sulfate chains of perlecan (in the case of TGFβ this is through a covalent interaction with CTGF). TGFβ has also been described as binding to fibrillin and fibulin (Guilak F et al., 2018). Mechanotransduction in the PCM is facilitated by type IV collagen that links with type II collagen fibers in the further removed ECM, while also anchoring mechanosensory receptors on chondrocytes (Guilak F et al., 2018).

1.2.5 ECM homeostasis

Chondrocytes are responsible for the maintenance and repair of the ECM. They do so by maintaining a delicate balance between synthesis of matrix-degrading enzymes and matrix macromolecules. As discussed earlier, chondrocytes are responsible for the biosynthesis of collagen, proteoglycans and other matrix molecules. On the other hand, proteolytic enzymes involved in cartilage turnover include metalloproteinases and cathepsins (Sophia Fox A et a., 2009). Metalloproteinases participate in the breakdown of collagen fibers, while cathepsins aid in aggrecan degradation (Sophia Fox A et a., 2009). Articular cartilage has limited capacity for intrinsic repair, and collagen fibers that are laid down in the ECM essentially last a lifetime. The half-life of

collagen is estimated to be 117 years, while the turnover rate of proteoglycans and glycoproteins is estimated to be a couple weeks to 25 years (Correa D et al., 2017).

1.2.6 ECM changes in OA

During OA development, native chondrocytes that are normally considered to be quiescent cells undergo a phenotype change. They take on a catabolic profile that results in fibrillation and cartilage degradation. This is associated with increased cartilage calcification and vascular invasion from the subchondral bone (Li G et al., 2013). Additionally, byproducts from cartilage-degrading enzymes may contribute catabolic and inflammatory activation, hypertrophic differentiation of chondrocytes and chondrocyte apoptosis (Goldring M., 2012). The increased expression of matrix degrading enzymes is a hallmark feature in OA cartilage. The biology resembles aspects of endochondral ossification during bone formation, where chondrocytes attain a hypertrophic-like phenotype (van der Kraan P et al., 2012). Hypertrophic chondrocytes express *MMP13*, *COL10A1*, and *VEGF*, that are upregulated in OA (Dreier R., 2010). Thus, chondrocyte hypertrophy is usually an indicator of OA progression.

The activation of pathways that lead to cartilage damage induces transcriptional and post transcriptional events in chondrocytes that promote aberrant expression of inflammatory genes such as nitric oxide synthase 2 (*NOS2*) and cyclooxygenase 2 (*COX2*), and catabolic genes such as matrix metalloproteinases (*MMP 1, 3*, and *13*), and A Disintegrin and

Metalloproteinase with Thrombospondin motifs (*ADAMTS 4* and *5*). Endogenous inhibitors of MMPs include cathepsin B and tissue inhibitors of MMPs (TIMPs) are also increased, although these factors are usually found in lower abundance in OA tissue compared to their catabolic counterparts (Akkiraju H et al., 2015). Pro-inflammatory mediators such as IL-1β, IL-6, IL-8, TNF-α, and NO are also found in higher abundance in damaged cartilage and synovial fluid (Borrelli J et al., 2019). Anti-inflammatory mediators IL-10, IL-4, IL-1Rα are also found readily available in human synovial samples of the injured joint, and these may act to initiate tissue repair (Borrelli J et al., 2019).

OA-induced cartilage damage activates a myriad of signaling cascades that trigger either additional joint inflammation or help to initiate tissue repair. These cascades, activated by growth factors, inflammatory and mechanical stimuli include the MAPK cascade (ERK, p38, JNK), which subsequently activate AP1, ETS, Runx2, C/EBP and NF-κB transcription factors (Goldring M., 2012). Other catabolic mediators are the secreted damage-associated molecular patterns (DAMPs) that act on toll like receptors (TLRs) and receptor for advanced glycation end products (RAGE) (Goldring M., 2012). These events may cause oxidative stress, chondrocyte death and mitochondrial dysfunction.

The mechanical environment is altered in OA cartilage. Loss of collagen, aggrecan and hydration results in higher stiffness of cartilage, making cartilage less compliant to tension, compression, and shear stresses

(Akkiraju H et al., 2015). Thickening of collagen fibrils have been reported as well, which further deteriorate mechanical integrity (Silver F et al., 2002). Such changes contribute to the constant deterioration of the cartilage biomechanical environment, leading to the formation of fibrocartilaginous tissue to replace degraded cartilage and osteophyte formation (the formation of bony spurs around joints as an adaptive response to maintain joint balance) (Gelse K et al., 2003). Our group has shown that mechanical factors alone are necessary and sufficient to promote OA, as immobilization of the joint prevents murine OA by surgical destabilization (Burleigh A et al., 2012).

1.3 Cartilage injury

Mechanical stress is one of the key factors that influence cartilage homeostasis. Articular cartilage is subjected to a combination of mechanical stresses including tensile, compressive and shear stress. A healthy joint achieves mechanoprotection by having thick cartilage that can withstand a lifetime of constant cyclic loading and physiological magnitudes of mechanical strain. Dynamic compression at normal/moderate levels can be beneficial to cartilage by providing anti-catabolic effects and inhibit cytokine release, but overloading above a strain threshold can become detrimental to cell and tissue function. Excessive and injurious loading can produce structural damage and osteoarthritic-like changes in the ECM including increased collagen denaturation, reduced proteoglycan synthesis and chondrocyte apoptosis in injured cartilage (Chen C et al., 2001; D'Lima D et al., 2001). This can lead to tissue swelling and reduced tissue stiffness and

ultimately alteration of contact dynamics between articular cartilage surfaces (Li Y et al., 2013). However, how mechanical thresholds are activated in vivo is unknown.

The cartilage injury response can be categorized into signals that confer cartilage repair (chondroprotection), or deleterious signals that drive cartilage degradation (mechanoflammation), which will be described in the next sections.

1.3.1 Mechanoflammation

Mechanical injury is a key hallmark of OA, and our lab has researched extensively into the cartilage injury response, with an emphasis on the upregulation of inflammation upon cartilage injury, termed mechanoflammation. Mechanically-induced inflammation is not exclusive to cartilage but also involves the synovium and subchondral bone (Sokolove J et al., 2013; Burleigh A et al., 2012). In OA, pathological changes to the synovium include synovial hypertrophy and hyperplasia, an increased number of synovial lining cells and modest infiltration of inflammatory cells. These subsequently activate chondrocytes to produce proteases and other catabolic factors that are responsible with the degradative phenotype in OA (Pelletier J et al., 2001).

The upstream mechanism by which chondrocytes sense mechanical injury is not known but subsequent rapid activation of signaling cascades induce a

plethora of inflammatory genes, that ultimately lead to cartilage degradation. Many intracellular signaling pathways have been shown to be activated upon cartilage injury including the mitogen activated protein kinase (MAPK), nuclear factor kappa light chain enhancer of activated B cells (NF-κB) pathway, the wingless/integrated (Wnt) pathway, Src pathway and Hippo-YAP pathway (Deng Y et al., 2018; Fanning P et al., 2003; Ismail H et al., 2017; Vincent T et al., 2019; Vincent T et al., 2002; Watt F et al., 2013). These signaling pathways will be described later in Section 1.4.

1.3.2 Chondroprotection

Dynamic compression can stimulate anabolic responses in cartilage which promote cartilage matrix repair and chondroprotective pathways (Li Y et al., 2013; Vincent T et al., 2019). These signals are mainly delivered via the release of sequestered growth factors and regulatory molecules in the PCM (Vincent T., 2013) (Figure 1.3).

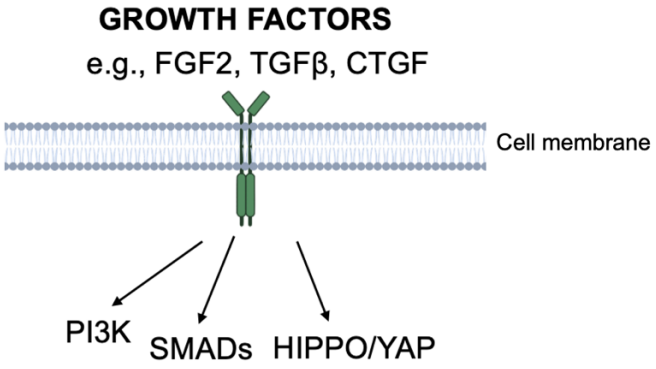

Figure 1.3: Activation of chondroprotective pathways upon cartilage injury
Mechanical compression of cartilage releases sequestered growth factors that drive tissue repair responses (chondroprotective). Growth factors are sequestered in the chondrocyte pericellular matrix and include fibroblast growth factor 2 (FGF2), transforming growth factor beta (TGFβ) and connective tissue growth factor (CTGF)

(Vincent T et al., 2007; Tang X et al., 2018). These are known to activate various downstream cascades such as PI3K, Smads and ERK MAPK (Di-Luoffo M et al., 2021; Neu C et al., 2007). Hippo/Yap are also activated by injury (unpublished data, Vincent group).

A well described chondroprotective factor is fibroblast growth factor 2 (FGF2), sequestered on perlecan, is released upon cutting or cyclical compression of cartilage (Vincent T et al., 2007). FGF2 is chondroprotective in OA, as mice deficient in FGF2 developed accelerated OA following surgical destabilization of the medial meniscus (DMM). Furthermore, FGF2 inhibited interleukin 1 (IL1)-driven aggrecanolysis in human cartilage explants (Sawaji Y et al., 2008). In FGF2 total KO mice, there was higher induction of *Adamts5* mRNA, suggesting that FGF2 normally suppresses *Adamts5* in vivo (Vincent T., 2011). Variants in the FGF2 response may be determined by signaling through different FGF receptors (FGFRs). FGF2 exerted catabolic signaling, such as the induction of matrix proteases *Mmp13* and *Adamts5* when signaling through FGFR1 but signaling through FGFR3 favored anabolic responses (Yan D et al., 2011). To support this, FGFR3 total KO mice demonstrated early cartilage destruction and arthritis (Valverde-Franco G et al., 2006), while tamoxifen-induced cartilage-specific deletion of *Fgfr1* in 8-week mice inhibited cartilage degeneration in surgically induced OA (Weng T et al., 2012). This evidence suggests that variable biological responses can arise from differences in receptor-ligand signaling or that FGF2 is acting on tissues that have different expression levels of FGFRs. FGF18, which preferentially signals through FGFR3, attenuated cartilage degradation by stimulating proteoglycan synthesis, suppressing matrix proteolytic enzymes and promoting chondrocyte proliferation, and is currently in clinical trial under the name Sprifermin (Yao X et al., 2019; Li J et al., 2021).

Another mechanosensitive PCM growth factor is transforming growth factor beta (TGFβ). TGFβ is a pleiotropic growth factor that regulates diverse cellular functions such as cellular differentiation, proliferation, apoptosis, and wound healing in many cell systems (Choi M et al., 2012). TGFβ is initially bound to two latency associated peptides (LAPs), where it is then secreted extracellularly and binds to latent TGFβ binding proteins (LTBPs) to form a complex. This TGFβ complex is then thought to bind to fibrillin and fibulin (Massam-Wu et al., 2010). The canonical TGFβ signaling cascade occurs through phosphorylation of downstream Smad proteins. *Smad3* knockout (through vector-targeted mutation of Smad3) germline chimeric mice showed reduction in TGFβ signaling, and was accompanied with abnormal terminal differentiation of chondrocytes, progressive cartilage loss and osteophyte formation (van de Laar et al., 2011). A single nucleotide polymorphism in *SMAD3* conferred an increased risk of knee and hip OA (Gao S et al., 2018). Shear stress loading on bovine cartilage explants activated TGFβ signaling in a phospho-Smad2/3 manner, suggesting that TGFβ is a potential mediator of mechanosensitive responses (Neu C et al., 2007). Some studies suggest a dual role for TGFβ in OA, depending on the source of upstream Smad signals from activin receptor-like kinases (ALKs). ALK5 phosphorylates Smad2/3, while ALK1 phosphorylates Smad1/5/8 (van der Kraan P et al., 2012). The authors saw a shift in ALK1/ALK5 balance in ageing and OA, whereby ALK5 (and Smad2/3 phosphorylation) was lost in OA and ageing cartilage while ALK1 (and Smad1/5/8 phosphorylation) did not diminish to a comparable extent. This shift from Smad2/3 to Smad1/5/8 during ageing and OA was associated with increased *MMP13* expression and reduced aggrecan synthesis (Blaney Davidson E et al., 2009). They postulated that TGFβ exerts its function as a repair factor via Smad2/3 to keep chondrocytes in the quiescent state; in OA, Smad1/5/8 becomes dominant and triggers

chondrocytes to leave their quiescent state and pursue a hypertrophic-like phenotype that aggravates osteophyte formation (van der Kraan P et al., 2012; Wang X et al., 2018).

Our group has demonstrated that connective tissue growth factor (CTGF) is released upon cartilage injury (Tang X et al., 2018). CTGF has been reported to mediate many processes in the joint, including ECM remodeling, endochondral ossification, angiogenesis and chondrocyte survival (Nishida T et al., 2007; Tu M et al., 2019). In our group's study, CTGF was found to be required for sequestration of a latent TGFβ by binding covalently to it and facilitating its activation through TGFβR3 cell surface receptors (Tang X et al., 2018). We hypothesized that CTGF would have a protective role in OA, but postnatal cartilage-specific CTGF KO mice (deletion at 8 weeks) had thicker articular cartilage that was more resistant to degradation in murine DMM (Tang X et al., 2018). It is possible that lack of CTGF allows uncontrolled activation of TGFβ because it is no longer sequestered in the matrix. In the wider literature, however, it is unclear whether CTGF is truly a protective growth factor. CTGF overexpression in synovium in OA caused upregulation of *MMP3* and reduced proteoglycan synthesis, resulting in transient fibrosis (Shi-Wen X et al., 2008). CTGF also promoted IL1β-mediated synovial inflammation in knee OA (Wang Z et al., 2013). On the other hand, some experiments have indicated an anabolic role for CTGF. Intra-articular injection of recombinant CTGF in rats repaired damaged articular cartilage (Nishida T et al., 2004). There has been evidence in preclinical studies that targeting CTGF may have a potential therapeutic role in OA treatment. For example, CTGF-induced IL1β expression in OA synovial fibroblasts was inhibited by the treatment with berberine, a drug that reversed cartilage damage in a

collagenase-induced OA rat model. Overall, more investigations are needed to validate the role of CTGF in OA.

1.4 Signalling events upon cartilage injury

Upon cartilage injury, mitogen activated protein kinase (MAPKs) signaling pathways are rapidly activated (Ismail H et al., 2017). The mechanism by which chondrocytes sense mechanical injury is still unknown, but injury-driven MAPK activation is led by phosphorylation and polyubiquitination of TGFβ-activated kinase 1 (TAK1), which is briefly summarized in Figure 1.4.

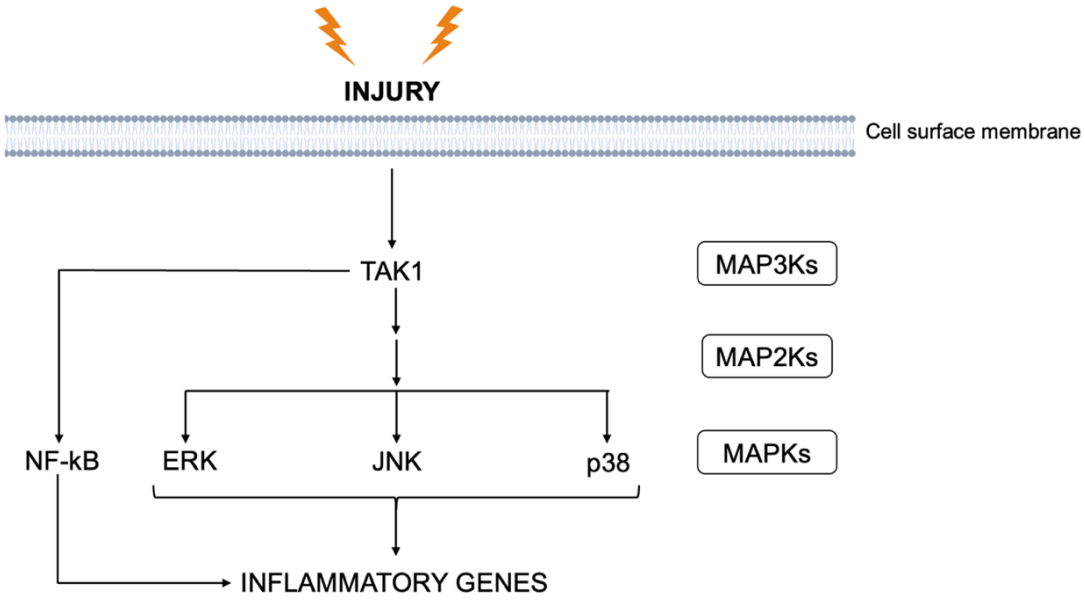

Figure 1.4: Activation of mechanoflammatory pathways upon cartilage injury by TAK1
Mechanical injury on cartilage activates transforming growth factor beta-activated kinase 1 (TAK1). TAK1 activates downstream mitogen activated protein kinases (MAPKs) that include extracellular signal kinase (ERK), c-Jun N-terminal kinase (JNK) and p38. TAK1 also activates nuclear factor kappa- light-chain-enhancer of activated B cells (NF-kB) signalling. Activation of MAPKs and NF-kB results in the increased expression of inflammatory genes, causing the release of key cartilage-degrading enzymes and inflammatory mediators.

1.4.1 TAK1

TAK1 has been demonstrated as a key driver of inflammation and joint homeostasis. TAK1 is a mitogen activated protein kinase kinase kinase (MAP3K) and is known to be an upstream mediator of MAPKs and NF-kB signaling (Figure 1.4). It can be activated by a host of stimuli, including cytokines (i.e., TNF, IL1), chemo-attractants, and growth factors to elicit different signal transduction cascades depending on the cell stress and cell type (Sylvain-Prevost S et al., 2015; Klatt A et al., 2006; Xu Y et al., 2020). TAK1 was originally discovered as the direct downstream mediator of TGFβ signaling (Yamaguchi K et al., 1995). TAK1 activation is facilitated by recruitment of its binding partners, TAK1-binding proteins (TABs). Binding of the TAB-TAK1 complex to K63-polyubiquitination chains facilitates autophosphorylation of TAK1 at Thr184/Thr187 and its subsequent activation. TAK1 then phosphorylates IκB kinases (IKKs) and MAP2Ks, leading to the activation of NF-κB and MAPKs (Xu Y et al., 2020). Cartilage-specific deletion of TAK1 in mice resulted in severe musculoskeletal abnormalities, such as chondrodysplasia and impaired formation of secondary ossification centers (Shim J et al., 2009). However, TAK1 constitutive KO in mice (by germline TAK1 mutation) is embryonic lethal due to abnormal development of the neural tube (Shim J et al., 2005), and postnatal pan-tissue conditional knockout of TAK1 causes death of mice within 48 hours (unpublished data, Vincent group). These results indicate that TAK1 a key regulator of many processes in our body. In vitro, TAK1 inhibition by siRNA downregulated IL1β-induced inflammatory genes, MMP13, MMP1 and TNFα (Klatt A et al., 2006). Furthermore, TAK1 inhibition by intra articular injection of a TAK1 pharmacological inhibitor 5Z-7 blocked MAPK and NF-κB activation in OA

chondrocytes and synoviocytes, leading to decreased expression of matrix degrading enzymes and other anti-inflammatory effects (Cheng J et al., 2016). 5Z-7 also prevented ECM loss in OA cartilage explants (Cheng J et al., 2016).

In the context of mechanical injury, our group has shown that TAK1 is phosphorylated and activated within 30 seconds upon cartilage injury, using a porcine trotter injury model (Ismail H et al., 2017). This acute and rapid response triggers activation of downstream ERK, JNK, p38 and NF-κB signaling, all of which are activated in less than 2 minutes post-injury. They attempted to uncover a TAK1 upstream mediator by generating TNF receptor-associated factor 6 (TRAF6) total KO and myeloid differentiation primary response 88 (MyD88) total KO mice. Both Myd88 and TRAF6 are reported as receptor-proximal mediators of cytokine receptors such as IL1Rs and TNFRs, and a reported to lie upstream of the TAK1 signaling cascade (Verstak B et al., 2008). Both KO mice models failed to show any change in TAK1 signaling upon injury, suggesting that conventional inflammatory receptors such as TLRs and IL1Rs do not play a role in injury-induced mechanoflammation (Ismail H et al., 2017). TAK1 was also shown to be mechanosensitive in vitro when low/physiological magnitudes of loading onto fibrochondrocytes inhibited TAK1 phosphorylation and consequently suppressed NF-κB activation (Madhavan S et al., 2007). It is believed that the TAK1 upstream mediator is neither soluble nor secreted upon injury (Vincent T., 2019).

TAK1 has been reported to cross talk with the Hippo/YAP pathway in chondrocytes and cartilage. Yes-associated protein (YAP) is a mediator of the Hippo signaling pathway, that is implicated in stem cell fate regulation, organ development and regeneration (Karystinou A et al., 2015; Fu L et al., 2019). Deng et al. showed that inflammatory cytokines (i.e., TNF, IL1) facilitate YAP proteasomal degradation via TAK1-mediated YAP Ser127 phosphorylation and ubiquitination. Reciprocally, YAP inhibits cartilage degradation through association with TAK1 to prevent NF-κB translocation into the nucleus (Deng Y et al., 2018). Several studies have confirmed that YAP is overexpressed in animal OA models and human OA tissue, on both gene and protein levels (Kania K et al., 2020; Zhang Q et al., 2019; Gong Y et al., 2019). There was also preferential nuclear localization (over cytoplasmic localization) of YAP in OA cartilage compared with normal cartilage (Zhang X et al., 2020), suggesting that highly expressed YAP maybe involved in OA pathogenesis. Some studies support a protective role for YAP in OA progression. One study showed that loss of YAP1 in murine chondrocytes exaggerated cartilage degradation (Deng Y et al., 2018). For in vivo studies, *Yap* siRNA injection intra-articularly in mice decreased chondrocyte apoptosis, attenuated cartilage degeneration and reduced abnormal subchondral bone formation (Gong Y et al., 2019).

MAPKs are protein serine/threonine kinases that transduce extracellular stimuli into a wide range of cellular responses. MAPKs are common among all eukaryotic cells, which regulate gene expression, mitosis, metabolism, motility, survival, and differentiation. Among the 14 MAPKs that have been

characterized, the most extensively studied mammalian MAPKs are extracellular signal-regulated kinases (ERK), c-Jun amino N-terminal kinases (JNK) and p38 (Cargnello M et al., 2011; Kyriakis J et al., 2001). MAPK pathways are comprised of a hierarchical group of three acting kinases: a MAPKK kinase (MAPKKK/MAP3K), a MAPK kinase (MAPKK/MAP2K) and a MAPK. These proteins sequentially activate each other by phosphorylation on their serine/threonine/tyrosine residues. MAP3K leads to activation and phosphorylation of a MAP2K on conserved Thr-X-Tyr motifs; MAP2Ks then phosphorylate and activate MAPKs. Activated MAPKs then localize to interact with target proteins (often transcription factors) or genes of interest (Cargnello M et al., 2011). Upstream receivers of MAPK signals include cell surface receptors, such as receptor tyrosine kinases (RTKs), G-protein-coupled receptors (GPCRs), integrins, and GTPases Ras and Rap (Morrison D et al., 2012). In the following sections, the three MAPKs ERK, JNK and p38 will be discussed in greater detail.

1.4.2 ERK

ERK was the first mammalian MAPK to be identified and characterized. It was primary found to be activated by growth factors and mitogens, like platelet-derived growth factor (PDGF), epidermal growth factor (EGF), and nerve growth factor (NGF), and also in response to insulin (Boulton T et al., 1990). The classic ERK1/2 MAPK is activated upstream by MAP2Ks MEK1 and MEK2 (Cargnello M et al., 2011).

Our group has shown that ERK1/2 is phosphorylated and activated within 30 seconds of cartilage injury, and that FGF2 released from the cartilage matrix upon injury can activate ERK (Vincent T et al., 2002; Gruber J et al., 2004). In a model of dog OA, inhibition of ERK by using a ligand of voltage gated Ca^{2+} channels reduced OA lesions (Boileau C et al., 2006). Similarly, a MEK1/2 inhibitor, which inhibits ERK activation also prevented OA lesions by a presumed reduction of MMPs (Pelletier J et al., 2003). In a rabbit OA model, treatment with a MEK1/2 inhibitor decreased cartilage lesions, osteophyte formation and synovial inflammation (Pelletier J et al., 2003). Conversely, there is evidence of ERK being a negative regulator of proteoglycan synthesis in chondrocytes (Starkman B et al., 2005).

1.4.3 JNK

The JNK family, consisting of JNK1-3, is primarily activated by environmental stresses (ionizing radiation, heat, oxidative stress, and DNA damage), cytokines, and to a lesser extent by growth factors, GPCR ligands, and serum (Cargnello M et al., 2011). The JNK MAPKs are activated upstream by the MAP2Ks, MKK4 and MKK7, both of which are substrates of TAK1 and ASK1 (Cargnello M et al., 2011). Various studies have implicated the involvement of JNK in OA. Stimulation of chondrocytes with chemokines CXCL8/11 induced chondrocyte proliferation, alongside JNK activation and increased expressions of other pro-inflammatory cytokines (Yang P et al., 2016). Accumulating evidence indicate that inhibition of the JNK pathway can reduce cartilage degradation associated with OA (Ge H et al., 2017). Suppression of IL1-induced JNK/p38 attenuated *MMP1*, *MMP3* and *MMP13*

gene expression in chondrocytes (Jeong J et al., 2015). Our group has shown that JNK is phosphorylated and activated within 2 minutes cartilage injury, in a TAK1-dependant manner (Ismail H et al., 2017). In an earlier study, our group observed a delay in the development of surgically induced OA in JNK2 total KO mice through the suppression of aggrecanolysis and inflammatory genes (Ismail H et al., 2016).

1.4.4 p38

The p38 MAPK is generally more responsive to stress stimuli, inflammatory cytokines (i.e., TNF and IL1), oxidative stress, UV irradiation, and hypoxia. p38 MAPKs are activated upstream by the MAP2Ks, MKK3 and MKK6, both of which are substrates of TAK1 and ASK1 (Cargnello M et al., 2011). p38 is activated in OA cartilage and p38 inhibition (using a p38 inhibitor, SB203580) in cartilage tissue in vitro suppressed apoptosis and expression of proinflammatory cytokines (Sun H et al., 2017). Similarly, SB203580 reduced joint degeneration and pain in a rat OA model (Brown K et al., 2008). A different p38 inhibitor (R-130823) protected cartilage breakdown and was associated with MMP1, MMP13 and PGE2 release, alongside *COX2* mRNA suppression (Wada Y et al., 2006). In a different study, only p38 inhibition (and not ERK or JNK) blocked Mmp13 expression mediated by the discoidin domain receptor in murine chondrocytes (Xu L et al., 2007). These results suggest that activated p38 accelerates cartilage breakdown. Unfortunately, p38 inhibitors were somewhat unsuccessful for disease attenuation in vivo,

possibly because p38 possesses both pro and anti-inflammatory effects (Tomida T et al., 2015).

1.4.5 ASK1

ASK1 is another member of the MAP3K family and is a serine/threonine kinase like TAK1. It activates MKK4/7 JNK and MKK3/6 p38 signaling cascades. ASK1 is primary known as a signal transducer to cell stress stimuli, namely oxidative stress, inflammatory cytokines, lipopolysaccharides, endoplasmic reticulum stress, and calcium influx (Fujino G et al., 2007). Of these stimuli, ASK1 is best characterized as a potent activator of oxidative stress. ASK1 has been implicated diseases such as neurodegenerative, renal, liver and cardiovascular disorders (Hayakawa R et al., 2012).

1.4.5.1 ASK1 in OA

Studies investigating the role of ASK1 in OA or cartilage are scarce.
In vitro, H_2O_2, TNFα and calcium have been reported to activate ASK1, p38 and JNK signaling in chondrocytes (Eaton G et al., 2013). They also showed ASK1-dependant upregulation of *MMP13*, alkaline phosphatase and *COL10A1* mRNA (Eaton G et al., 2013). In human articular cartilage tissue retrieved from joint replacement surgeries, increased ASK1 expression was observed with OA progression (Zhang Q et al., 2016). In the same study, joint degeneration was slowed in ASK1 total KO mice, demonstrated by decreased cartilage and proteoglycan loss (Zhang Q et al., 2016). The authors also generated two OA mouse models (partial meniscectomy and

joint destabilization) and showed that ASK1 inhibition in these models attenuated cartilage breakdown (Zhang Q et al., 2016). Immunohistochemistry of the growth plate revealed that ASK1 expression correlated with chondrocyte hypertrophy (Zhang Q et al., 2016). This finding resonated with a different study, which observed increased ASK1 expression in the hypertrophic zone of the growth plate (Eaton G et al., 2014). According to a review paper, ASK1 total KO mice are viable, healthy, long lived and show no developmental abnormalities (Ogier J et al., 2020). Bone development appeared accelerated in ASK1 total KO mice compared to WT mice, although no skeletal malformations were reported (Eaton G et al., 2014). Recently, the use of a selective ASK1 inhibitor named serlonsertib was tested in pre-clinical studies of OA. In chondrocytes, serlonsertib attenuated IL1β-induced inflammatory gene upregulation and cartilage degradation, via blockade of the ASK1/p38/JNK/NF-kB cascade (Yan J et al., 2021). Intra articular injection of serlonsertib into anterior cruciate ligament transection and partial medial meniscus rat OA models prevented cartilage erosions, proteoglycan loss and chondrocyte apoptosis. From this study and others, serlonsertib might act via regulating ASK1/p38/JNK pathways in OA (Yoon Y et al., 2020).

The ASK1 inhibitor serlonsertib was initially used for a phase 2 trial for treatment of diabetic kidney disease (Chertow G et al., 2019), and most recently, a phase 3 trial for treatment for non-alcoholic steatohepatitis (NASH), a fibrotic liver disease (Harrison S et al., 2020). Serlonsertib led to anti-inflammatory and anti-apoptotic effects such as improvement of liver

fibrosis and presented no adverse effects in patients (Loomba R et al., 2018). The NASH trial did not reach its primary study endpoint (Harrison S et al., 2020).

1.4.5.2 ASK1 Mechanism of action

In non-stressed conditions, ASK1 forms a homo-oligomer through direct interaction through its C-terminal coiled-coil domain (Shiizaki S et al., 2013). At the same time, ASK1 is bound to thiol-containing antioxidant protein, Thioredoxin-1 (Trx) which represses ASK1 activity in normal homeostatic conditions. This high molecular weight complex (1500-2000 kDa) is termed the ASK1 signalosome (Shiizaki S et al., 2013). In conditions that activate ASK1, such as elevated oxidative stress, Trx is oxidized and dissociates from ASK1, leading to ASK1 activation by autophosphorylation at Thr838 (for humans) Thr845 (for mice) (Saitoh M et al., 1998; Tobiume K et al., 2002). It is also reported that reactive oxygen species (ROS) such as hydrogen peroxide (H_2O_2) activates ASK1 by recruiting TNF receptor-associated factor 2 (TRAF2) and TNF receptor-associated factor 6 (TRAF6) to the ASK1 signalsome, where they interact with ASK1's N-terminal region (Fujino G et al., 2007). It has been described before that TRAF2 and TRAF6 are upstream of ASK1-dependant MAPK and NF-κB signaling (Noguchi T et al., 2005). Upon ASK1 activation, ASK1 phosphorylates and activates downstream MAP2Ks 3,4,6, and 7, which subsequently phosphorylate and activate p38 and JNK MAPKs. ASK1 is best known for promoting pro-apoptotic activation of p38/JNK and was also implicated in p38/JNK-

mediated fibrosis and inflammation (Tobiume K et al., 2001; Ogier J et al., 2020). Recently, a another ASK1 phospho-site has been reported, Ser966, that takes part in inhibiting ASK1 under non-stressed conditions by interacting with Trx (Petrvalska O et al., 2016).

1.4.6 NF-κB

Nuclear factor-kappa B (NF-κB) are a family of nuclear transcription factors, that regulate an array of genes involved in different immune and inflammatory responses. The NF-κB family has five structurally related members: NF-κB1, NF-κB2, RelA, RelB and c-Rel (Liu T et al., 2017). These transcription factors facilitate transcription of their target genes by binding to specific DNA motifs called κB enhancers (Liu T et al., 2017). NF-κB proteins are normally sequestered in the cytoplasm by inhibitory proteins, such as the inhibitor of nuclear factor-κB (IκB) proteins. The best studied IκB family member is IκBα (Liu T et al., 2017).

1.4.6.1 Canonical NF-κB signaling

The canonical NF-κB cascade is induced by ligand-based activation of various cytokine receptors, pattern-recognition receptors, TNF receptor superfamily members, as well as T-cell receptors and B-cell receptors (Zhang H et al., 2015). Activating stimuli include cytokines, growth factors, mitogens, microbial components and stress agents (Israel A et al., 2010). Canonical activation of NF-κB occurs via the inducible degradation of IκB triggered through its phosphorylation, by the kinase that phosphorylates IκBs called the

IκB kinase (IKK) complex (Liu T et al., 2017). Upon IKK complex activation, IKK phosphorylates IκB at serine residues, triggering ubiquitin-dependent IκB degradation in the proteasome and consequent transient nuclear translocation of canonical NF-κB proteins. Post-translational modifications of IκB, IKK and the NF-κB proteins can also modify response of the signaling cascade (Oeckinghaus A et al., 2009).

1.4.6.2 Non-canonical NF-κB signaling

The non-canonical NF-κB pathway is activated by a small subset of TNF receptor superfamily members, notably in response to oncogenic viruses and bacteria. This pathway relies on the phosphorylation of p100, a precursor of NF-κB2. This causes nuclear translocation of the non-canonical p52/RelB complex (Sun S., 2012). Functionally, the non-canonical NF-κB pathway serves as a supplementary signaling axis that cooperates with the canonical NF-κB pathway to regulate specific functions of the adaptive immune system (Liu T et al., 2017).

1.4.6.3 NF-κB in OA

NF-κB has been implicated in many inflammatory and autoimmune diseases such as rheumatoid arthritis. The significance of NF-kB in OA pathogenesis was first determined through loss of function studies. Treatment with NF-κB inhibitors on human osteoarthritic chondrocytes suppressed IL1β-induced *MMP3* and *MMP13* mRNA (Liacini A et al., 2002). siRNA specific knockdown

of *p65* NF-κB alleviated injury induced cartilage lesions in a rat OA model (Chen L et al., 2008). Furthermore, intra articular injection of an IKK inhibitor suppressed OA development in surgically induced OA mouse model and downregulated IL1β-induced catabolic gene expression in chondrocytes (Murahashi Y et al. 2018). Tamoxifen-induced cartilage specific knockout of IKK in 10-week old mice subjected to DMM showed reduced cartilage degradation and hypertrophy-like features compared to wild-type controls, but growth plates displayed aberrant architecture and correlated with chondrocyte apoptosis (Culley K et al., 2019).

In vitro and in vivo studies of OA have demonstrated that increased NF-κB activity positively correlated with higher cartilage destruction (Choi M et al., 2019). NF-κB induces inflammation in cartilage and chondrocytes by promoting catabolic gene expression directly via the binding of NF-κB response elements to the promoters of *MMP1*, *MMP9* and *ADAMTS5* genes, or by indirectly elevating pro inflammatory mediators including cyclooxygenase 2 (COX2), prostaglandin E2 (PGE2), and inducible nitric oxide synthase (iNOS) (Kobayashi H et al., 2013; Lianxu C et al., 2006; Vincenti M et al., 1998). Intermediate mediators of NF-κB that have been reported include hypoxia-inducible factor 2 (HIF-2), ETS domain-containing protein-1 (ELK1), and E74-like factor 3 (ELF3) (Choi M et al., 2019). HIF-2 is required for hypertrophic differentiation of chondrocytes and is an inducer of *MMP13*, *COL10A1*, and *VEGF* by its binding to hypoxia-responsive elements (Saito T et al., 2010). NF-κB binding proteins SAM68 and KPNA2 were reported to interact with NF-κB signaling to promote chondrocyte catabolism

(Xu L et al., 2015; Tao R et al., 2015). The Wnt pathway also cross-talks with NF-κB via TCF4 (Ma B et al., 2016).

Many extracellular factors associated with OA can induce the expression of matrix degrading enzymes and pro-inflammatory mediators. For example, ghrelin (also known as the 'hunger hormone') was protective against OA in DMM-induced OA and IL1β-induced NF-κB activation (Qu R et al., 2018). Osteopontin (OPN), a factor involved in adipose tissue inflammation and bone remodeling, was found elevated in synovial fluid and articular cartilage of OA patients (De Fusco C et al., 2017; Gao S et al., 2010). OPN promoted *Mmp13* upregulation and *Hif-2* suppression via NF-κB, supporting a catabolic role, but OPN total KO mice exhibited enhanced OA progression (Choi M et al., 2019). Thus, more detailed investigations are required to validate the contradictory findings. Conventional cytokines, such as IL1 and TNF have been implicated in OA on many occasions (Wojdasiewicz P et al., 2014) but there is little substantive in vivo data (in mice or humans) for a direct role. IL-6 and IL-36 also activate NF-κB and have been implicated in OA (Conde J et al., 2015; Latourte A et al., 2017). One particular study found that aberrant signaling through the TGFβ type II receptor (TGFBR2) can cause NF-κB and MAPK activation (Li T et al., 2019).

There is also multiple evidence that excessive mechanical loading causes NF-kB activation in OA development, while normal/physiological loading protects cartilage degeneration and inhibits NF-kB. Mechanical regulation of

NF-kB has been reported to occur at the level of TAK1 and IKK (Dossumbekova A et al., 2007; Madhavan S et al., 2007; Nam J et al., 2009;).

1.5 Models of cartilage injury

The Vincent lab has used a few ex vivo models to investigate the signaling pathways activated upon cartilage injury. These include articular cartilage explantation (cartilage cut or carved out directly from the intact joint surface), re-cutting (cartilage is rested in vitro for 48 hours and then re-injured by cutting), avulsion (shearing the immature femoral head from the mouse hip) and mechanical compression (Vincent T., 2019). These models have been validated by the group in multiple studies, as characterized by the activation of catabolic pathways that drive inflammation (mechanoflammation) and the release of sequestered growth factors that drive cartilage repair (Vincent T et al., 2002; Zhu L et al., 2017). In vivo, cartilage injury leading to OA, can be induced by surgical joint destabilization. Past work by the Vincent group suggests that differences in type of mechanical loading led to differences in cartilage response outcomes. Specifically, shear stress is more likely to activate mechano-inflammatory responses and compressive load is more likely to promote chondroprotection (Burleigh A et al., 2012). These models are used by our lab to delineate known pathways or discover new mechanosensitive signaling pathways, to understand the pathological processes that underlie OA and thereby facilitate the discovery of new drug targets.

1.6 ROS

Reactive oxygen species are oxygen-containing free radical molecules (Zahan O et al., 2020). These molecules contain unpaired valence electrons that causes ROS to be short lived, unstable and highly reactive (Zahan O et al., 2020). Notable examples of ROS include the hydroxyl radical (OH^-), hydrogen peroxide (H_2O_2), superoxide anion (O_2^-), nitric oxide (NO^-) and hypochlorite ion (OCl^-). Low levels of ROS produced by cells is essential for cellular homeostasis and function (Trachootham D et al., 2008). However excessive ROS is usually considered to be deleterious, as they can oxidize protein and lipid constituents, cause DNA damage, and stimulate release of inflammatory mediators (Zahan O et al., 2020). The notion of chronic ROS production is considered central to many inflammatory diseases, including OA, thus it has been of increased interest to study the role of ROS in cartilage homeostasis.

1.6.1 Sources of ROS

There are three major sites of ROS production in chondrocytes: the mitochondria (via oxidative phosphorylation), non-mitochondrial membrane-bound nicotinamide adenine dinucleotide phosphate (NADPH) oxidase and xanthine oxidase (XO) (Zahan O et al., 2020).

ROS in the mitochondria arise as a byproduct of oxidative phosphorylation (Turrens F et al., 2003). In mitochondria, the superoxide anion ($O_2^-\bullet$) is generated by the one electron reduction of O_2 (Turrens F et al., 2003).

Dismutation of the superoxide anion generates hydrogen peroxide (H_2O_2), which can be fully reduced to water or partially reduced to form a hydroxyl radical (OH•) (Turrens F et al., 2003). The majority of mitochondrial ROS processes are catalyzed by complexes of the electron transport chain that lie on the inner membrane of the mitochondria. Complex I is the primary contributor of ROS in pathological scenarios (Turrens F et al., 2003). Complex I serves as the entry point for electrons into the electron transport chain, where a flavin mononucleotide (FMN) cofactor takes electrons from NADH and passes them through a series of iron-sulfur centers to the coenzyme Q (CoQ) reduction site, at which reduction of oxygen takes place (Murphy M et al., 2009). When there is a high NADH/NAD+ pool or a large amount of reduced CoQ, production of the superoxide anion is favored (Murphy M et al., 2009). It is estimated that 2-3% of O_2 used in mitochondrial oxidative phosphorylation is converted to superoxide anions (Lepetsos et al., 2016).

NAPDH oxidase (NOX) enzymes are heme-containing transmembrane proteins that aid electron transport. NOXs receive electrons from a cytosolic donor (usually NAPDH) and transfer them to an electron acceptor, O_2 (Drevet S et al., 2018). The chemical reaction for this is $2O_2 + NADPH \rightarrow 2O_2^- + NADP^+ + H^+$. NOXs are expressed ubiquitously in humans (Drevet S et al., 2018). Increased NOX activity is correlated in many pathologies, in particular cardiovascular and neurodegenerative diseases (Bedard K et al., 2007).

Lastly, xanthine oxidase (XO) catalyzes the oxidation of hypoxanthine to xanthine, producing the byproduct H_2O_2 (Turrens F et al., 2003).

1.6.2 Antioxidant systems

Enzymatic and non-enzymatic antioxidant systems have been described for scavenging ROS. Antioxidant enzymes include thioredoxin, superoxide dismutase (SOD), catalase (CAT), glutathione peroxidase (GPX), to name a few (Zahan O et al., 2020). These enzymes act by eliminating ROS directly or by catalyzing the regeneration of other antioxidants (Tudorachi N et al., 2021). SOD enzymes catalyze the conversion of superoxide anions to oxygen and hydrogen peroxide (Tudorachi N et al., 2021). Downregulation in expression of SODs have been reported in OA cartilage in humans and animal models (Scott J et al., 2010), although our group have shown that SOD genes are strongly upregulated by cartilage injury (Hermansson M et al., 2003). CAT enzymes catalyze the conversion of hydrogen peroxide to water and oxygen (Tudorachi N et al., 2021). GPx serves the same function by converting hydrogen peroxide to water and oxygen but is also capable of reducing peroxide radials (such as lipid peroxides) to alcohol and oxygen (Tudorachi N et al., 2021).

Examples of non-enzymatic antioxidants include glutathione (GSH), carotenoids, vitamins and Coenzyme Q10. GSH is an endogenous antioxidant that is found in mitochondria or peroxisomes (Lushchak V., 2012). GSH acts in concert with antioxidant enzymes to scavenge free radicals, where it is oxidized into glutathione disulfide (GSSG) (Lushchak V., 2012).

GSSG can be recycled back into GSH via glutathione reductase: GSSG + NADPH + $H^+ \rightarrow$ 2GSH + $NADP^+$ (Lushchak V., 2012). Carotenoids are naturally occurring pigments found in many plants and animals, and also encompass a few classes of vitamins (Vitamins A, C and E) (Tudorachi N et al., 2021). They possess antioxidant effects by directly eliminating oxidized radicals or by interfering with oxidative stress-induced signaling, such as NF-κB, IL-6 and TNFα (Tudorachi N et al., 2021). Coenzyme Q10 (commonly known as just coenzyme Q/CoQ), is a coenzyme localized on the inner membrane of mitochondria and is responsible for transferring electrons across respiratory complexes of the electron transport chain (Tudorachi N et al., 2021). The reduced form of CoQ10 can be oxidized by oxygen radicals and is recycled back into the reduced form by the action of NADPH oxidoreductases (Tudorachi N et al., 2021).

1.6.3 ROS in OA and cartilage

Oxygen tension of the joint is particularly relevant when considering ROS, as exposure of cartilage to high oxygen tension can induce formation of ROS. The oxygen tension surrounding articular chondrocytes is reported to be 6% in the superficial zone and 1% in the deep zone (Fermor B et al., 2007). Since articular cartilage is avascular, oxygen and nutrients must diffuse into the cartilage tissue from the synovial fluid surrounding the joint. The oxygen tension in synovial fluid is estimated to be 7-9% (Fermor B et al., 2007). Mobilization of the joint can increase the cartilage's oxygen supply. One group investigated the effects of oxygen tension on articular cartilage. Culturing cartilage explants at 5% O_2 significantly increased proteoglycan

and collagen synthesis compared to culturing at 20% O_2, but culturing at 1% O_2 showed decreased proteoglycan and collagen synthesis compared to culturing at 20% O_2 (Fermor B et al., 2004). These findings suggest that 5% O_2 maybe an optimal level of oxygen for cartilage matrix homeostasis. In vitro, hypoxia promoted the chondrogenic phenotype and cartilage matrix synthesis, indicating that the chondrocyte phenotype is oxygen sensitive (Henrotin Y et al., 2005). Cyclic loading or compression of cartilage could also enhance the diffusion and transport of nutrients towards the cartilage, affecting the metabolism and hence oxygen consumption of cartilage. (Murphy C., 2011)

Recent studies have cemented a role for oxidative stress and ROS in OA progression. Oxidative stress-related OA pathologies include disruption of cartilage signaling, chondrocyte senescence and apoptosis, mitochondrial dysfunction, cartilage degradation, synovial inflammation and subchondral bone dysfunction (Drevet S et al., 2018; Li D et al., 2012). These observations often correlated with an elevated profile of lipid peroxidation products such as oxidized low-density lipoprotein (ox-LDL), nitrite ($NO2^-$), nitrotyrosine, and nitrated ($NO3^-$) in the fluids and cartilage of OA patients and away animal models (Ostalowska A et al., 2006; Zahan O et al., 2020). A decrease in antioxidant systems has also been described in OA patients (Zahan O et al., 2020; Ostalowska A et al., 2006; Sakurai H et al., 1995).

ROS are produced at low concentrations in chondrocytes, with the primary source of ROS being NADPH oxidase (NOX) in the native tissue (Zahan O et

al., 2020). In unstimulated isolated human chondrocytes, the production of ROS was estimated to be 10 nmol of H_2O_2 per 10^6 cells (Henrotin Y et al., 1993). One study demonstrated that porcine articular chondrocytes could release ROS through an NADPH oxidase-like complex (Nemirovskiy O et al., 2009). Additionally, treatment of post-traumatic murine OA with selective NAPDH oxidase inhibitors or a *Nox4* total knockout showed reduced OA pathology (Wegner A et al., 2019).

Nitric oxide synthase (NOS) is an enzyme that catalyzes the production of free radical nitric oxide (NO) (Forstermann U et al., 2012). NOS expression can be induced by inflammatory cytokines and shear stress (Hiran T et al., 1997). *NOS* mRNA can be upregulated by NF-κB and MAPK pathways (Pelletier J et al., 2012). Excessive ROS and NO production deregulate the GSH antioxidant system and induces chondrocyte apoptosis. The proposed mechanisms by which ROS-induced apoptosis occurs include activation of caspase 3,9; regulation of PI3K/Akt, MAPK signaling pathways; and cyclooxygenase 2 (*COX2*)-induced prostaglandin E2 (PGE2) production (Beecher B et al., 2007; Palmer R et al., 1993; Notoya K et al., 2000; Yin W et al., 2009). H_2O_2 treatment of chondrocytes in vitro induces apoptosis in a dose-dependent manner (Mathy-Hartert et al., 2002). In vitro, administration of H_2O_2, or upregulation of endogenous superoxides, inhibited proteoglycan synthesis by suppressing mitochondrial oxidative phosphorylation (Zahan O et al., 2020). Both superoxide anions and NO are required for IL1-dependant inhibition of proteoglycan and collagen synthesis (Oh M et al., 1998). The

authors proposed that NO blocks collagen II biosynthesis by hydroxylation of proline residues on collagen II post-translationally (Oh M et al., 1998).

Mitochondrial dysfunction can perpetuate a harsh cycle of increased ROS and mitochondrial DNA damage, which are hallmarks of chronic degenerative diseases (Mao X et al., 2020). Depletion of superoxide dismutase 2 (SOD2), a major mitochondrial antioxidant protein, was found in early and end-stage OA cartilage (Scott J et al., 2010). This depletion of SOD2 also correlated with increase ROS production and collagenase expression in chondrocytes (Scott J et al., 2010). Another study showed that hypercholesterolemia promoted OA progression by mitochondrial dysfunction in chondrocytes, by stimulating ROS production and apoptosis (Farnaghi S et al., 2017). In a study using a rat OA model, administration of CoQ10 attenuated cartilage degeneration, suppressed inflammatory gene expression and demonstrated an antinociceptive effect (Lee J et al., 2013). Furthermore, blocking mitochondrial respiration, using inhibitors of mitochondrial complexes, attenuated collagen and proteoglycan synthesis in articular chondrocytes in vitro (Johnson K et al., 2000).

The relationship between ROS and pain is poorly understood. So far, it has been reported that H_2O_2 and $ONOO^-$ are involved in inflammation derived pain. (Pelletier J et al., 2000). Since NO is a known nociceptive signaling molecule, it may be worth investigating the relationship between NO abundance and pain in OA (Guingamp C et al., 1997)

ROS levels are subject to fluctuations upon mechanical stress in many cell types, including myocytes and endothelial cells (Zahan O et al., 2020). Chronic mechanical overloading was reported to stimulate NO production in articular chondrocytes in vivo and in vitro (Hashimoto S et al., 1998). Mechanically induced mitochondrial ROS stimulated ATP production in bovine osteochondral explants, that was suppressed by a mitochondrial-specific ROS scavenger, MitoQ (Wolff K et al., 2013). Taken together, mechanical forces can alter oxygen tension and release of ROS in cartilage, but the precise mechanisms of this requires further investigation.

1.7 IL1

The Interleukin-1 (IL1) family is a group of 11 cytokines, that can regulate and initiate a host of inflammatory responses in many cell types and tissues (Dinarello C et al., 2011). IL1α and IL1β are the two best studied cytokines as they were discovered first. IL1β was shown to be released by activated macrophages to activate T cells (Gery I et al., 1972). IL1α, then known as catabolin, was purified from synovium was noted for its ability to degrade cartilage (Saklatvala J et al., 1980). IL1α and IL1β are acidic and basic proteins respectively, both of which signal by binding to the high affinity IL1 receptor (IL1R) (Saklatvala J et al., 1986).

1.7.1 IL1 Mechanism of action

The current canonical mechanism for signaling of IL1 is as follows. IL1α and IL1β pro-proteins are retained in the cytoplasm. Pro-IL1β, but not pro-IL1α,

lacks biological activity and must first be catalyzed by caspase-1/ICE (IL1 converting enzyme). This allows IL1β to be secreted from the cell in its active form (Gross O et al., 2011). Mature IL1 ligands IL1α and IL1β bind to the extracellular domain of IL1 receptors (IL1Rs). A series of conserved cytosolic regions called Toll- and IL-1R–like (TIR) domains assemble the ligand-receptor-co-receptor trimeric complex and recruits two intracellular signaling proteins, myeloid differentiation primary response gene 88 (Myd88) and interleukin-1 receptor–activated protein kinase (IRAK). Next, tumor necrosis factor–associated factor (TRAF) 6, an ubiquitin E3 ligase, is recruited. TRAF6 and its binding partners attach K63-linked polyubiquitin chains to IRAK, adaptor proteins TAB2 and TAB3 (transforming growth factor beta activated protein kinase binding protein 2 and 3) and TAK1 (transforming growth factor beta activated kinase 1). NF-κB activation by IL1 involves upstream activation of the IKK complex. Activation of IKK phosphorylates IκB, causing its K^{48}-linked polyubiquitination and subsequent proteasomal degradation. IκB degradation facilitates nuclear translocation of the p50 and p65 NF-κB subunits to initiate gene expression (Weber A et al., 2010). IL1 signaling is conserved across many cell types and can also responds to stimulation by other cytokine family members such as IL-18 and IL-33 (Dinarello C et al., 2009). IL1 signals can also crosstalk with protein kinase C, Notch and Wnt pathways (Jenei-Lanzl Z et al., 2019).

IL1 signaling is transient and is terminated by a few mechanisms. Firstly, there is a naturally occurring IL-1 receptor antagonist (IL-1Ra), homologous to IL1α and IL1β, that competitively binds IL1Rs (Dinarello C., 1991). IL1R

binds to adaptor toll-interacting protein (TOLLIP) that inhibits IRAK and targets IL1R internalization into endosomes for proteolytic degradation. IL1 also possesses negative feedback loops to turn off IL1R signaling. p38-mediated phosphorylation of TAB1 deactivates TAK1 (Mendoza H et al., 2008), p65 NF-κB subunits mediates IκB synthesis that inhibits the NF-κB response (Sun S et al., 1993), expression of MAPK phosphatase 1 (MKP1) dephosphorylates MAPKs (Toh M et al., 2004).

1.7.2 IL1 in OA

Pro and anti-inflammatory cytokines have been implicated in the development of joint arthritides, such as OA (Dinarello C., 2011). As an inflammatory cytokine capable of tissue damage, IL1 has been widely used to treat cultured chondrocytes or synovial cells to mimic osteoarthritic characteristics in vitro (Goldring S et al., 2004). IL1 can induce the activity of matrix metalloproteinases (MMPs) and a disintegrin with thrombospondin motifs (ADAMTs) in vitro, mitochondrial dysfunction, inhibit proteoglycan synthesis and stimulate release of nitric oxide (Saklatvala J et al., 1980; Tyler J et al., 1985; Li T et al., 2022; Joosten L et al., 2004; Vaamonde-Garcia C et al., 2012). Intra-articular injection of IL1 causes loss of articular cartilage glycosaminoglycans (GAGs) and leads to plasma cell infiltration (Towle C et al., 1997). IL1 signaling and IL1R levels are increased in osteoarthritic chondrocytes (Ahmad R et al., 2007). Furthermore, superoxide radicals and hydrogen peroxide can mediate IL1-induced NF-κB activation (Mendes A et al., 2003).

Detection of IL1 in vivo has been a challenge because of difficulties in obtaining normal tissue as a control comparator. Furthermore, IL1 is present at very low concentrations and is not easily detected by conventional enzyme-linked immunosorbent assays or by higher-sensitivity assays such as the MesoScale Discovery platform (Watt F et al., 2016). Some have managed to detect IL1 in less than 1pM concentrations in OA synovial fluid and even lower concentrations in normal joints (Denoble A et al., 2011). Others have reported positive immunohistochemistry staining and presented in situ hybridization data for IL1α, IL1β in human OA cartilage (Moldovan F et al., 2000; Saha N et al., 1999). Interestingly, expression of IL1α and IL1β may not be the same in different stages of osteoarthritic cartilage. One study found that IL1α and IL1β expression in patients with severely degenerated cartilage was lower than that in mild or asymptomatic individuals (Towle C et al., 1997) and this was also seen in early microarray studies of OA cartilage (Fan Z et al., 2007).

The source of IL1 release is unclear as both cartilage and synovium can make IL1. One group were unable to show that OA cartilage explants released IL1β nor IL-18 (Bougault C et al., 2012). Our group demonstrated that cutting of articular cartilage activated inflammatory pathways and induced *IL1α* and *IL1β* mRNA (Gruber J et al., 2004). In the same study, active IL1α (presumed to be the pro-form) was also detectable in cartilage lysates (Gruber J et al., 2004). Increased *IL1β* and *IL1R1* mRNA was detected in synovial cells of collagenase-induced OA mouse joints compared to control joints (van Dalen S et al., 2017).

On paper, IL1 appears to be an excellent contender for a primary driver of OA, but little in vivo evidence supports this either in mice or in humans. IL1 appears to be a potent inducer of cartilage degradation in vitro, but IL1 data in pre-clinical mouse models did not show promising results. IL1β total KO, ICE (Interleukin-1 converting enzyme, also known as capsase-1) total KO and IL1α/IL1β double KO OA mouse models did not show reduced disease. If anything, there was a modest increase in disease instead (Clements K et al., 2003; Fukai A et al., 2012). In our group we have failed to see protection in IL1R total KO mice (unpublished data, Vincent group). There has been only one report (in a review article) of protection against OA in a IL1β total KO mouse, which saw a 40% reduction at the 8 weeks timepoint (Glasson S., 2017).

1.7.3 IL1 in human clinical studies

Randomized controlled trials in OA using IL1 targeting therapies have not been successful. An IL1α/IL1β dual neutralizing antibody for use in hand and knee OA failed to reach their primary endpoint due to lack of efficacy (Kloppenburg M et al., 2019; Fleischmann R et al., 2019). A clinical trial involving intra articular injection of anakinra (an interleukin-1 receptor antagonist (IL-1Ra) mimic) (Chevalier X et al., 2009) and another involving an IL1R neutralizing antibody also failed to meet the primary outcome (Cohen S et al., 2011).

1.8 Work that has led up to this thesis

1.8.1 All-trans retinoic acid suppression of mechanoflammation

In recent years, the Vincent lab has taken interest in the role of all-trans retinoic acid (atRA) in the cartilage injury response. This work was based on a genome-wide association study (GWAS) in an Icelandic discovery dataset of 2230 individuals. The GWAS was carried out to search for single nucleotide polymorphisms that conferred an increased risk of hand osteoarthritis. One significantly associated loci was found in the *ALDH1A2* gene, which was further supported by findings in replication datasets from the Netherlands and the UK (Styrkarsdottir U et al., 2014).

ALDH1A2 (aldehyde dehydrogenase 1 family, member A2) encodes the enzyme that catalyzes the formation of retinoic acid. atRA is synthesized from all-trans retinol (Vitamin A) and is metabolized by cytochrome P450 enzyme Cyp26. Functional studies for ALDH1A2 showed significantly lower levels of this gene in OA tissue compared to non-diseased tissue (Shepherd C et al., 2018). Our lab saw a reciprocal relationship between ALDH1A2 gene expression (or atRA bioavailability) and inflammatory genes (Zhu L et al., 2022). This effect was defined by a drop in atRA-response genes upon cartilage injury (Zhu L et al., 2022). This response was reversed using a retinoic acid metabolism blocking agent (RAMBA) talarazole, a Cyp26 inhibitor. Talarazole suppressed inflammatory genes in articular cartilage in a mouse knee joint destabilization model and reduced OA structural phenotype according to histological assessment (Zhu L et al., 2022). Furthermore, our group observed a link between atRA signaling and mechanoflammation and observed that the anti-inflammatory effects of atRA occur at the nucleus and

not at the level of signaling (Vincent group, unpublished data). Altogether, this provides compelling evidence that boosting atRA levels can suppress cartilage mechanoflammation and puts forward RAMBAs as potential disease modifying drugs for OA and highlights other potential mechano-inflammatory targets.

1.8.2 Generation of ROS in cartilage injury

My work for this thesis was built upon the findings of Dr Pragash Kamalathevan, a former DPhil student of the Vincent group. Kamalathevan investigated the involvement of atRA and ROS in the cartilage injury response.

Kamalathevan first showed that cellular and mitochondrial ROS were involved in driving the activation of TAK1 upon cartilage injury. He injected different commercial ROS inhibitors (NAC, NOXi, CoQ10) that target various sources of ROS and observed that all ROS inhibitors suppressed MAPK and TAK1 activation upon injury (Figure 1.5B). In particular, the injection of the mitochondrial ROS inhibitor CoQ10 had the least effect of inhibition on TAK1 (Figure 1.5B), suggesting that mitochondrial ROS generated upon injury enhances TAK1 in a positive feedback loop. Moreover, inflammatory gene upregulation upon cartilage injury was also suppressed using ROS inhibitors (Figure 1.5C).

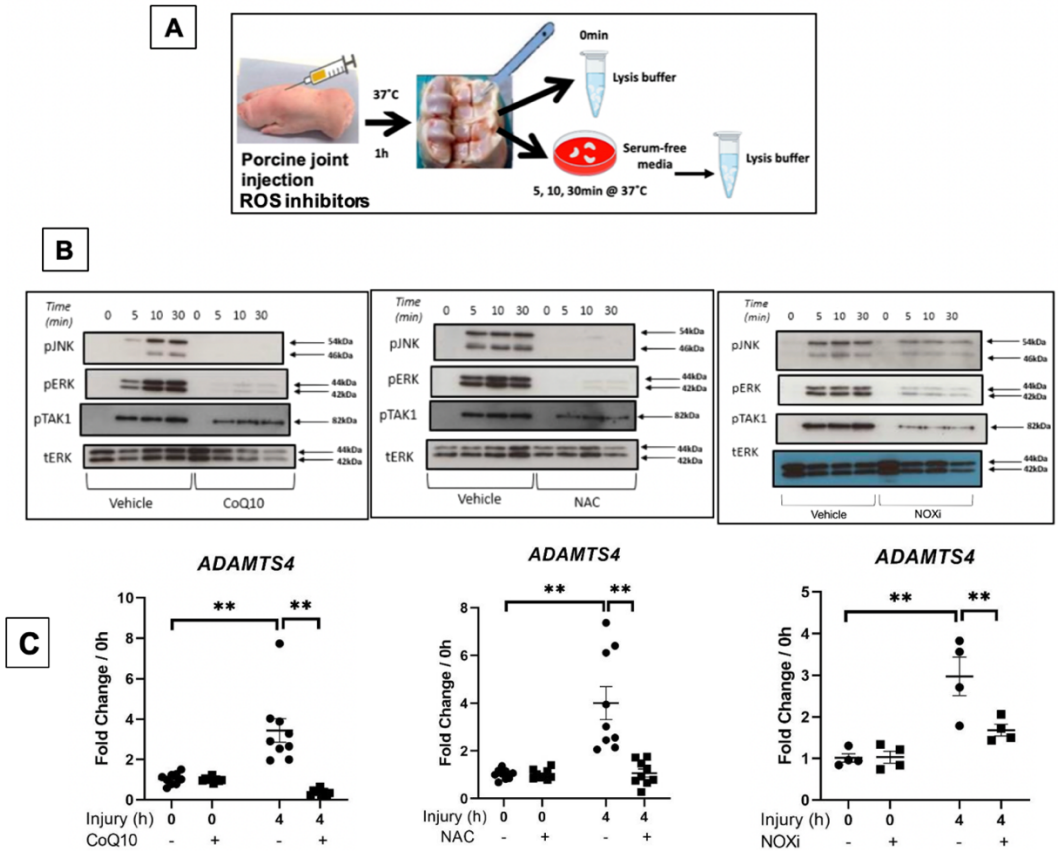

Figure 1.5: Inhibition of ROS suppresses MAPK activation and inflammatory gene upregulation upon cartilage injury (data from Dr Pragash Kamalathevan, Vincent group)

(A) Schematic showing the protocol for porcine MCP joint inhibitor injection. Porcine MCP joints were injected with commercial ROS inhibitors or vehicle. After 1h at 37°C, cartilage was explanted as described in Materials and Methods.

(B) Trotter MCP joints were pre-injected with commercial ROS inhibitors (CoQ10, NAC, NOXi) or vehicle prior to cartilage explantation. Explanted cartilage from ROS inhibitor or vehicle groups were used to create protein lysates for various periods of time (0min, 5min, 10min and 30min) at 37 °C, 5% CO2. Lysates were measured for pJNK, pERK, pTAK1 protein expression by SDS-PAGE and Western Blotting. Total ERK (tERK) was immunoblotted as the loading control

(C) Trotter MCP joints were pre-injected with ROS inhibitors prior to cartilage explantation. Cartilage explants were either snap frozen or incubated for 4 hours in serum free DMEM containing either ROS inhibitor or vehicle. RNA was extracted, converted to cDNA and RT-PCR was performed to measure expression for inflammatory genes (ADAMTS4 shown as example, as subjected to ROS inhibition). Bars show the mean ± SEM of 3 independent experiments. ∗ = $P < 0.05$; ∗∗ = $P < 0.01$, ns= not significant.

Dr Kamalathevan was first in our group to uncover a role for ASK1 in the cartilage injury response. Using an ASK1 inhibitor (serlonsertib) in the porcine trotter injury model (Figure 1.6A), he observed a decrease in ERK

and JNK MAPK activation, but TAK1 activation was unaffected (Figure 1.6B). This was paralleled with suppression of inflammatory gene upregulation post-injury (Figure 1.6C). In conjunction with key experiments shown in Figure 1.5, Dr Kamalathevan hypothesized that TAK1 was activating MAPKs indirectly by first inducing ROS production from the mitochondria and subsequent activation of ASK1.

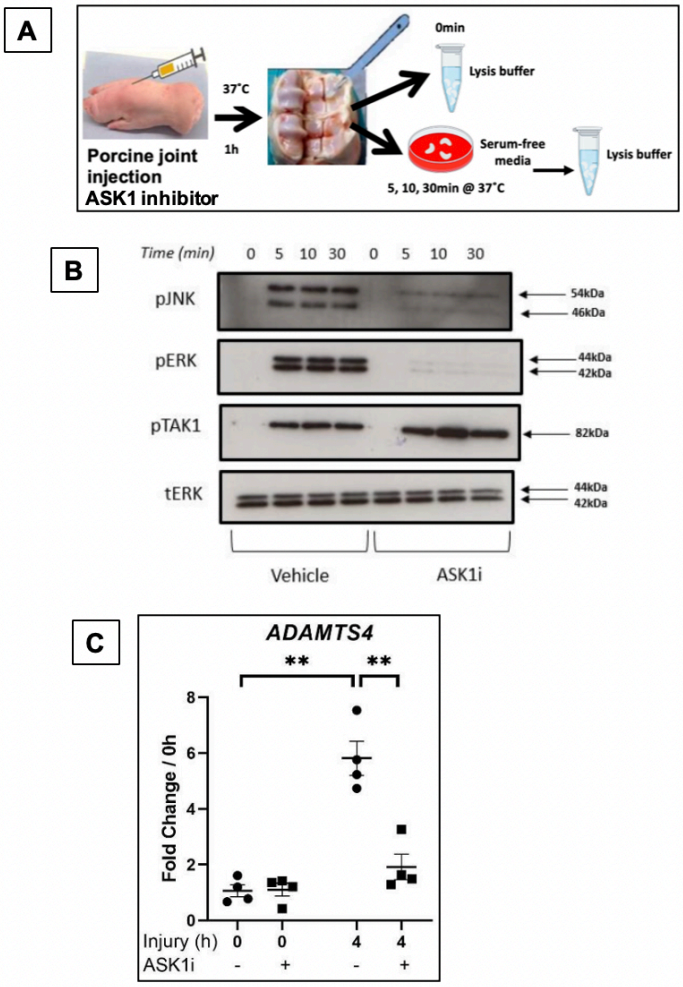

Figure 1.6: Inhibition of ASK1 suppresses MAPK activation and inflammatory gene upregulation upon cartilage injury (data from Dr Pragash Kamalathevan, Vincent group)

(A) Schematic showing the protocol for porcine MCP joint inhibitor injection. Porcine MCP joints were injected with ASK1 inhibitor (ASK1i) or vehicle. After 1h at 37 ^{O}C, cartilage was explanted as described in Materials and Methods.

(B) Trotter MCP joints were pre-injected with 10uM ASK1 inhibitor (ASK1i) prior to cartilage explantation. Explanted cartilage from ASK1i or vehicle groups were used to create protein lysates for various periods of time (0min, 5min, 10min and 30min)

at 37 °C, 5% CO2. Lysates were measured for pJNK, pERK, pTAK1 protein expression by SDS-PAGE and Western Blotting. Total ERK (tERK) was immunoblotted as the loading control
(C) Trotter MCP joints were pre-injected with 10uM ASK1 inhibitor (ASK1i) prior to cartilage explantation. Cartilage explants were either snap frozen or incubated for 4 hours in serum free DMEM containing either ASK1i or vehicle. RNA was extracted, converted to cDNA and RT-PCR was performed to measure expression for inflammatory genes (ADAMTS4 shown as example). Bars show the mean ± SEM of 3 independent experiments. $*$ = $P < 0.05$; $**$ = $P < 0.01$, ns= not significant.

Lastly, Kamalathevan also defined the atRA-dependent pathway that is activated upon injury, mediated upstream by cytosolic phospholipase A2 (cPLA2). cPLA2 is an enzyme that catalyzes arachidonic acid formation from polyunsaturated fatty acids (PUFAs) in the lipid bilayer (Sun G et al., 2021). Using the same porcine trotter injury model, he showed that cPLA2 is activated upon cartilage injury and cPLA2 activation is partially TAK1-dependant (Kamalethevan et al., unpublished data). Inhibition of cPLA2 prevented the downregulation of atRA-responsive genes on cartilage injury, meaning that inflammatory gene regulation on cartilage injury is cPLA2-dependent (Kamalethevan et al., unpublished data). Downstream mediators of arachidonic acid and cPLA2, such as 12/15 LOX and 4-HNE, were also strongly ROS dependent because it could be inhibited by a number of anti-oxidant treatments (Kamalethevan et al., unpublished data).

In summary, Kamalathevan characterized two mechanoflammatory pathways, one pathway which involves the TAK1-driven MAPK cascade, and another pathway involving the cPLA2-dependant regulation of atRA. The summary of these unpublished data is illustrated in Figure 1.7.

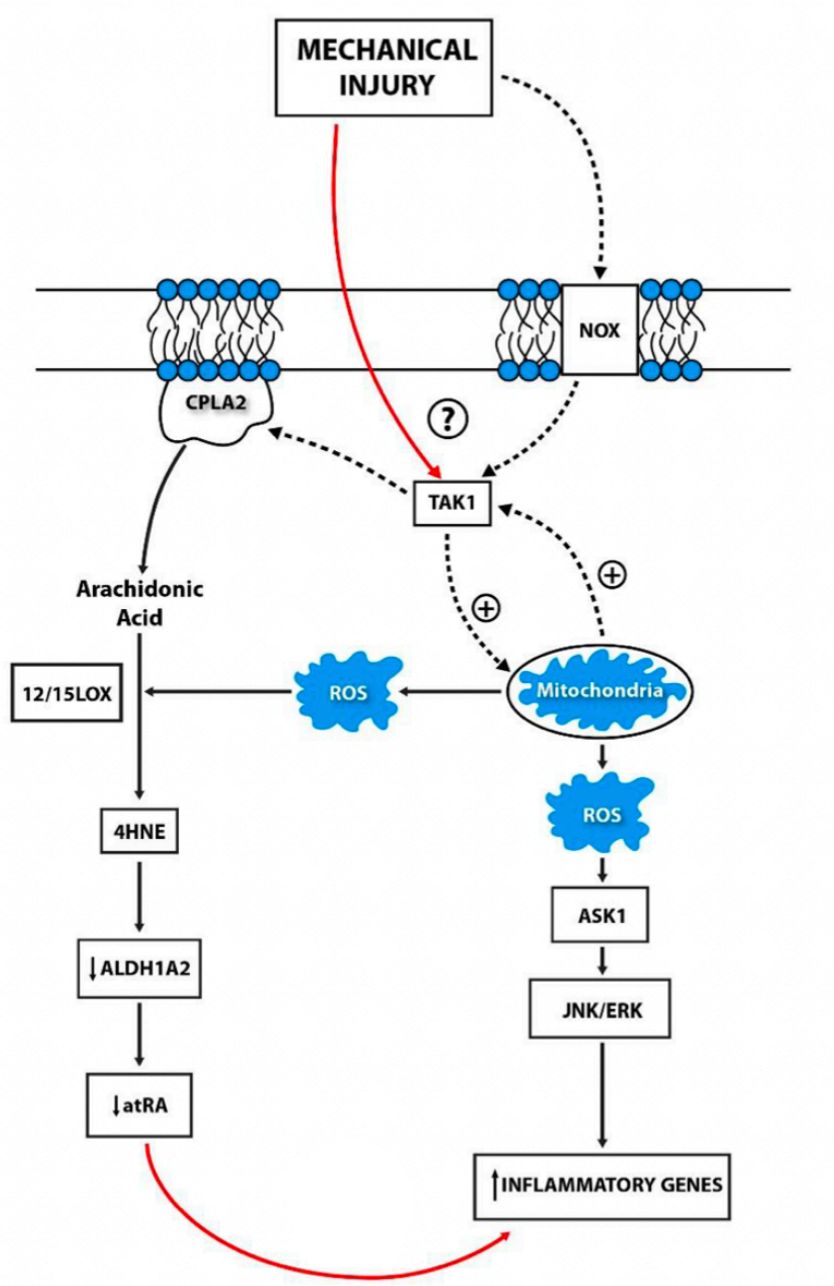

Figure 1.7: MAPK and atRA-dependant pathways of mechanoflammation (work by Dr Pragash Kamalathevan, Vincent group)
Mechanical injury downregulates all-trans-retinoic acid (atRA)-dependent genes in both a reactive oxygen species (ROS)-dependent and cytosolic phospholipase A2 (cPLA2)-dependent manner. Transforming growth factor activated-beta kinase 1 (TAK1) is responsible for partially phosphorylating cPLA2 on cartilage injury. The phosphorylation of cPLA2 on cartilage injury is also NOX-dependent and likely mediated via TAK1. It was yet to be determined what activated TAK1 on cartilage injury and whether TAK1 was acting upstream or downstream of mitochondrial/cellular derived ROS. Block red line = undetermined; block black line = full activation; dotted black line = partial activation.

1.9 Aims

Based on the results produced from Kamalathevan, a number of interesting questions arise. How is ASK1 activated upon cartilage injury? Can I measure phosphorylation of ASK1 after injury? What is the role of ASK1 in murine OA? I hypothesized that ASK1 is another mediator of the injury response and planned to study its mechanism of action upon cartilage injury, the dependency of ASK1 upon stimulation of chondrocytes with biochemical stresses and the role of ASK1 and related mechanoflammatory pathways in mouse models.

Therefore, my thesis is divided into three main aims:

1. To validate the acute signaling response in cartilage and explore tools for examining ASK1 activation in the tissue.
2. To address whether ASK1 is also an important pathway in ROS and IL1 driven responses in isolated chondrocytes
3. To address whether ASK1 inhibition and other related mechano-inflammatory pathways influence disease in vivo.

CHAPTER 2: MATERIALS AND METHODS

2.1 Cell culture

Porcine metacarpophalangeal (MCP) joints were disinfected in 2% Virkon for 10 minutes. MCP joints were opened and cartilage was explanted. Explanted cartilage was incubated in DMEM containing Collagenase A (25ml of 1mg/ml collagenase per trotter) (ThermoFisher Scientific, Massachusetts, USA) overnight at 37°C. Collagenase digest was washed by centrifugation at 25200 RCF for 5 minutes three times. Pellets were resuspended in Dulbecco's modified Eagle's medium (DMEM) containing 4.5 g/L of glucose and L-Glutamine (Lonza, Verviers, Belgium) and were supplemented with 10 % or 20% fetal bovine serum (FBS) (ThermoFisher Scientific, Massachusetts, USA), 1 % penicillin, streptomycin and amphotericin B (Gibco, NY, USA). Primary porcine chondrocytes were isolated from the collagenase digest and were used for cell culture. Primary chondrocytes were plated at a density of 2 million per well in each well of a 6-well plate in DMEM containing 10% or 20% FBS for 24 hours at 37°C, 5% CO_2. Primary chondrocytes were then serum starved by incubating for 24 hours in serum-free DMEM and then stimulated with either 100uM H2O2 or serum-free media as a vehicle control. After stimulation, primary chondrocytes were gently washed with ice-cold 1X sterile PBS and incubated with ice-cold 1X RIPA Buffer for 45 minutes, 4°C. Chondrocytes were harvested using a cell scraper and centrifuged at 18900 RCF, 4°C. Supernatant was collected and used to generate cell lysates for Western Blotting analysis.

2.2 Porcine trotter cartilage injury model

Freshly slaughtered 3-6 month old porcine forelimbs were ordered from the local abattoir. Porcine metacarpophalangeal (MCP) joints were disinfected in 2% Virkon for 10 minutes. The MCP joints were opened, rinsed with ice-cold 1X sterile PBS and cartilage was explanted. Explanted cartilage was either immediately cooled in ice-cold 1X RIPA Buffer (zero minute time point) or cultured in serum free DMEM for various periods of time (5 minutes, 10 minutes and 30 minutes) at 37 °C, 5% CO2 before being transferred to ice cold, 1X RIPA buffer. Explants with 1X RIPA buffer were mildly shaken for 45 minutes at 4°C to generate protein lysates for Western Blotting analysis.

2.3 Western Blotting

1X radioimmunoprecipitation assay (RIPA) buffer, was prepared from stock 10X RIPA Buffer (Abcam, Cambridge, UK). 1X RIPA buffer was supplemented with protease and phosphatase inhibitor cocktail (ThermoFisher Scientific, Massachusetts, USA). Porcine protein lysates containing 1X RIPA buffer was obtained as described in Materials and Methods.

Lysates were first reduced with Laemmli SDS sample buffer and 2-mercaptoethanol according to the manufacturer's instructions. Lysates were denatured at 95°C for 2 minutes, followed by sonication for 10 minutes at room temperature, and then denatured at 95°C for 2 minutes. Lysates were finally centrifuged at 18900 RCF, room temperature. Samples were resolved on hand-made 10% Sodium Dodecyl Sulphate-Polyacrylamide Gel (SDS-PAGE) in Tris-Glycine buffer conditions. Gel was transferred to poly (vinylidene) (PVDF) membranes (ThermoFisher Scientific, Massachusetts, USA). PVDF membrane was blocked in 5% skim milk powder dissolved in 1X

tris-buffered saline with 0.1% Tween-20 detergent (TBST) for 1 hour at room temperature. Membrane was incubated overnight in primary antibody at 4°C, washed 3 times 10 minutes each for a total of 30 minutes in 1X TBST and incubated for a further hour in 1:2000 secondary antibody. Membrane was further washed 3 times 10 minutes each for a total of 30 minutes in 1X TBST. Blots were developed by the use of chemiluminescence ECL reagent (Sigma-Aldrich, St. Louis, Missouri, USA) and subsequently visualised using autoradiography films (Cytiva, Malborough, USA). The blot was stripped using 1X ReBlot stripping solution (Merck, New Jersey, USA), re-blocked in 5% milk in 1X TBST and then re-probed for GAPDH or beta-actin as the loading control. The quantitication of at least three separate biological replicate experiments was performed using FIJI-App, ImageJ-win64 Gel Analysis software and normalised to loading control GAPDH or beta-actin.

2.4 List of antibodies used for western blot work

Table 2.1 List of western blotting antibodies

Antibody	**Species**	**Catalog Number**	**Dilution**	**Provider**
Phospho-P38 (pP38)	Rabbit	9211S	1:1000	Cell Signalling Technology (Massachusetts, USA)
Phospho-p44/42 (pERK)	Rabbit	4370	1:1000	Cell Signalling Technology (Massachusetts, USA)

Phospho-SAPK/JNK (pJNK)	Rabbit	9251S	1:1000	Cell Signalling Technology (Massachusetts, USA)
IkBα	Mouse	4814	1:500	Cell Signalling Technology (Massachusetts, USA)
Phospho-YAP (pYAP)	Rabbit	4911	1:1000	Cell Signalling Technology (Massachusetts, USA)
Phospho-ASK1 (pASK1)	Rabbit	PA5-64541	1:500	ThermoFisher Scientific, Massachusetts, USA
Phospho-ASK1 (pASK1)	Rabbit	3765	1:500	Cell Signalling Technology (Massachusetts, USA)
ASK1	Rabbit	8862	1:500	Cell Signalling Technology (Massachusetts, USA)
ASK1	Rabbit	3762	1:500	Cell Signalling Technology (Massachusetts, USA)

ASK1	Mouse	sc-5294	1:500	Santa Cruz Biotechnology (Dallas, USA)
GAPDH	Rabbit	2118	1:2000	Cell Signalling Technology (Massachusetts, USA)
Beta actin	Mouse	4697	1:6000	Cell Signalling Technology (Massachusetts, USA)
Goat anti-Rabbit Secondary Antibody, HRP	Goat	31460	1:2000	ThermoFisher Scientific, (Massachusetts, USA)
Rabbit Anti-Mouse Secondary Antibody, HRP	Rabbit	P0260	1:2000	Dako, Agilent Technologies (Santa Clara, USA)

2.5 Immunoprecipitation

Immunoprecipitation was performed using Dynabeads™ Protein G Immunoprecipitation Kit (ThermoFisher Scientific, Massachusetts, USA) according to the manufacturer's instructions. 100 µl of protein lysate was mixed with 50 µl of Protein G beads and 5 µl antibody. A non-protein-specific isotype antibody was also used for immunoprecipitation as a negative control. Samples were rotated overnight at 4°C. Beads were subjected to

SDS-PAGE and Western Blotting analysis for assessment of immunoprecipitation.

2.6 Protein Kinase Assay

Protein G beads containing immunosorbed protein kinase, were assayed for protein kinase activity using the Universal Kinase Assay Kit (Fluorometric) (Abcam, Cambridge, UK). Briefly, 20 µl of protein kinase eluted from Protein G beads was mixed with 20 µl ADP Sensor Buffer and 10 µl ADP Sensor to create a 50 µl reaction mixture. Reaction mixtures were pipetted on 96-well solid black flat-bottom microplates (Corning, New York, USA). Fluorescence intensity was measured using the FLUOstar Omega plate reader (BMG Labtech, Ortenberg, Germany) on Omega software (version 5.10 R2), at an excitation/emission wavelength of 544/590 nm respectively.

2.7 RNA extraction from murine cartilage

RNA extraction was performed using the RNeasy Micro Kit (Qiagen, Hilden, Germany). Snap-frozen cartilage was pulverized into fine powder using a mortar and pestle in liquid nitrogen.
Four murine hip caps were pooled and suspended in 150 µl Buffer RLT. RNA was extracted following the manufacturer's instructions. RNA concentration was quantified using a Nanodrop machine and RNA purity was estimated by 260:280 nm wavelength ratio of approximately 2.0.

2.8 cDNA synthesis (Reverse Transcription)

Complementary DNA (cDNA) was generated from RNA using a High-Capacity cDNA Reverse Transcription kit (ThermoFisher Scientific, Massachusetts, USA) according to the manufacturer's instructions.

2.9 TaqMan microfluidic gene array

TaqMan Low-Density Array (TLDA) microfluidic cards were custom designed and ordered from Applied Biosystems. TLDA cards were run on a ViiA™ 7 Real-Time PCR System (Applied Biosystems) thermocycler. Each sample was amplified using commercial TaqMan probes used listed in Table 2.2. Expression of genes was normalised to 18s as a housekeeping control.

Table 2.2 Microfluidic TaqMan array gene list

GENE	GENE NAME	TAQMAN ASSAY ID
18S	Eukaryotic 18S rRNA	Hs99999901_s1
Adamts4	a disintegrin-like and metallopeptidase (reprolysin type) with thrombospondin type 1 motif, 4	Mm00556068_m1
Adamts5	a disintegrin-like and metallopeptidase (reprolysin type) with thrombospondin type 1 motif, 5 (aggrecanase-2)	Mm00478620_m1
Ccl2	chemokine (C-C motif) ligand 2	Mm00441242_m1
Cyp26a1	cytochrome P450, family 26, subfamily a, polypeptide 1	Mm00514486_m1
Cyp26b1	cytochrome P450, family 26, subfamily b, polypeptide 1	Mm00558507_m1

Hoxa4	homeobox A4	Mm01335255_g1
Il6-	interleukin 6	Mm00446190_m1
Il1β	interleukin 1 beta	Mm00434228_m1
Mmp3	matrix metallopeptidase 3	Mm00440295_m1
Ngf	nerve growth factor	Mm00443039_m1
Ptgs2	prostaglandin-endoperoxide synthase 2	Mm00478374_m1
Rara	retinoic acid receptor, alpha	Mm01296312_m1
Rarb	retinoic acid receptor, beta	Mm01319677_m1
Rarg	retinoic acid receptor, gamma	Mm00441091_m1
Timp1	tissue inhibitor of metalloproteinase 1	Mm00441818_m1

2.10 Mice

Animals were housed in the approved animal care facilities at the Kennedy Institute of Rheumatology Biological Services Unit, in compliance with care and usage protocols. Standard individually ventilated cages were used to house 4-6 mice per cage at 21°C, maintained under a 12 hour light/dark

cycle. Mice were fed a certified mouse diet (RM3, Special Dietary Systems) and water ad libitum. C57BL/6 mice were purchased from Harlan UK.

2.10.1 Surgeries

Animal surgeries were performed by trained personnel, Jadwiga Zarebska at the Kennedy Institute of Rheumatology. Before surgery, mice were anesthetized by inhalation of isoflurane (3% induction and 1.5-2% maintenance) in 1.5-2 L/min O_2 and given a subcutaneous injection of buprenorphine (Vetergesic; Alstoe Animal Health). Mice were fully mobile 5 minutes after withdrawal of isoflurane.

2.10.2 Partial medial meniscectomy model

Partial meniscectomy (PMX) surgery was performed for surgical induction of osteoarthritis. PMX or sham surgery was performed in 10-week old C57BL/6 male mice. Joints were collected 24 days after surgery. Female mice were not assessed in this study because they typically have substantially lower disease scores. PMX surgery was conducted on the right leg of mice, where surgical procedures were followed as previously described (Vincent et al., 2020).

2.10.3 ASK1 inhibitor

15 week old male C57BL/6 mice received ASK1 inhibitor (GS-4997, MedChem Express) or vehicle by gavage daily for 28 days after PMX surgery. ASK1 inhibitor was dissolved in DMSO, PEG 400 (polyethylene glycol, molecular weight 400) and PBS to a daily dosage of 10 mg/kg.

2.10.4 Modified Diet

Mice were fed the modified (completely deuterated arachidonic acid, AIN93 low fat) and (normal arachidonic acid) control diets from weaning at 3-4 weeks old. PMX was performed at 10 weeks old and the mice were culled after 6 weeks and knees were collected for histological processing. Modified diets were acquired from Kristina Zec, University of Oxford.

2.10.5 JNK2 KO

JNK2$^{-/-}$ mice (also known as MAPK9$^{-/-}$) were performed on C57BL/6 background.

2.10.6 Avulsion of hip cartilage

Mice (4-6 weeks old) were culled by cervical dislocation, and the acetabulofemoral joint was exposed by blunt dislocation. The cartilaginous femoral epiphysis was avulsed using forceps, as described previously (Chong K et al., 2013). Epiphyseal cartilage was immediately snap frozen (timepoint 0) or rested for 4 hours in serum free media and then snap frozen at -80°C.

2.11 Histology

Paraffin embedded tissue was processed and embedded by the histology department at the Kennedy Institute of Rheumatology. Dissected murine knee joints were fixed in 10% formalin, decalcified in formic acid and embedded in paraffin. Coronal sections were cut through the whole joint, producing 4 µm thick sections at 80 µm intervals. Sections were stained with Safranin O.

2.11.1 Histological assessment of OA

Severity of cartilage destruction was assessed by a modified Osteoarthritis Research Society International (OARSI) grading system by two blinded, independent scorers. Two independent scorers graded the coronal knee sections using a semi-quantitative scoring system (0 - Normal; 0.5 - Loss of proteoglycans (Safranin O staining) without structural changes; 1 - Superficial fibrillation without loss of cartilage; 2 - Loss of superficial cartilage; 3 - Cartilage delamination at the tidemark; 5 - Loss of tissue extending into the calcified cartilage; 6 - Loss of tissue extending into subchondral bone). For each joint, at least eight sections were assessed in their tibial and femoral surfaces for both medial and lateral compartments (resulting in four subscores per section). These four subscores were summed to produce a final summed score per section. The three highest summed scores of one joint were added together to generate a final score for the joint.

Osteophyte severity was assessed by an osteophyte scoring system. Osteophytes scores were given for osteophyte size (0 = none, 1 = small ~ the same thickness as the adjacent cartilage, 2 = medium ~ 1–3 × the thickness as the adjacent cartilage, 3 = large >3 × the thickness as the adjacent cartilage), osteophyte maturity (0 = none, 1 = predominantly cartilaginous, 2 = mixed cartilage and bone with active vascular invasion and endochondral ossification, 3 = predominantly bone), and articular staining of the tibia surface adjacent to osteophyte (0 = no loss of staining, 0.5 = patches of loss of staining, 1 = total loss of Safranin-O staining). A summed osteophyte score was calculated for each osteophyte measurement per anterior-medial section. A total of 4 sections per knee scored from middle of joint with distinct triangle menisci. Osteophyte scoring system was adapted from Little et al (Little C et al., 2009).

2.12 Statistical Analysis

Statistical analysis was performed using Prism 9 (GraphPad Software Inc, USA). Degree of significance was calculated and reported as in a p-value format ($p \geq 0.05$: (ns), $p \leq 0.05$: (*), $p \leq 0.01$ (**), $p \leq 0.001$ (***), $p \leq 0.0001$ (****)). An unpaired t-test was performed to compare two distinct sets of measurements. Experiments that included three or more groups of data were analysed a one-way ANOVA. A two-way ANOVA was performed when two independent variables were considered in three or more groups of data. Multiple comparisons analyses was performed via a Tukey's range test which compared the means of each group.

2.13 List of reagents

Table 2.3 List of reagents

Reagent	Catalog Number	Provider
2-Mercaptoethanol	21985023	ThermoFisher Scientific (Massachusetts, USA)
30% Hydrogen Peroxide solution	Q18755	ThermoFisher Scientific (Massachusetts, USA)
Amphotericin B	15290018	ThermoFisher Scientific (Massachusetts, USA)
Collagenase A	10103586001	Sigma-Aldrich (St. Louis, Missouri, USA)

Corning 96-well Solid Black Flat Bottom Polystyrene TC-treated Microplates	3916	Corning (New York, USA)
DMEM, high glucose, pyruvate	41966-029	ThermoFisher Scientific (Massachusetts, USA)
Fetal Bovine Serum	F9665	Sigma-Aldrich (St. Louis, Missouri, USA)
Halt™ Protease Inhibitor Cocktail (100X)	78429	ThermoFisher Scientific (Massachusetts, USA)
Laemmli SDS sample buffer	1610747	Bio-Rad (California, United States)
Penicillin-Streptomycin	11548876	ThermoFisher Scientific (Massachusetts, USA)
Porcine TGF-beta 1 Protein (carrier free)	101-B1/CF	R&D Systems, Bio-Techne (Minneapolis, USA)
Proteasome Inhibitor I	539160	Sigma-Aldrich (St. Louis, Missouri, USA)
Protein G Immunoprecipitation Kit	10007D	ThermoFisher Scientific (Massachusetts, USA)
ReBlot Plus Strong Antibody Stripping Solution	2504	Merck (Darmstadt, Germany)
Recombinant Human IL-1α	200-01A	PeproTech (London, UK)

Recombinant Human IL-1β	200-01B	PeproTech (London, UK)
RIPA Lysis and Extraction Buffer	89900	ThermoFisher Scientific (Massachusetts, USA)
Serlonsertib (ASK1 inhibitor)	GS-4997	MedChem Express (Monmouth Junction, USA)
Talarozole (TLZ)	HY-14531-10	MedChem Express (Monmouth Junction, USA)
Universal Kinase Assay Kit (Fluorometric)	ab138879	Abcam (Cambridge, United Kingdom)

CHAPTER 3: DETERMINING THE ACUTE SIGNALING EVENTS ACTIVATED UPON CARTILAGE INJURY

Introduction

Articular cartilage in a joint is mechanosensitive and can respond to mechanical and biochemical signals, which play roles to maintain cartilage homeostasis and further OA. The principal catabolic process in OA is mechanoflammation. Mechanoflammation is described as the activation downstream inflammatory signaling that leads to production of matrix-degrading proteases and consequent cartilage breakdown upon cartilage injury. Cartilage injury also activates anabolic processes involved in repair, regeneration, and chondroprotection. These are largely driven by the release of sequestered growth factors from the cartilage pericellular matrix upon injury. Since mechanical injury is a key hallmark of OA, our lab has researched extensively into the cartilage injury response.

Our lab has previously shown that cartilage injury by cutting/explantation using the porcine trotter model activates the MAPK signalling cascade (Ismail H et al., 2017, Vincent T et al., 2002, Vincent T et al., 2019). The MAP3K, TAK1, is activated upon cartilage injury and subsequently activates downstream MAPK pathways (ERK, JNK and p38) and NF-κB signaling (Ismail H et al., 2017, Vincent T et al., 2002, Vincent T et al., 2019). The upstream mediator of TAK1 is not known but it is believed to be neither soluble nor secreted upon cartilage injury (Ismail H et al., 2017). As the role of ASK1 upon cartilage injury had not been directly investigated before, I hypothesised that ASK1 is another MAPK mediator activated upon injury and

determined the mechanism of action for ASK1 activation in the cartilage injury response.

3.1 Mitogen-activated protein kinases (MAPKs) and NF-κB signaling are activated upon cartilage injury

First, I validated previous findings from the lab showing the activation of MAPKs and NF-κB signaling cascades upon cartilage injury.

Porcine cartilage injury lysates were generated at 0 minutes, 5 minutes, 10 minutes and 30 minutes post cartilage injury. Lysates were immunoblotted for phospho-p38, phospho-ERK, phospho-JNK and IκBα. β-actin or GAPDH was immunoblotted as the loading control. Quantitication of at least three separate experiments was performed using FIJI-App, ImageJ Gel Analysis software. Results were normalized to β-actin or GAPDH and statistical significance of comparison between groups analyzed by a one-way ANOVA.

The MAPKs p38, ERK and JNK were not phosphorylated in native cartilage (0 minutes) but were all rapidly phosphorylated at 5 minutes post cartilage injury, which lasted up to 30 minutes post injury (Figure 3.1A). IκBα expression decreased at 5 minutes post cartilage injury (0.5-fold compared to 0 minutes, $p<0.05$), which recovered between 10 and 30 minutes, indicative of IkBα degradation and activation of the canonical NF-κB pathway (Figure 3.1B). Quantitication of at least three independent biological replicates is shown for each pathway in Figure 3.1C.

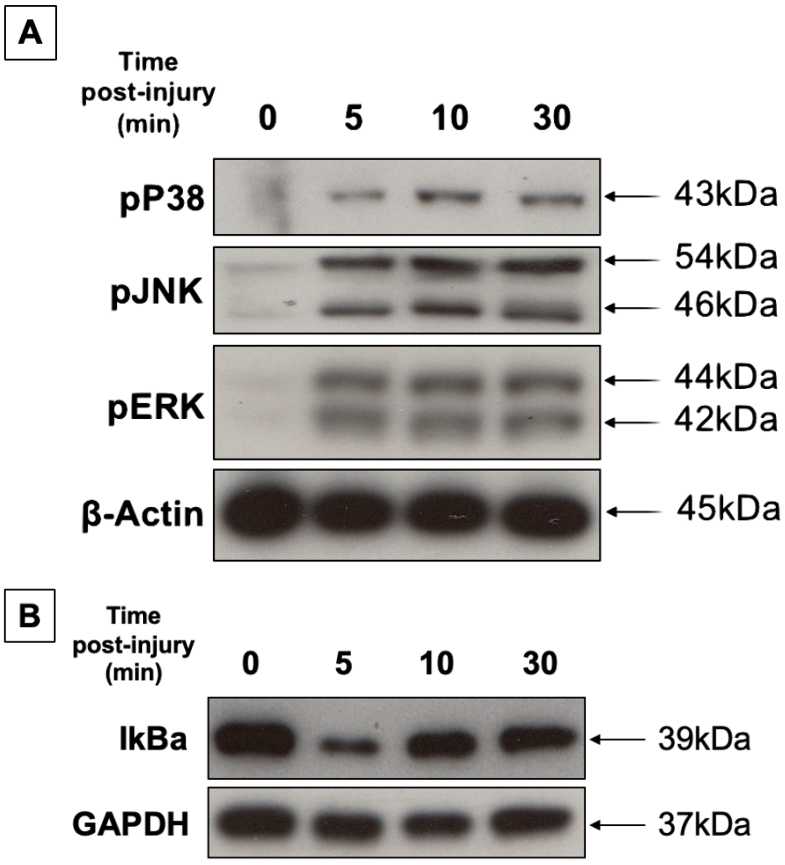
A
Time post-injury (min)
0
5
10
30
pP38
43kDa
pJNK
54kDa
46kDa
pERK
44kDa
42kDa
β-Actin
45kDa
B
Time post-injury (min)
0
5
10
30
IkBa
39kDa
GAPDH
37kDa

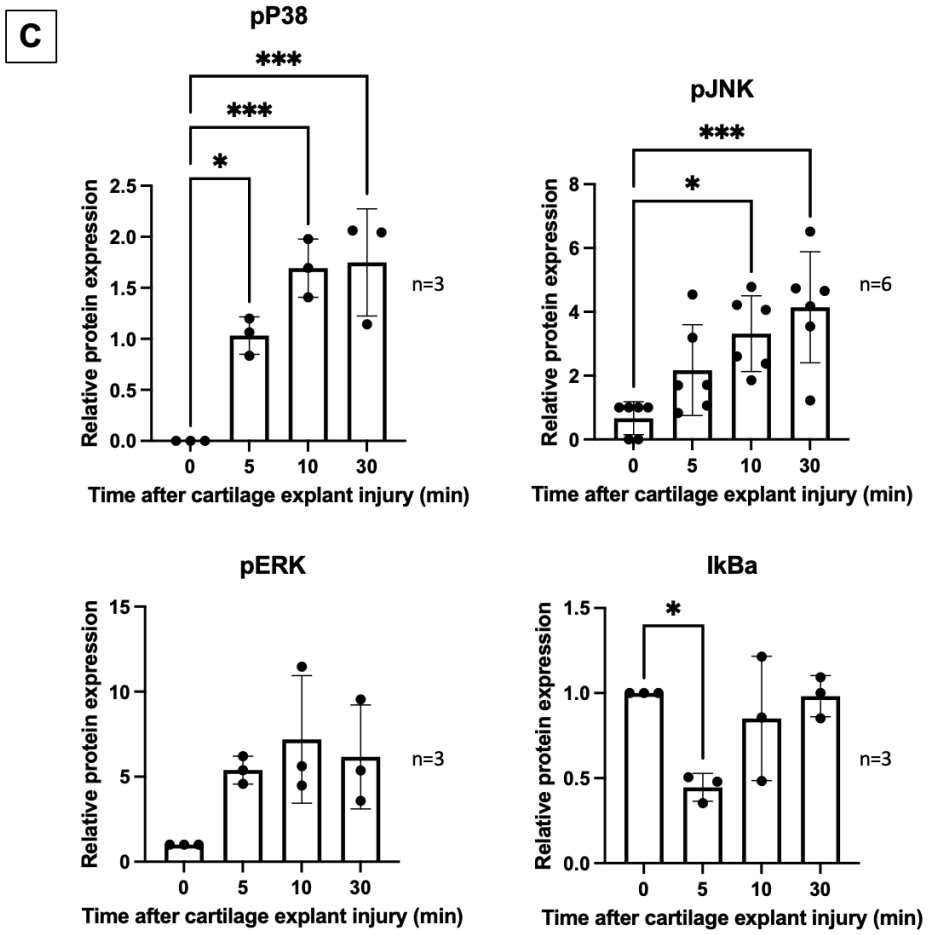

Figure 3.1: Mitogen-activated protein kinases (MAPKs) and NF-κB signaling are activated upon cartilage injury

Porcine metacarpophalangeal (MCP) joints were decontaminated in 2% Virkon for 15 minutes. MCP joints were opened and cartilage was rapidly explanted into ice cold 1X RIPA Buffer (0min) or cultured for various periods of time after explanation (5min, 10min and 30min) in serum free DMEM at 37°C, 5% CO2 before being transferred to ice cold, 1X RIPA buffer. Explants with 1X RIPA buffer, were mildly shaken for 45 minutes at 4°C. Lysates were run on 10% Sodium Dodecyl Sulphate-Polyacrylamide Gel (SDS-PAGE) and transferred to polyvinylidene (PVDF) membrane. PVDF membrane was blocked in 5% milk for 1hour at room temperature, incubated overnight in 1:1000 primary antibody ((A) pP38, pJNK, pERK, (B) IκBa), washed 3 times in 1X TBST and incubate for 1 hour in 1:2000 secondary antibody. Protein signal was enhanced by chemiluminescence and visualised using autoradiography. Blots were stripped and re-probed for β-actin or GAPDH as the loading control.

(C) Quantitication of at least three independent biological replicates was performed using ImageJ and normalised to β-actin or GAPDH. * = $p<0.05$; ** = $p<0.01$; *** = $p<0.001$.

3.2 YAP is dephosphorylated upon cartilage injury

Earlier, I showed that MAPKs and NF-κB signaling are activated upon cartilage injury. YAP is another factor that plays a role in cartilage, notably chondrocyte differentiation and overall cartilage protection. Our lab has recently taken interest in researching the role of YAP in cartilage, especially if the reparative properties of YAP are switched on upon cartilage injury. Of note, YAP and TAK1 have been reported to reciprocally inhibit each other in chondrocytes upon cytokine stimulation (Deng Y et al., 2018). Given the potential link to TAK1 and MAPK signaling upon cartilage injury, I determined if YAP signaling is activated upon cartilage injury.

To determine if YAP is activated upon cartilage injury, I used the porcine cartilage injury model as previously described. Porcine cartilage injury lysates were generated at 0 minutes, 5 mins, 10 mins and 30 mins post cartilage injury. Lysates were immunoblotted for phospho-YAP. β-actin was blotted as the loading control. Quantitication at least three separate experiments was performed using FIJI-App, ImageJ Gel Analysis software. Results were normalized to β-actin and statistical significance of comparison between groups analyzed by a one-way ANOVA.

YAP is initially phosphorylated at 0 minutes but loses phosphorylation over time. At 5 minutes, phosphorylation is approximately 0.25-fold compared to 0 minutes. At 10 to 30 minutes, YAP is phosphorylation was completely abolished ($p<0.0001$) (Figure 3.2).

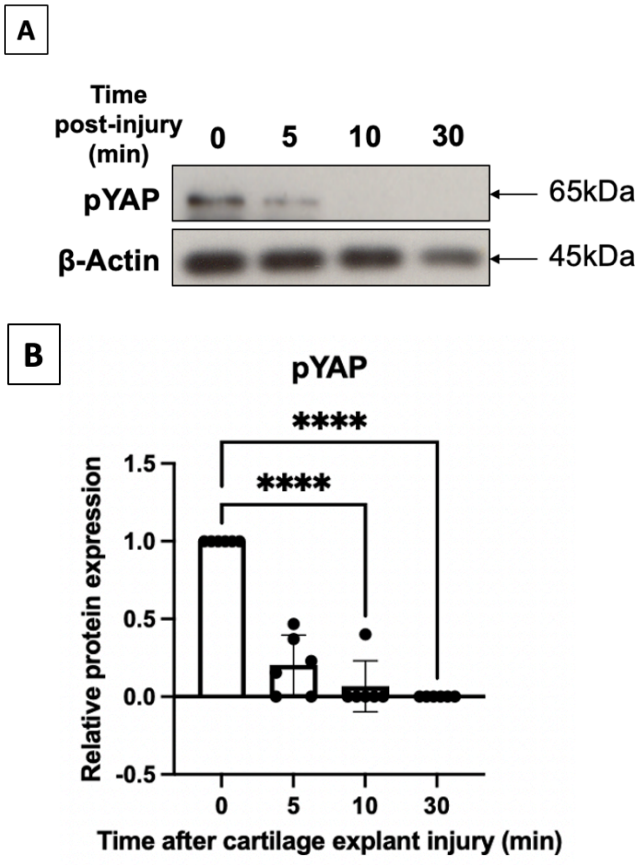

Figure 3.2: YAP is dephosphorylated upon cartilage injury
(A) Porcine metacarpophalangeal (MCP) joints were decontaminated in 2% Virkon for 15 minutes. MCP joints were opened and cartilage was rapidly explanted into ice cold 1X RIPA Buffer (0min) or cultured for various periods of time after explanation (5min, 10min and 30min) in serum free DMEM at 37°C, 5% CO2 before being transferred to ice cold, 1X RIPA buffer. Explants with 1X RIPA buffer, were mildly shaken for 45 minutes at 4°C. Lysates were run on 10% Sodium Dodecyl Sulphate-Polyacrylamide Gel (SDS-PAGE) and transferred to polyvinylidene (PVDF) membrane. PVDF membrane was blocked in 5% milk for 1 hour at room temperature, incubated overnight in 1:1000 with a phospho-YAP (Ser127) primary antibody, washed 3 times in 1X TBST and incubate for 1 hour in 1:2000 secondary antibody. Protein signal was enhanced by chemiluminescence and visualised using autoradiography. Blots were stripped and re-probed for β-actin as the loading control.
(B) Quantitication of at least three independent biological replicates was performed using ImageJ and normalised to β-actin. * = $p<0.05$; ** = $p<0.01$; *** = $p<0.001$.

3.3 ASK1 is phosphorylated and accumulates upon cartilage injury

Next, porcine cartilage injury lysates were generated at 0 minutes, 5 minutes, 10 minutes and 30 minutes post cartilage injury to explore ASK1 activation. Lysates were immunoblotted for phospho-ASK1 or ASK1 total protein. β-actin was immunoblotted as the loading control. Quantitication at least three separate experiments was performed using FIJI-App, ImageJ Gel Analysis software. Results were normalized to β-actin and statistical significance of comparison between groups analyzed by a one-way ANOVA.

ASK1 was not phosphorylated at 0 minutes but was phosphorylated at 5 to 10 minutes post cartilage injury (approximately 1.5-2 fold), which had decreased by 30 minutes post injury. This antibody, which is the best validated from the published literature was not robust, so although there was a trend to increase phosphorylation of ASK1 in three biological replicates (Figure 3.3A), these did not reach statistical significance (Figure 3.3B).

I also observed total ASK1 appeared to increase in a time-dependant manner post injury. There was an approximately 4-fold increase of ASK1 at 30 minutes compared to 0 minutes ($p<0.001$) (Figure 3.3C), with robust quantitication in nine biological replicates (Figure 3.3D).

These results suggested that ASK1 was phosphorylated (activated) upon cartilage injury by directly detecting phosphorylated ASK1 in cartilage injury lysates. ASK1 appeared transiently phosphorylated at 5 to 10 minutes post injury, which had not been shown before, but this response was difficult to reproduce in a robust manner.

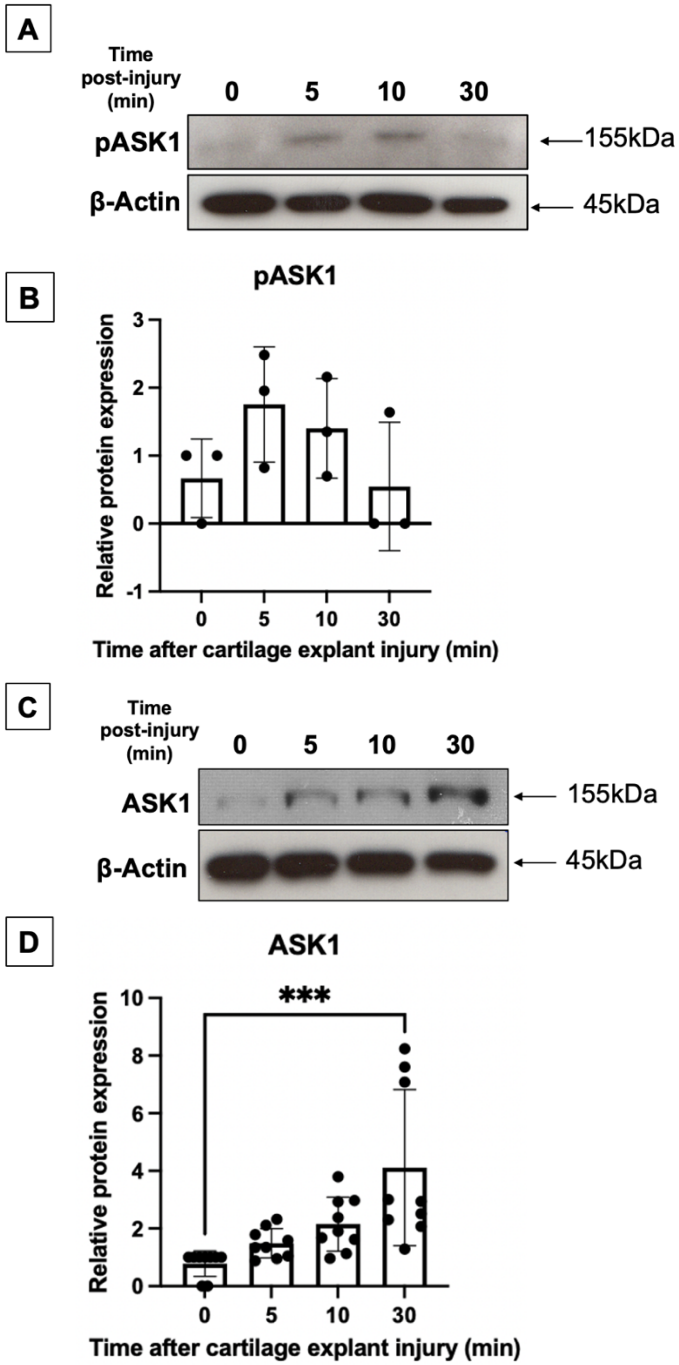

Figure 3.3: ASK1 is phosphorylated and accumulates upon cartilage injury
Porcine metacarpophalangeal (MCP) joints were decontaminated in 2% Virkon for 15 minutes. MCP joints were opened and cartilage was rapidly explanted into ice cold 1X RIPA Buffer (0min) or cultured for various periods of time after explanation (5min, 10min and 30min) in serum free DMEM at 37°C, 5% CO2 before being transferred to ice cold, 1X RIPA buffer. Explants with 1X RIPA buffer, were mildly shaken for 45 minutes at 4°C. Lysates were run on 10% Sodium Dodecyl Sulphate-Polyacrylamide Gel (SDS-PAGE) and transferred to polyvinylidene (PVDF) membrane. PVDF membrane was blocked in 5% milk for 1hour at room

temperature, incubated overnight in 1:1000 with (A) phospho-ASK1 (Thr838) or (C) total ASK1 primary antibody, washed 3 times in 1X TBST and incubate for 1 hour in 1:2000 secondary antibody. Protein signal was enhanced by chemiluminescence and visualised using autoradiography. Blots were stripped and re-probed for β-actin as the loading control.
(B,D) Quantitication of at least three independent biological replicates was performed using ImageJ and normalised to β-actin. * = $p<0.05$; ** = $p<0.01$; *** = $p<0.001$.

3.4 Determining the mechanism of ASK1 accumulation upon cartilage injury

3.4.1 ASK1 accumulation is suppressed when its phosphorylation is inhibited

To perform this, I first injected an ASK1 inhibitor (ASK1i), serlonsertib, into the porcine cartilage injury model. Serlonsertib is a clinical stage ASK1 inhibitor (up to Phase 3 clinical trials) that has been used in experimental treatment for diabetic nephropathy and kidney fibrosis (Lin J et al., 2015). Mechanistically, serlonsertib has been reported to compete with ATP in the ASK1 catalytic kinase domain, thereby inhibiting ASK1 phosphorylation (Lin J et al., 2015). I hypothesized that inhibiting phosphorylation of ASK1, using serlonsertib, would prevent the accumulation of ASK1 after cartilage injury.

I preinjected porcine MCP joints with either 10 μM ASK1i or vehicle control. Injured cartilage explants were incubated for various timepoints in serum-free media containing either ASK1i or vehicle. Lysates were extracted and immunoblotted for ASK1. β-actin was immunoblotted as the loading control. Quantitication at least three separate experiments was performed using FIJI-App, ImageJ Gel Analysis software. Results were normalized to β-actin and statistical significance of comparison between groups analyzed by a two-way ANOVA, with post hoc multiple comparisons corrected using Tukey's tests.

As previously observed, there was time-dependant accumulation in ASK1 post injury, with an approximate 4-fold increase at 30 minutes compared to 0

minutes ($p<0.05$). In the presence of the ASK1i (serlonsertib), ASK1 accumulation was completely suppressed to baseline levels (Figure 3.4.1A). Suppression of ASK1 was significant at 10 minute and 30 minute timepoints ($p<0.05$) (Figure 3.4.1B). This result indicated that inhibition of ASK1 phosphorylation using an ASK1 inhibitor suppressed ASK1 accumulation upon cartilage injury.

3.4.2 Inhibition of ASK1 accumulation occurs via a proteasome-dependant mechanism

I further hypothesized that stabilization and accumulation of ASK1 by phosphorylation could indicate that it becomes less prone to proteolytic degradation by the proteasome. Proteasome degradation is the primary process for the degradation of intracellular proteins, where proteins targeted for degradation are marked with ubiquitin chains and then shuttled to the proteasome for proteolysis (Tanaka K., 2009).

Thus, I next investigated ASK1's dependency on the proteasome pathway using a proteasome inhibitor. A proteasome inhibitor 1 (PI1) was used to halt proteasome degradation in cartilage. I first sought to validate the efficacy of the proteasome inhibitor in halting protein degradation. I preinjected porcine MCP joints with either 100 μM PI1 or vehicle control. Injured cartilage explants were incubated for various timepoints in serum-free media containing either PI1 or vehicle. Lysates were extracted and immunoblotted for ASK1. β-actin was immunoblotted as the loading control. Only one

biological replicate was performed for validation purposes. In the presence of PI1, ASK1 suppression by ASK1i was recovered, signifying that ASK1 is sensitive to proteasomal degradation (Figure 3.4.2A).

Next, I carried out an experiment to determine whether phosphorylation-mediated accumulation of ASK1 is due to a reduction in proteasome degradation. I preinjected porcine MCP joints with either 10 μM ASK1i or a combination of 10 μM ASK1i and 100 μM PI1 together. Injured cartilage explants were incubated for various timepoints in serum-free media containing either PI1 or vehicle. Lysates were extracted and immunoblotted for ASK1. β-actin was immunoblotted as the loading control. Quantitication of at least three separate experiments was performed using FIJI-App, ImageJ Gel Analysis software. Results were normalized to β-actin and statistical significance of comparison between groups analyzed by a two-way ANOVA, with post hoc multiple comparisons corrected using Tukey's tests.

The suppression of ASK1 in the ASK1i group after injury was similar to vehicle alone (Figure 3.4.1A) in the presence of PI1 at 30 minutes. At 30 minutes, ASK1 expression in the ASK1i+PI1 group was approximately 6-fold higher than the ASK1i group ($p<0.05$) (Figure 3.4.2B, C). Together, these results show that ASK1 phosphorylation stabilizes the ASK1 protein and preventing its proteasomal degradation.

The primary objective of my project was to determine and characterise whether the ASK1 MAP3K is activated upon cartilage injury. As shown earlier,

I performed preliminary experiments by directly western blotting for phospho-ASK1 on protein lysates generated from the porcine cartilage injury model (Figure 3.3). From the few experiments which worked, I was able to see transient phosphorylation of ASK1 upon cartilage injury. However, the antibody I used for this method proved to be very inconsistent and unreliable. Thus, I next performed a kinase assay on ASK1 as an alternate way of measuring ASK1 activation.

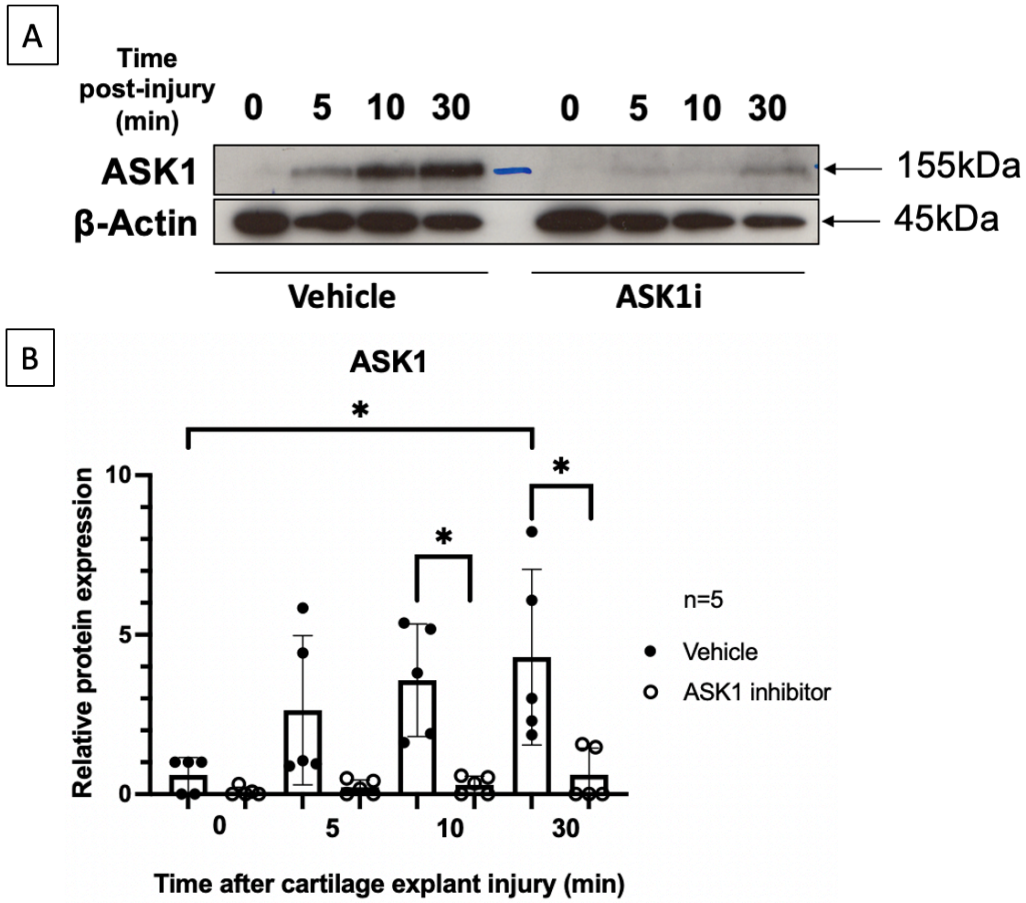

Figure 3.4.1: ASK1 accumulation is suppressed when its phosphorylation is inhibited

(A) Porcine metacarpophalangeal (MCP) joints were decontaminated in 2% Virkon for 15 minutes. MCP joints were injected with either an ASK1 inhibitor or vehicle control and incubated for another 1 hour at 37 °C. The ASK1 inhibitor binds the catalytic kinase domain of ASK1 to prevent its phosphorylation and activation. MCP joints were opened and cartilage was rapidly explanted into ice cold 1X RIPA Buffer (0min) or cultured for various periods of time after explanation (5min, 10min and 30min) in serum free DMEM at 37°C, 5% CO2 before being transferred to ice cold, 1X RIPA buffer. Explants with 1X RIPA buffer, were mildly shaken for 45 minutes at 4°C. Lysates were run on 10% Sodium Dodecyl Sulphate-Polyacrylamide Gel (SDS-PAGE) and transferred to polyvinylidene (PVDF) membrane. PVDF membrane was blocked in 5% milk for 1hour at room temperature, incubated overnight in 1:1000 primary antibody (ASK1), washed 3 times in 1X TBST and incubate for 1 hour in 1:2000 secondary antibody. Protein signal was enhanced by chemiluminescence and visualised using autoradiography. Blots were stripped and re-probed for β-actin as the loading control.

(B) Quantitication of five independent biological replicates was performed using ImageJ and normalised to β-actin. * = $p<0.05$

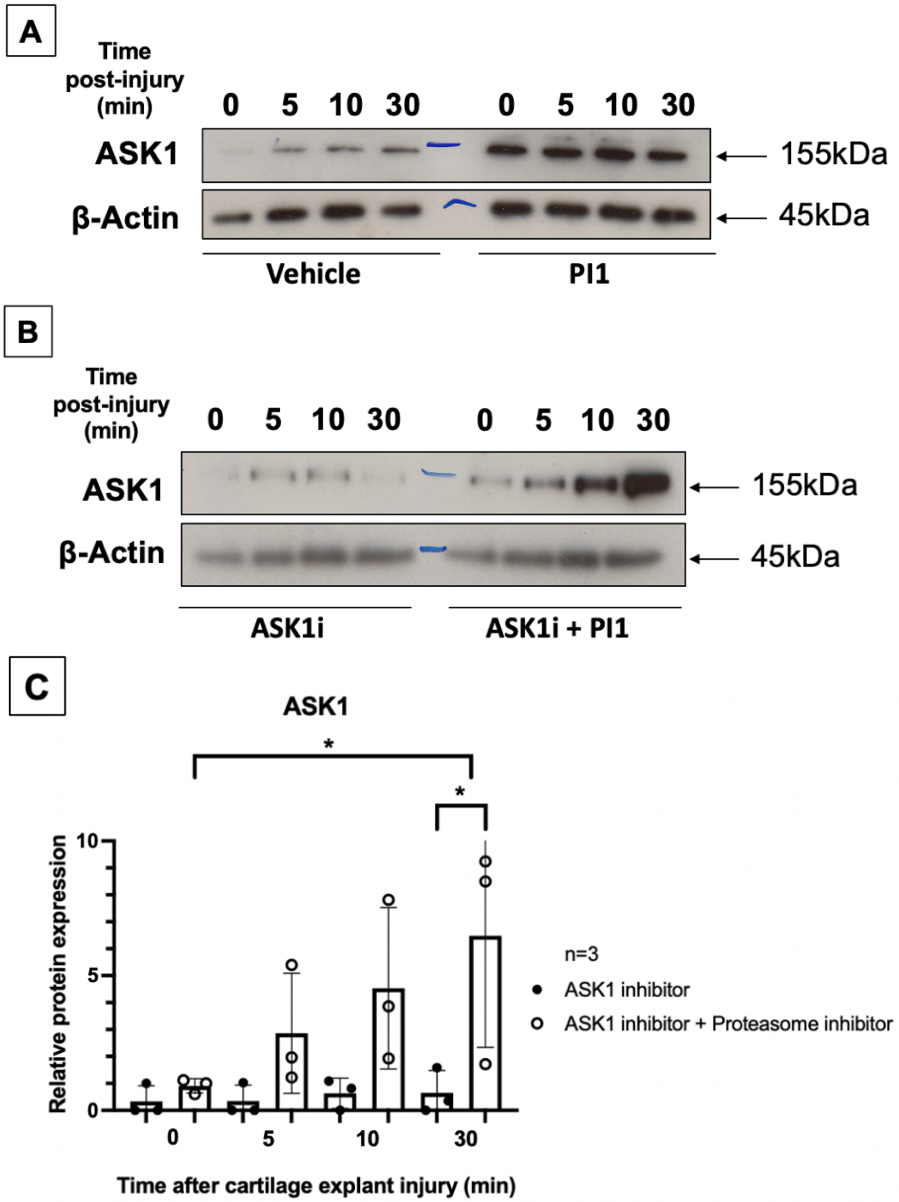

Figure 3.4.2: Inhibition of ASK1 accumulation occurs via a proteasome-dependant mechanism

(A) Porcine metacarpophalangeal (MCP) joints were decontaminated in 2% Virkon for 15 minutes. MCP joints were injected with either a proteasome inhibitor or vehicle. MCP joints were incubated for another 1 hour at 37 °C. The proteasome inhibitor (PI1) inhibits the activity of the 20S proteasome complex. MCP joints were opened and cartilage was rapidly explanted into ice cold 1X RIPA Buffer (0min) or cultured for various periods of time after explanation (5min, 10min and 30min) in serum free DMEM at 37°C, 5% CO2 before being transferred to ice cold, 1X RIPA buffer. Explants with 1X RIPA buffer, were mildly shaken for 45 minutes at 4°C. Lysates were run on 10% Sodium Dodecyl Sulphate-Polyacrylamide Gel (SDS-PAGE) and transferred to polyvinylidene (PVDF) membrane. PVDF membrane was blocked in 5% milk for 1hour at room temperature, incubated overnight in 1:1000 primary antibody (ASK1), washed 3 times in 1X TBST and incubate for 1 hour in

1:2000 secondary antibody. Protein signal was enhanced by chemiluminescence and visualised using autoradiography. Blots were stripped and re-probed for β-actin as the loading control.
(B) Porcine metacarpophalangeal (MCP) joints were decontaminated in 2% Virkon for 15 minutes. MCP joints were injected with either an ASK1 inhibitor or a combination of the ASK1 inhibitor and proteasome inhibitor. MCP joints were incubated for another 1 hour at 37 °C. The ASK1 inhibitor (ASK1i) binds the catalytic kinase domain of ASK1 to prevent its phosphorylation and activation. The proteasome inhibitor (PI1) inhibits the activity of the 20S proteasome complex. MCP joints were opened and cartilage was rapidly explanted into ice cold 1X RIPA Buffer (0min) or cultured for various periods of time after explanation (5min, 10min and 30min) in serum free DMEM at 37°C, 5% CO2 before being transferred to ice cold, 1X RIPA buffer. Explants with 1X RIPA buffer, were mildly shaken for 45 minutes at 4°C. Lysates were run on 10% Sodium Dodecyl Sulphate-Polyacrylamide Gel (SDS-PAGE) and transferred to polyvinylidene (PVDF) membrane. PVDF membrane was blocked in 5% milk for 1hour at room temperature, incubated overnight in 1:1000 primary antibody (ASK1), washed 3 times in 1X TBST and incubate for 1 hour in 1:2000 secondary antibody. Protein signal was enhanced by chemiluminescence and visualised using autoradiography. Blots were stripped and re-probed for β-actin as the loading control.
(C) Quantitication of three independent biological replicates for (B) was performed using ImageJ and normalised to β-actin. * = $p<0.05$

3.4 ASK1 kinase activity is elevated upon cartilage injury

In this section, I use a different technique to indirectly measure ASK1 activation and phosphorylation - through a kinase assay. A kinase assay allows for the measurement of the enzymatic kinase activity of proteins, which in this experiment will be ASK1.

To perform an ASK1 kinase assay, immunoprecipitation of ASK1 from generated porcine cartilage injury lysates is required. Porcine cartilage injury lysates were generated at 0 minutes and 30 minutes post cartilage injury. Immunoprecipitation of ASK1 was performed using the Dynabeads™ Protein G Immunoprecipitation Kit according to the manufacturer's instructions.

0 minute and 30 minute cartilage injury explant lysates were also included as negative and positive controls respectively (Lane 1 and 2, Figure 3.5A). A non-immunized antibody was used in the immunoprecipitation protocol as a negative control (Lane 3, Figure 3.5A). The 30 minutes cartilage injury lysate was used to immunoprecipitate ASK1 for validation by Western Blotting (Lane 4, Figure 3.5A). Lane 5 was left empty. Leftover lysate from the immunoprecipitation protocol was also included in the western blot validation (Lane 6, Figure 3.5A). ASK1 was successfully immunoprecipitated, as shown in the lower exposed blot (Figure 3.5A)

Next, a kinase assay was performed on immunoprecipitated ASK1 (ASK1 IP) from the porcine cartilage injury lysates generated at 0 minutes, 5 minutes, 10 minutes and 30 minutes post cartilage injury (Columns 2-4 respectively, Figure 3.4B). A 30 minute porcine cartilage injury lysate was included as a positive control (Column 1, Figure 3.5B). A non-immunized negative control

group should have been included in this experiment, but was not performed. Results were normalized to the ‘ASK1 IP 0 min explant’ (Column 2, Figure 3.5B) and statistical significance of comparison between groups analyzed by a one-way ANOVA.

The result shows that ASK1 kinase activity was significantly upregulated at all timepoints after injury. Compared to the 0 minute ASK1 immunoprecipitated group, ASK1 kinase activity increased by 537% in the 5 minute and 10 minute groups ($p<0.0001$) and increased by 480% in the 30 minute groups ($p<0.001$) (Figure 3.5B).

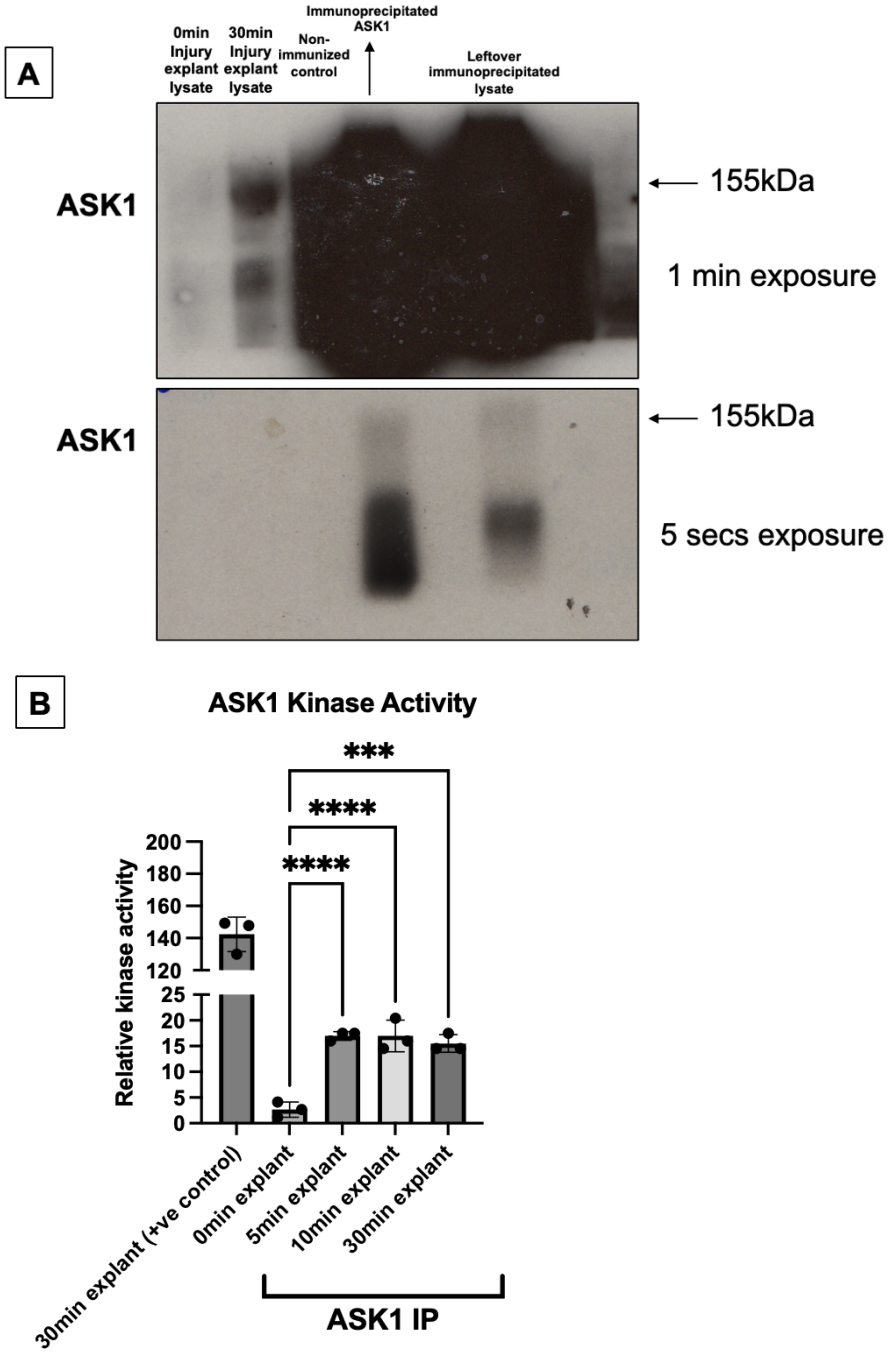

Figure 3.5: ASK1 kinase activity is elevated upon cartilage injury
(A) Immunoprecipitation of ASK1 was validated by western blotting. Porcine cartilage injury lysates were immunoprecipitated for ASK1. Lysates were run on 10% Sodium Dodecyl Sulphate-Polyacrylamide Gel (SDS-PAGE) and transferred to polyvinylidene (PVDF) membrane. PVDF membrane was blocked in 5% milk for 1hour at room temperature, incubated overnight in 1:1000 with ASK1 primary antibody, washed 3 times in 1X TBST and incubate for 1 hour in 1:2000 secondary antibody. Protein signal was enhanced by chemiluminescence and visualised using autoradiography.

(B) Immunoprecipitated ASK1 (ASK1 IP) from the cartilage injury lysate timecourse experiment (0 minutes, 5 minutes, 10 minutes, 30 minutes) was assayed for protein kinase activity using the Universal Kinase Assay Kit (Fluorometric). Fluorescence intensity was measured at an excitation/emission wavelength of 544/590 nm respectively. Quantitication of three technical replicates was performed and normalised to 'ASK1 IP 0min explant' (Lane 2). * = $p<0.05$; ** = $p<0.01$; *** = $p<0.001$; **** = $p<0.0001$.

Discussion

I was able to replicate findings that had been performed by multiple members of the group in the past. Published work in our group showed that activation of all three MAPKs (p38, ERK, JNK) were acute, and in some cases, transient (Ismail H et al., 2017). For example, our group previously showed p38 was phosphorylated as early as 30 seconds and was sustained for 60 minutes post injury; JNK was phosphorylated to be phosphorylated at by 2 minutes and was similarly sustained for 60 minutes post injury; ERK was phosphorylated by 30 seconds and remained elevated for the duration of the experiment (240 minutes) (Ismail H et al., 2017; Vincent T et al., 2002). I was unable to validate the phospho-TAK1 antibody, but this protein had been shown to be activated upon injury. TAK1 was phosphorylated within 30 seconds post injury, and was sustained up to 60 minutes post injury (longest timepoint of the experiment) (Ismail H et al., 2017). Additionally, the use of a TAK1 inhibitor (5Z-7) abolished injury-induced TAK1 and MAPK phosphorylation and suppressed upregulation of inflammatory genes (Ismail H et al., 2017).

IκBα proteins are inhibitors of NF-κB signalling (Liu T et al., 2017). Phosphorylation of IκBα triggers its proteasomal degradation, resulting in nuclear translocation of canonical NF-κB factors and activation of NF-κB signaling (Liu T et al., 2017). Thus, low expression of IκBα protein is indicative of NF-κB signaling. I showed that IκBα was downregulated at 5 minutes post cartilage injury but recovered by 10 minutes. This also aligned with our group's historical work, where IκBα degradation was observed from 0 to 5 minutes post injury, and IκBα was resynthesized by 10 minutes (Ismail H et al., 2017). The authors of this paper also showed that newly synthesized

IκBα was phosphorylated and degraded, using a phospho-IκBα antibody (Ismail H et al., 2017).

I next determined the activation of YAP upon cartilage injury. According to literature, phosphorylation of YAP (at Ser127) causes its cytosolic retention and proteasomal degradation, whereas unphosphorylated YAP translocates to the nucleus to initiate gene transcription (Mo J et al., 2014). YAP's target genes promote repair and regenerative pathways (Wang K et al., 2009). I observed YAP to be rapidly dephosphorylated upon cartilage injury, implying that YAP nuclear translocation is promoted to allow transcription of YAP target genes. Our group previously found that YAP gene expression is strongly and significantly upregulated at 4 hours post cartilage injury, which aligns with this assumption (unpublished data, Abigail Claridge, Vincent group). *Yap1* mRNA induction upon injury was also highly FGF2-dependent and aligns with the rapid release of FGF2 from the PCM of cartilage after injury (unpublished data, Vincent group). Neither of these observations have been described before in the literature. Furthermore, we observed a mean increase in YAP nuclear localization upon cutting injury of cartilage from 0 to 4 hours post injury, although the experiment was too underpowered to see statistical significance (unpublished data, Vincent group). To summarize, these results support the notion that the reparative functions of YAP are stimulated upon cartilage injury.

YAP, like FGF2, has been reported to facilitate chondrocyte differentiation but inhibit chondrocyte maturation during the endochondral ossification process (Zarka M et al., 2021). Endochondral ossification is the principal process of bone tissue formation. Briefly, mesenchymal stem cells at the site of bone formation first differentiate into chondrocytes. Proliferating chondrocytes

undergo hypertrophy and mineralization to form cartilaginous callus tissues where new bone is deposited (Deng Y et al., 2016). YAP has been reported to promote the proliferation of chondrocytes via increasing Sox6 expression and inhibit hypertrophy via suppressing Sox9, Col10 and the Wnt/β-catenin pathway (Zarka M et al., 2021). YAP has also been shown to be important in cartilage repair in vivo as synovial-derived cells and chondrocytes, strongly up-regulate it during the repair process (Roelofs et al., 2017). The regulation of YAP target genes upon cartilage injury was not explored in this work but should certainly be included as a future step. Moreover, the mechanism of YAP crosstalk with the MAPK cascade should be further explored, as it has been previously reported that YAP and TAK1 MAP3K reciprocally inhibit each other in chondrocytes upon cytokine stimulation and promotion of Hippo signaling is chondroprotective (Deng Y et al., 2018).

As a previous student had also identified ASK1, another MAP3K, in the injury cascade (Figure 1.6). By knowing that I attempted to visualise the activation of this kinase upon cartilage injury. The bulk of this chapter was dedicated to characterising the mechanism of ASK1 activation upon cartilage injury. Previous studies have shown upregulation of ASK1 expression in OA tissue compared to healthy tissue (Yan J et al., 2021; Zhang Q et al., 2016). ASK1 has been described to be a mechanosensitive in a few studies. For instance, osteoblasts respond to cyclic stress activated ROS by activating ASK1-p38/JNK pathways to induce apoptosis (Matsui H et al., 2014). Mechanical stretch also activates ASK1-mediated endoplasmic reticulum stress and stimulates extracellular vesicle release from alveolar epithelial cells (Tang R et al., 2022).

In cartilage ASK1 activation appears to sit on the TAK1-dependent pathway that is induced by shear stress and which we have termed "mechanoflammation". The primary trigger for activation of this pathway remains elusive, but may involve, at least in part, proximal generation of ROS from the cell membrane in an NADPH oxidase dependent manner (unpublished data, Vincent group). Our group have been unable to find evidence for a soluble, secreted factor for TAK1 and MAPK activation upon cartilage injury, by showing that explanted cartilage-conditioned medium was unable to activate TAK1 in cultured chondrocytes (unpublished data, Vincent group). However, a previous student (Kamalathevan) did show that MAPK activation upon injury was ROS-dependent (Figure 1.5) and that these came both from the cell membrane and the mitochondrion. ASK1 inhibitors and Coenzyme Q10 (that suppresses mitochondrial ROS production) both completely abrogate MAPK signaling and inflammatory gene regulation.

ASK1 is a serine/threonine kinase, and to date only has two phosphorylation sites that have been functionally characterized. The first is the Threonine 838 site, which is canonically associated with ASK1 activation and kinase activity (Shiizaki S et al., 2013). The activation of ASK1 at the Thr838 site has been widely reported in many cell types and can be induced by various cell stresses, such as oxidative stress, endoplasmic reticulum (ER) stress and inflammatory mediators (Shiizaki S et al., 2013). Autophosphorylation of Thr838 is important in oxidative stress-mediated ASK1 activation (Obsilova V et al., 2021). The other less-reported functional phosphorylation site of ASK1 is the Serine 966 site, which is associated with ASK1 inactivation (Goldman E et al., 2004). Unstressed ASK1 is phosphorylated on the Ser966 site and a 14-3-3 protein negatively regulates ASK1 by binding to ASK1 via the Ser966 site (Goldman E et al., 2004). Upon ROS stimulation, ASK1 is

dephosphorylated at Ser966, resulting in dissociation of 14-3-3 from ASK1 and ASK1 activation (Goldman E et al., 2004; Zhang L et al., 1999).

As discussed earlier, our group previously observed that ASK1 inhibition suppressed cartilage injury-induced MAPK activation (Figure 1.6). We also showed that ASK1i (serlonsertib) significantly suppressed the upregulation of inflammatory genes in the porcine cartilage injury model, namely IL6, COX2, ADAMTS4, CCL2, TIMP1, CDKN1A and NGF (Figure 1.6, and other data not shown). Moreover, ASK1 inhibition did not alter TAK1 activation upon injury (Figure 1.6). This suggests that ASK1 is either downstream of TAK1 or lies in a separate parallel axis to TAK1. In other words, ASK1 drives mechanoflammation in a TAK1-independent manner. As Coenzyme Q10 and NAC also prevent down-stream MAPK activation, and ASK1 is known to be activated by ROS, it is highly likely that TAK1 somehow modulates the mitochondrion to make ROS, which then leads to ASK1 activation. This notion is supported by other studies showing that TAK1 mediates mitochondrial permeability and mitochondrial ROS generation (Suzuki M et al., 2020). This order of events is also supported by the fact that although TAK1 is important in the downregulation of atRA-response genes on cartilage injury, ASK1 inhibition does not affect this (unpublished data Kamalathevan et al; Zhu L et al., 2022), There is some reduction in TAK1 phosphorylation with Coenzyme Q10, but this was only by 50% and may indicate a positive feedback loop with mitochondrial ROS (Figure 1.5B).

In the published literature, TRAF6 is a ubiquitin E3 ligase that is known to activate both ASK1 and TAK1, through different mechanisms (Fujino G et al., 2007; Shim J et al., 2005). TRAF6 and TRAF2 bind to the N-terminal region of ASK1 to induce its activation (Fujino G et al., 2007). TRAF6 aids in the

production of K^{63}-linked polyubiquitin chains that bind to TAK1-binding proteins (TABs), leading to subsequent oligomerization and autophosphorylation of TAK1 (Tobiume K et al., 2002). Despite TAK1 and ASK1 sharing common upstream activators (TRAF6, TRAF2), they are generally considered to be independently activated MAP3Ks. TAK1 and ASK1 share similar MAP2Ks, namely MKK3/6 (Meijles D et al., 2020). Of note, published work from our Centre has shown that the cartilage mechano-inflammatory signaling response is neither TRAF2 nor TRAF6 dependent and that the pattern of ubiquitination of TAK1 after injury does not resemble either IL1 or TNF induced ubiquitination, suggesting that the upstream ubiquitination complex for injury is quite distinct (Ismail H et al., 2017). Heba Ismail (a past OA Centre post doc) is pursuing this with a Versus Arthritis Fellowship at Sheffield University.

Of note, the phospho-ASK1 antibody I used was unreliable. I often did not see a band at all in many of my lanes (data not quantified and not shown). This might have been due to differences in species reactivity of the antibody. The pASK1 Thr838 used in this work had only been validated against humans and mouse, but not against pigs/porcine tissues. The ASK1 protein structure may be different in humans compared to pigs, although MAPK protein structures are usually highly conserved across all mammals. In fact, none of the other MAPK antibodies used by our group had been validated against porcine tissue, yet we had been able to produce consistent and reliable results using them, due to the evolutionarily conserved similarities of MAPK sequences in humans and pigs. Using the National Center for Biotechnology Information's (NCBI) Basic Local Alignment Search Tool (BLAST), I confirmed that the gene and protein sequences for the ASK1 kinase domain to be almost identical in humans and pigs, meaning that the

pASK1 Thr838 antibody I possess should theoretically work on porcine tissue. I did purchase different pASK1 Thr838 antibodies from different suppliers, but none worked well. Further attempts in optimising the Western Blotting protocol had been attempted, but I was still unable to make the pASK1 Thr838 antibody work in a consistent manner. A phospho-ASK1 (Ser966) antibody had not been purchased nor attempted in this experiment due to the lack of evidence for the role of Ser966 in ASK1 activity and the lack of availability of this antibody by suppliers.

I used a total ASK1 antibody initially to persuade myself that there were indeed detectable levels of ASK1 in cartilage lysates. Serendipitously, I observed that total ASK1 expression increased post-injury, potentially due to the accumulation of ASK1 protein (over a short time course). Linking these results together, I hypothesised that phosphorylation of ASK1 causes stabilisation and subsequent accumulation of ASK1 total protein. Protein phosphorylation has long been established as a key mechanism for structural stabilization of proteins (Miranda F et al., 2004). The addition of a phosphorylated group to proteins induces conformational changes near the phospho-site, namely by forming more hydrogen bonds and residue contacts than non-phospho-sites, thus making the protein more resistant to proteolytic degradation (Nishi H et al., 2011). This may be the case for ASK1. I therefore next investigated whether injury caused the accumulation of ASK1 protein by reducing its degradation.

To do this I used a proteasome inhibitor that selectively inhibits the multi-catalytic proteinase complex (20S proteasome). The 20S proteasome is the core of the proteasome complex, that carries out proteolytic roles in all eukaryotic cells (Tanaka K et al., 2009). I hypothesized that ASK1 followed

proteasomal degradation like most intracellular proteins, and that ASK1 phosphorylation would prevent its proteasomal degradation. Since protein phosphorylation is one of the few mechanisms that enables structural stabilization of proteins (Miranda F et al., 2004), I hypothesized that phosphorylated ASK1 is better protected from proteolytic degradation than non-phosphorylated ASK1. My results were consistent with this hypothesis as ASK1 failure to accumulate with the ASK1 inhibitor was reversed when the proteosome inhibitor was also added.

ASK1 has been reported to negatively regulate proteasome activity (Um J et al., 2010). In this study, Um et al. demonstrated that ASK1 inhibited the ATPase activity of the 19S proteasome subcomplex (Um J et al., 2010). 19Ss are regulatory particles that support the 20S catalytic core of the proteasome. 19Ss are responsible for recognizing polyubiquitinated proteins, unfolding them, and subsequently translocating them into the 20S catalytic core, a process which is ATP-dependent (Tanaka K et al., 2009). Whether ASK1's phosphorylation state affected the deregulation of the proteasome was not explored in Um et al.'s study. A different study identified an LRLRGG sequence on ASK1's C-terminal domain that associates with 19S of the proteasome (Schneider J et al., 2013). Mutant forms of the LRLRGG sequence within ASK1 reduced ASK1's association with 19S and thus reduced ASK1's capacity to inhibit the proteasome (Schneider J et al., 2013). Mutant forms of ASK1 also showed reduced TNF-induced JNK and NF-κB signaling, but ASK1 kinase activity was unaffected (Schneider J et al., 2013). Following this publication, another group built upon these findings and found that the LRLRGG sequence was required for the recruitment of ubiquitin specific peptidase 9 X-linked (USP9X) to ASK1 (Nagai H et al., 2009). USP9X, a deubiquinating enzyme, was found to prevent oxidative stress-

induced ubiquitination and subsequent proteasomal degradation of activated ASK1, resulting in stabilization of activated ASK1 (Nagai H et al., 2009). This particular finding by Nagai H et al. supports my hypothesis that activated ASK1 (in their case, activation by oxidative stress) is stabilized and prevented from proteasomal degradation. My work showed that ASK1 is activated and phosphorylated upon cartilage injury, leading to its stabilization and accumulation on a total protein level. Furthermore, Nagai and colleagues identified a 15 amino acid region (aa 956–1235) on ASK1's C-terminal which was ubiquitinated and then consequently cleaved by USP9X upon oxidative stress stimulation (Nagai H et al., 2009). USP9X knockdown in vitro suppressed oxidative stress-induced MAPK p38/JNK activation similar to ASK1 knockdown cells (Nagai H et al., 2009). These results imply that USP9X is a strong regulator of ASK1 activity and stability.

As an alternate means to measure ASK1 activation, I attempted to measure the kinase activity directly using a commercial kinase assay with immunoprecipitated ASK1. My experiment did suggest that I might be able to immunoprecipitate ASK1 successfully, even though there were limitations with visualizing the immunoprecipitated protein. The results also showed that there was a difference in detected kinase activity between the 0 time points and later ones after injury. Taken together these results were consistent with the demonstration of ASK1 dependent kinase activity and consistent with activation of this pathway as noted above. This experiment omitted a non-immune control and was only performed once. Had I more time, I would have repeated this experiment with all relevant controls.

The off-target effects of serlonsertib on other members of the MAPK cascade are unknown. Therefore, supporting this data with the use of other ASK1

inhibitors or a combination of different ASK1 inhibitors may be more reassuring. Among the commercially available ASK1 inhibitors, serlonsertib is the only ASK1 inhibitor that has made it up to phase 3 clinical trials in an experimental study of non-alcoholic steatohepatitis, but unfortunately the primary study endpoint was not reached (Harrison S et al., 2020). Nevertheless, serlonsertib was selected for this work due to its reliability and efficacy as the most promising ASK1 inhibitor currently available. More in vivo and translational work is required to reveal the therapeutical potential of ASK1 inhibition for the treatment of OA and this will be explored in Chapter 5.

A final summary of the mechano-inflammatory response, adding to that already produced by Kamalathevan, is shown in Figure 3.6.

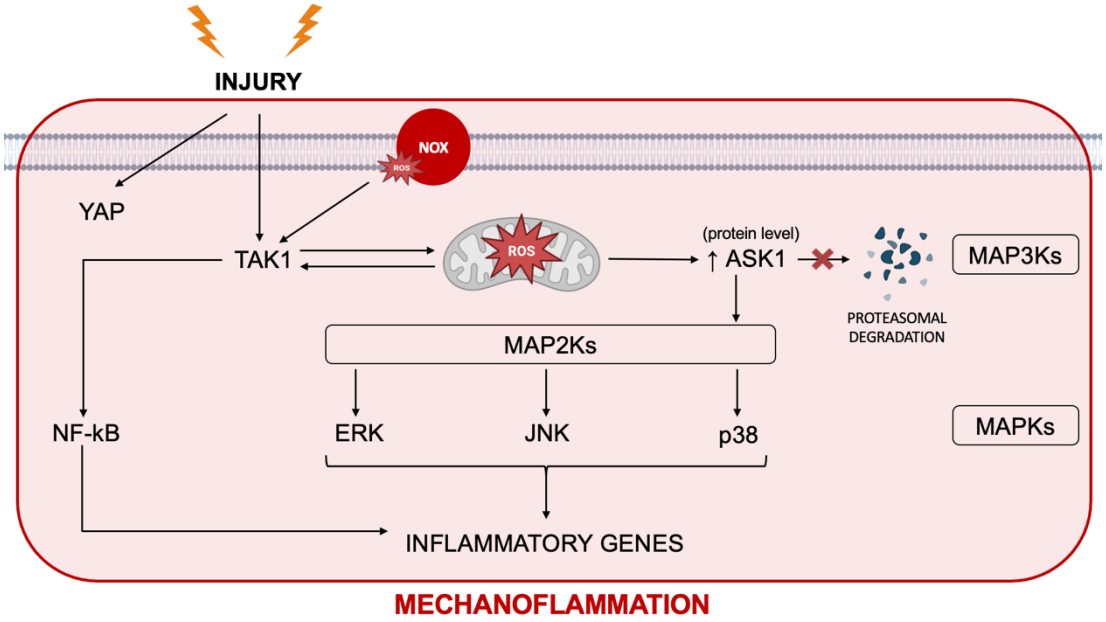

Figure 3.6: Schematic of mechanoflammation signalling in cartilage
Mechanoflammation activates Transforming growth factor beta-activated kinase 1 (TAK1) that drives mitochondrial production of reactive oxygen species (ROS). Apoptosis signal-regulating kinase 1 (ASK1) is activated by mitochondrial ROS that drives phosphorylation of the mitogen activated protein kinases (MAPKs) (extracellular signal-regulated kinase (ERK), Jun N-terminal kinase (JNK) and p38) which subsequently increases inflammatory gene regulation. TAK1 also activates downstream Nuclear factor kappa B (NF-κB) signalling but it is not currently known whether this requires ASK1. Yes-associated protein (YAP) signaling is also turned on upon injury. Block black line = direct, full activation.

CHAPTER 4: ROLE OF ASK1 IN IL1 OR H_2O_2-INDUCED CHONDROCYTE RESPONSES

Introduction

IL1 and ROS have overlapping adverse effects on chondrocytes, such as the induction of inflammatory mediators and production of matrix proteases. In this chapter, I explored the effect of IL1 or H_2O_2 stimulation on MAPK and NF-κB signaling. I further investigated ASK1's dependancy on these signaling cascades by using an ASK1 inhibitor.

The previous chapter indicated that ASK1 phosphorylation plays a much more important role in the cartilage injury response than we had previously recognised. Moreover, previous unpublished data from our group suggested that TAK1 phosphorylation was upstream of ASK1 and could activate ASK1 by directing mitochondria to make ROS. This raised the important question of whether another TAK1 activator, such as IL1, also activates inflammatory signalling in an ASK1 dependent manner. This would somewhat challenge the existing paradigm which suggests a direct activation of MAPKKs from TAK1. If IL1 did not activate MAPKs in an ASK1-dependent manner this would support distinct mechanisms of activation following injury compared to receptor mediated cytokine stimulation and would potentially identify novel therapeutic targets that would interfere with injury responses without disrupting important cytokine-driven defence mechanisms.

Our group have shown that TGFβ is among the growth factors released from the PCM upon cartilage injury (Tang X et al., 2018). Whether TGFβ contributes to TAK1-mediated MAPK mechanoflammation in cartilage is not

known. TAK1 was initially discovered as a downstream mediator of TGFβ, thus its name ‘TGFβ-activated kinase 1’. It could potentially be the primary driver of TAK1 activation upon injury or could contribute to another upstream TAK1 stimulus. The former is perhaps less likely as our group have previously shown that TAK1 activation was not mediated by a soluble factor; TGFβ is readily available in the medium after cartilage injury.

In this chapter I explore inflammatory signalling following IL1, TGFβ or H_2O_2 stimulation of isolated chondrocytes and determine whether their ASK1 dependence. I start by validating MAPK signalling in isolated cells then examine the effect of ASK1 inhibition on their activation.

4.1 IL1 and TGFβ activates MAPKs in chondrocytes

I first explored the effect of TGFβ on MAPK signaling in chondrocytes in vitro. I first validated my chondrocyte porcine cell culture model by stimulating cells with either TGFβ or IL1 (used as a positive control).

Cultures of primary porcine chondrocytes were treated with TGFβ1 or IL1 for vehicle for 5 minutes, 10 minutes or 30 minutes. The IL1 group was included as a positive control. Lysates were immunoblotted for phospho-p38, phospho-ERK, phospho-JNK. β-actin was immunoblotted as the loading control. Quantitication of at least two or three separate experiments was performed using FIJI-App, ImageJ Gel Analysis software. Results were normalized to β-actin and statistical significance of comparison between groups analyzed by a two-way ANOVA, with post hoc multiple comparisons corrected using Tukey's tests.

TGFβ activated all 3 MAPKs (phospho-p38, phospho-ERK, phospho-JNK). pJNK and pP38 activation peaked at 5 minutes and decreased over time. Activation of pP38 by TGFβ at 5 minutes was statistically significant ($p<0.01$). pERK was moderately activated at 5 minutes, which peaked at 10 minutes and decreased at 30 minutes. IL1 (positive control group) also activated all 3 MAPKs. IL1 activation was highest at 5 minutes ($p<0.001$), which gradually decreased at 10 ($p<0.05$) and 30 minutes.

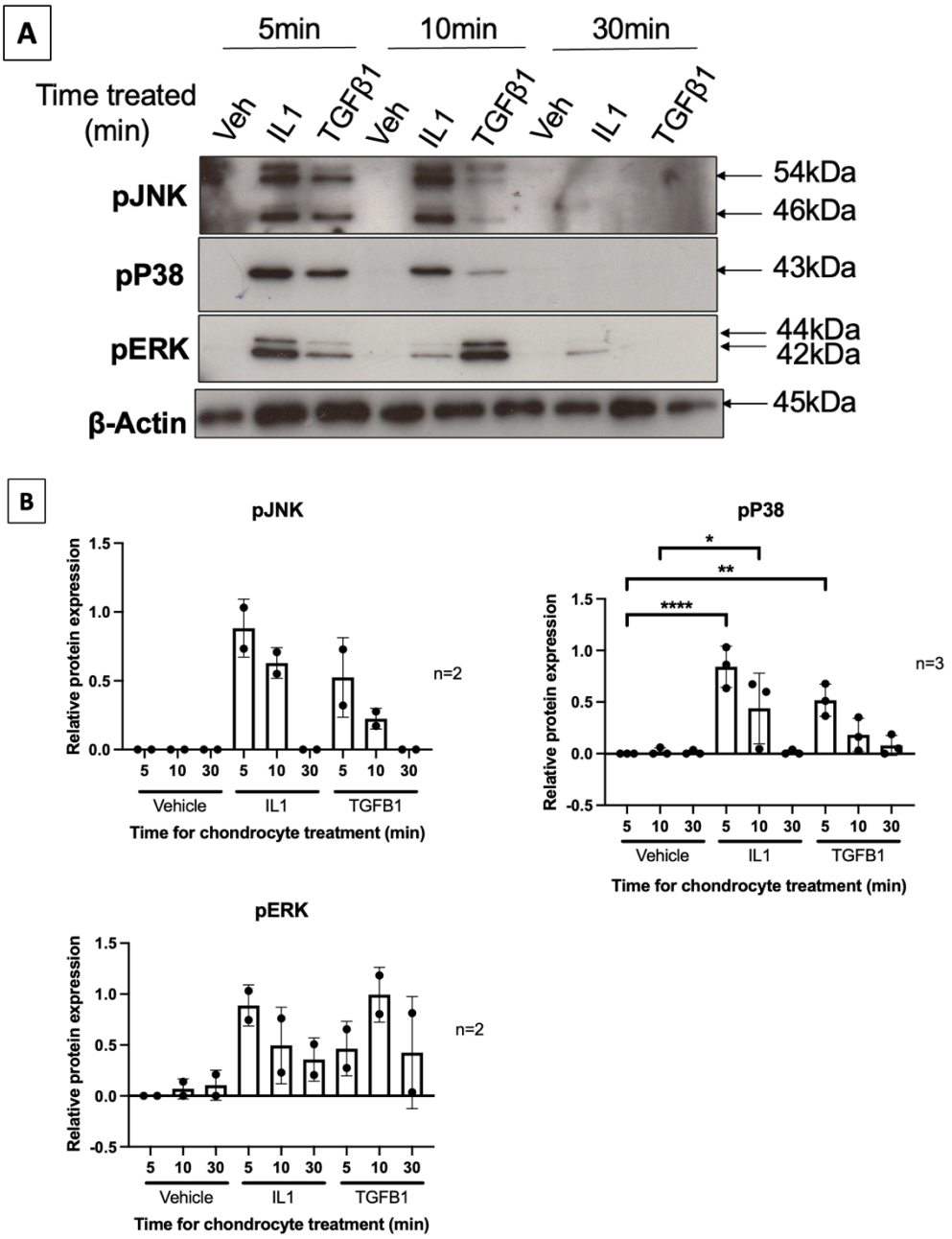

Figure 4.1: TGFβ activates MAPKs in chondrocytes
(A) Porcine metacarpophalangeal (MCP) joints were disinfected in 2% Virkon for 10 minutes. MCP joints were opened and cartilage was explanted. Explanted cartilage was incubated in DMEM containing 1m/ml Collagenase A overnight at 37°C. Collagenase digest was washed by centrifugation at 25200 RCF for 5 minutes three times Pellets were resuspended in DMEM containing 4.5 g/L of glucose and L-Glutamine and were supplemented with 10 % fetal bovine serum (FBS), 1 % penicillin, streptomycin and amphotericin B. Primary chondrocytes were plated at a density of 2 million per well in each well of a 6-well plate in DMEM containing 20% FBS for 24 hours at 37°C, 5% CO_2. Primary chondrocytes were then serum starved by incubating for 24 hours in serum-free DMEM and then stimulated with either 10 ng/ml TGFB1, 5 ng/ml IL1a or DMSO as the vehicle control (Veh). After stimulation,

primary chondrocytes were gently washed with 1X sterile PBS and incubated with ice-cold 1X RIPA Buffer for 45 minutes, 4°C. Chondrocytes were harvested using a cell scraper and centrifuged at 18900 RCF, 4°C. Supernatant was collected and used to generate protein lysates for Western Blotting analysis. Lysates were run on 10% Sodium Dodecyl Sulphate-Polyacrylamide Gel (SDS-PAGE) and transferred to polyvinylidene (PVDF) membrane. PVDF membrane was blocked in 5% milk for 1 hour at room temperature, incubated overnight in primary antibody (pP38, pJNK, pERK), washed 3 times in 1X TBST and incubate for 1 hour in 1:2000 secondary antibody. Protein signal was enhanced by chemiluminescence and visualised using autoradiography. Blots were stripped and re-probed for βactin as the loading control. (B) Quantitication of two or three independent biological replicates was performed using ImageJ and normalised to β-actin. Biological replicate number (n) is labelled for each experiment. * = $p<0.05$; ** = $p<0.01$; *** = $p<0.001$.

4.2 The effect of IL1 on MAPKs and NF-κB signalling in chondrocytes

4.2.1 IL1 activates MAPKs and NF-κB signalling in chondrocytes

Focusing on IL1, I next extended my observations to study a longer time course, and to include total ASK1 protein and NF-κB in my assay.

Cultures of primary porcine chondrocytes were treated with IL1 or vehicle for 0.25 minutes (15 seconds), 0.5 minutes (30 seconds) 5 minutes, 10 minutes, 30 minutes or 60 minutes. Porcine cartilage injury explant lysates generated using the porcine cartilage injury model (as described in Chapter 3.1) were included in the western blots as positive controls. Lysates were immunoblotted for ASK1, phospho-p38, phospho-ERK, IκBα. GAPDH was immunoblotted as the loading control. Quantitication at least three separate experiments was performed using FIJI-App, ImageJ Gel Analysis software. Results were normalized to GAPDH and statistical significance of comparison between groups analyzed by a one-way ANOVA

ASK1 total protein expression increased with IL1 stimulation in a time-dependant manner, up to around 1.8-fold at 60 minutes compared to 0 minutes, although not statistically significant. pP38 activation was transient, peaking at 10 minutes, after which it begins declining. pERK activation appears to start at 5 minutes which peaks at 30 minutes. IκBα degradation occurred acutely in less than a minute, after which IκBα was resynthesized at 5 minutes and subsequent timepoints (Figure 4.2.1).

4.2.2 ASK1i did not inhibit IL1-induced p38 signaling in chondrocytes

I also determined if treatment of an ASK1 inhibitor (serlonsertib) can inhibit IL1-induced MAPKs

Cultures of primary porcine chondrocytes were treated with IL1 or a combination of IL1 and ASK1i for 0.25 minutes (15 seconds), 0.5 minutes (30 seconds) 5 minutes, 10 minutes, 30 minutes or 60 minutes. Porcine cartilage injury explant lysates generated using the porcine cartilage injury model (described in Chapter 3.1) were included in the western blots as positive controls. Lysates were immunoblotted for phospho-p38. GAPDH was immunoblotted as the loading control. Quantitication at least three separate experiments was performed using FIJI-App, ImageJ Gel Analysis software. Results were normalized to GAPDH and statistical significance of comparison between groups analyzed by a one-way ANOVA

Curiously, pP38 activation appeared to be globally elevated in the presence of the ASK1 inhibitor at all timepoints. Statistical testing was not possible from this single experiment and further repeat experiments could not be included as the control (IL1 effect in the absence of ASK1i) failed to show a robust activation of signaling. Nonetheless, there was no evidence that ASK1 inhibition could suppress IL1 inflammatory signaling.

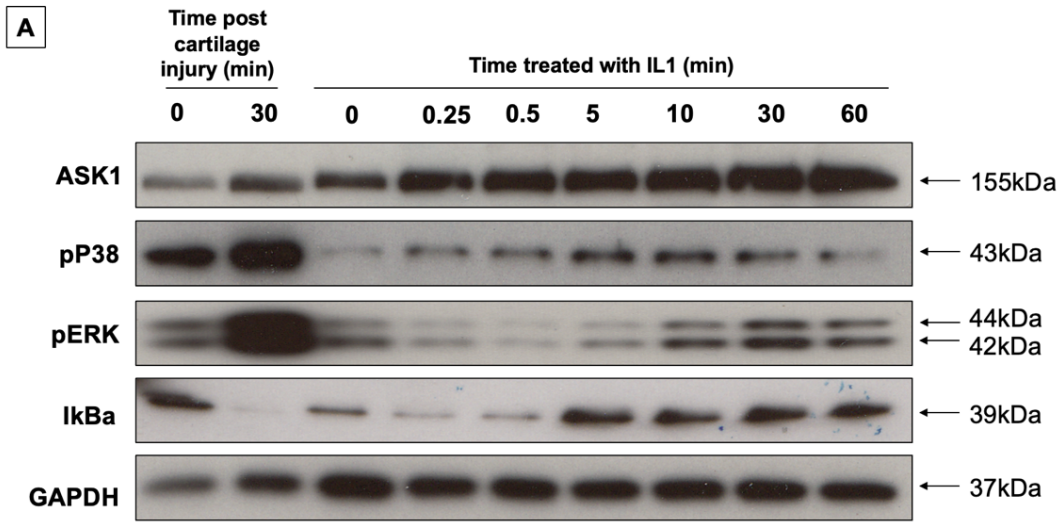

Figure 4.2 1: MAPK and NF-kB regulation upon IL1 treatment in chondrocytes
(A) Porcine metacarpophalangeal (MCP) joints were disinfected in 2% Virkon for 10 minutes. MCP joints were opened and cartilage was explanted. Explanted cartilage was incubated in DMEM containing 1m/ml Collagenase A overnight at 37°C. Collagenase digest was washed by centrifugation at 25200 RCF for 5 minutes three times Pellets were resuspended in DMEM containing 4.5 g/L of glucose and L-Glutamine and were supplemented with 20 % fetal bovine serum (FBS), 1 % penicillin, streptomycin and amphotericin B. Primary chondrocytes were plated at a density of 2 million per well in each well of a 6-well plate in DMEM containing 20% FBS for 24 hours at 37°C, 5% CO_2. Primary chondrocytes were then serum starved by incubating for 24 hours in serum-free DMEM and then stimulated for either 10 ng/ml IL1b or serum-free media as the 0 minute timepoint. After stimulation primary chondrocytes were gently washed with 1X sterile PBS and incubated with ice-cold 1X RIPA Buffer for 45 minutes, 4°C. Chondrocytes were harvested using a cell scraper and centrifuged at 18900 RCF, 4°C. Supernatant was collected and used to generate protein lysates for Western Blotting analysis. Lysates were run on 10% Sodium Dodecyl Sulphate-Polyacrylamide Gel (SDS-PAGE) and transferred to polyvinylidene (PVDF) membrane. PVDF membrane was blocked in 5% milk for 1 hour at room temperature, incubated overnight in primary antibody (ASK1, pP38, IkBα, pERK), washed 3 times in 1X TBST and incubate for 1 hour in 1:2000 secondary antibody. Protein signal was enhanced by chemiluminescence and visualised using autoradiography. Blots were stripped and re-probed for GAPDH as the loading control.

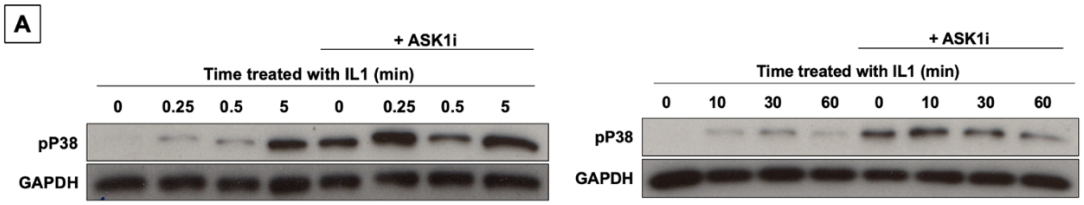

Figure 4.2.2: p38 MAPK regulation upon IL1 treatment in chondrocytes with an ASK1 inhibitor

(A) Porcine metacarpophalangeal (MCP) joints were disinfected in 2% Virkon for 10 minutes. MCP joints were opened and cartilage was explanted. Explanted cartilage was incubated in DMEM containing 1m/ml Collagenase A overnight at 37°C. Collagenase digest was washed by centrifugation at 25200 RCF for 5 minutes three times Pellets were resuspended in DMEM containing 4.5 g/L of glucose and L-Glutamine and were supplemented with 20 % fetal bovine serum (FBS), 1 % penicillin, streptomycin and amphotericin B. Primary chondrocytes were plated at a density of 2 million per well in each well of a 6-well plate in DMEM containing 20% FBS for 24 hours at 37°C, 5% CO_2. Primary chondrocytes were then serum starved by incubating for 24 hours in serum-free DMEM and then stimulated with either 10 ng/ml IL1b or serum-free media as the 0 minute timepoint. For the ASK1i group, cells was treated with 10uM ASK1i for 30 minutes after serum starvation but prior to IL1 treatment. After stimulation, primary chondrocytes were gently washed with 1X sterile PBS and incubated with ice-cold 1X RIPA Buffer for 45 minutes, 4°C. Chondrocytes were harvested using a cell scraper and centrifuged at 18900 RCF, 4°C. Supernatant was collected and used to generate protein lysates for Western Blotting analysis. Lysates were run on 10% Sodium Dodecyl Sulphate-Polyacrylamide Gel (SDS-PAGE) and transferred to polyvinylidene (PVDF) membrane. PVDF membrane was blocked in 5% milk for 1 hour at room temperature, incubated overnight in primary antibody (pP38), washed 3 times in 1X TBST and incubate for 1 hour in 1:2000 secondary antibody. Protein signal was enhanced by chemiluminescence and visualised using autoradiography. Blots were stripped and re-probed for GAPDH as the loading control.

4.3 The effect of H_2O2 on MAPKs and NF-κB signalling in chondrocytes

I next explored the effect of ROS on MAPK and NF-κB signaling in chondrocytes in vitro, using hydrogen peroxide (H_2O_2) as a means of ROS stimulation. I also investigated the effect of ASK1 inhibition on H_2O_2-treated chondrocytes.

4.3.1 H_2O_2 activates MAPKs and NF-κB signalling in chondrocytes

To investigate the effect of H_2O_2 in chondrocytes, I isolated primary chondrocytes from porcine cartilage, using the same method described in Chapter 4.1.

I first determined the concentration of H_2O_2 that was sufficient to stimulate MAPKs in my chondrocyte model. I performed a standalone validation experiment where I treated chondrocytes with different concentrations of H_2O_2 based on what others have used in the published literature (Figure 4.3.1A). ASK1 expression was largely unaffected by different H_2O_2 doses. For pP38, 50μM or higher H_2O_2 concentration was sufficient for activation.

Cultures of primary porcine chondrocytes were treated with H_2O_2 for 0.25 minutes (15 seconds), 0.5 minutes (30 seconds) 5 minutes, 10 minutes, 30 minutes or 60 minutes. Porcine cartilage injury explant lysates generated

using the porcine cartilage injury model (as described in Chapter 3.1) were included in the western blots as positive controls. Lysates were immunoblotted for ASK1, phospho-p38, phospho-ERK, IκBα. GAPDH was immunoblotted as the loading control. Quantitication at least three separate experiments was performed using FIJI-App, ImageJ Gel Analysis software. Results were normalized to GAPDH and statistical significance of comparison between groups analyzed by a one-way ANOVA.

ASK1 total protein expression appeared to remain relatively stable throughout the H_2O_2-timecourse, with no noticeable regulation of the protein throughout the experiment time course. pP38 was rapidly and transiently activated from 0.5 minutes, which peaked at 10 minutes (approximately 12-fold the 0 minute timepoint). pP38 activation returned to baseline by 30 minutes. pERK activation gradually increased upon stimulation, that peaked between 0.5 to 5 minutes after which the activation began to deteriorate slowly. IκBα degradation occurred rapidly in less than a minute, after which IκBα was resynthesized at 5 minutes and subsequent timepoints (Figure 4.3.1B)

4.3.2 ASK1i did not inhibit p38 signaling in H_2O_2-stimulated chondrocytes

I also determined if additional treatment of an ASK1i inhibitor (serlonsertib) can inhibit H_2O_2-induced MAPKs.

Cultures of primary porcine chondrocytes were treated with H_2O_2 or a combination of H_2O_2 and ASK1i for 0.25 minutes (15 seconds), 0.5 minutes (30 seconds) 5 minutes, 10 minutes, 30 minutes or 60 minutes. Porcine cartilage injury explant lysates generated using the porcine cartilage injury model (described in Chapter 3.1) were included in the western blots as positive controls. Lysates were immunoblotted for phospho-p38. GAPDH was immunoblotted as the loading control. Quantitication at least three separate experiments was performed using FIJI-App, ImageJ Gel Analysis software. Results were normalized to GAPDH and statistical significance of comparison between groups analyzed by a one-way ANOVA

pP38 regulation was not suppressed by the ASK1i inhibitor. If anything, it appeared slightly elevated and more sustained in the presence of the inhibitor. I also repeated this experiment several times but, similar to the IL1 experiments, several of these were not interpretable because I failed to show that my positive control (H_2O_2 alone) activated as expected. For both IL1 and H_2O_2 experiments there was a small increase in signaling in the inhibitor treated lanes suggesting that increased, rather than decreased, signaling was occurring in vitro with ASK1 inhibition.

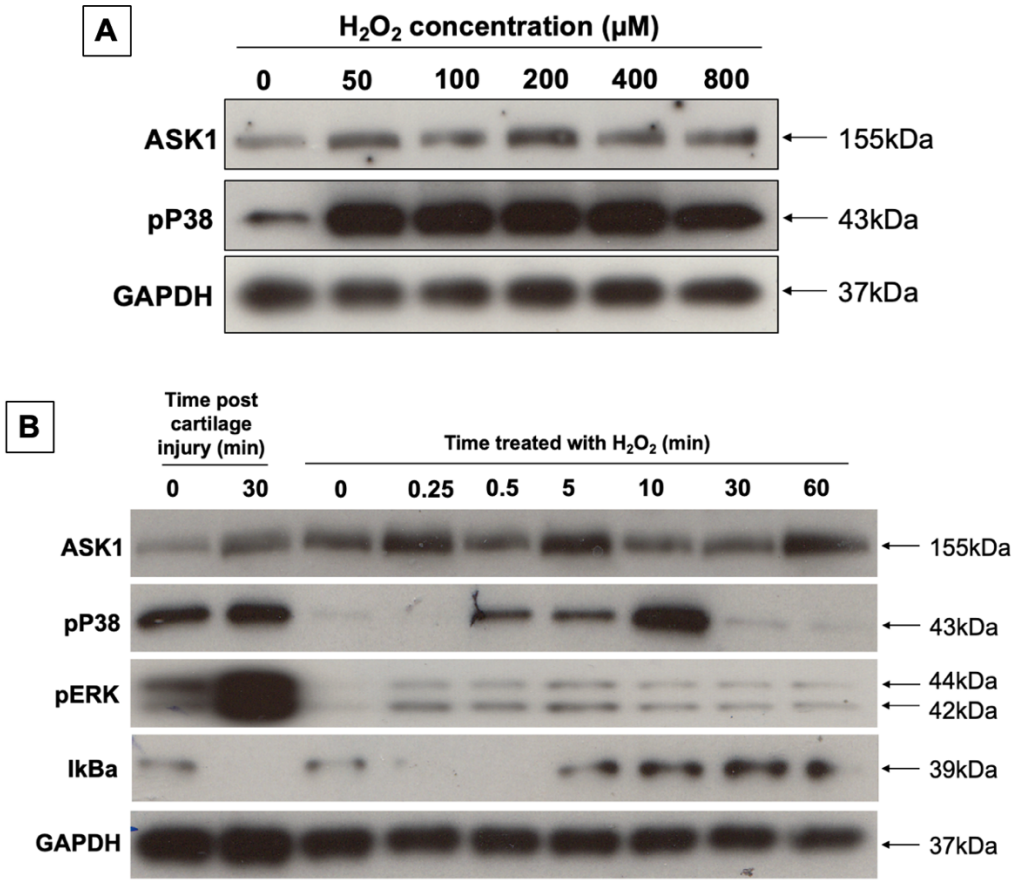

Figure 4.3.1: MAPK and NF-kB regulation upon H_2O_2 treatment in chondrocytes

(A) Porcine metacarpophalangeal (MCP) joints were disinfected in 2% Virkon for 10 minutes. MCP joints were opened and cartilage was explanted. Explanted cartilage was incubated in DMEM containing 1m/ml Collagenase A overnight at 37°C. Collagenase digest was washed by centrifugation at 25200 RCF for 5 minutes three times Pellets were resuspended in DMEM containing 4.5 g/L of glucose and L-Glutamine and were supplemented with 20 % fetal bovine serum (FBS), 1 % penicillin, streptomycin and amphotericin B. Primary chondrocytes were plated at a density of 2 million per well in each well of a 6-well plate in DMEM containing 20% FBS for 24 hours at 37°C, 5% CO_2. Primary chondrocytes were then serum starved by incubating for 24 hours in serum-free DMEM and then stimulated with different concentrations of H_2O_2 (50, 100, 200, 400, 800uM) or serum-free media as the 0 minute timepoint. After stimulation, primary chondrocytes were gently washed with 1X sterile PBS and incubated with ice-cold 1X RIPA Buffer for 45 minutes, 4°C. Chondrocytes were harvested using a cell scraper and centrifuged at 18900 RCF, 4°C. Supernatant was collected and used to generate protein lysates for Western Blotting analysis. Lysates were run on 10% Sodium Dodecyl Sulphate-Polyacrylamide Gel (SDS-PAGE) and transferred to polyvinylidene (PVDF) membrane. PVDF membrane was blocked in 5% milk for 1 hour at room temperature, incubated overnight in primary antibody (ASK1, pP38), washed 3 times in 1X TBST and incubate for 1 hour in 1:2000 secondary antibody. Protein signal was enhanced by chemiluminescence and visualised using autoradiography. Blots were stripped and re-probed for GAPDH as the loading control.

(B) Porcine metacarpophalangeal (MCP) joints were disinfected in 2% Virkon for 10 minutes. MCP joints were opened and cartilage was explanted. Explanted cartilage was incubated in DMEM containing 1m/ml Collagenase A overnight at 37°C. Collagenase digest was washed by centrifugation at 25200 RCF for 5 minutes three times Pellets were resuspended in DMEM containing 4.5 g/L of glucose and L-Glutamine and were supplemented with 20 % fetal bovine serum (FBS), 1 % penicillin, streptomycin and amphotericin B. Primary chondrocytes were plated at a density of 2 million per well in each well of a 6-well plate in DMEM containing 20% FBS for 24 hours at 37°C, 5% CO_2. Primary chondrocytes were then serum starved by incubating for 24 hours in serum-free DMEM and then stimulated with either 100uM H_2O_2 or serum-free media as the 0 minute timepoint. After stimulation, primary chondrocytes were gently washed with 1X sterile PBS and incubated with ice-cold 1X RIPA Buffer for 45 minutes, 4°C. Chondrocytes were harvested using a cell scraper and centrifuged at 18900 RCF, 4°C. Supernatant was collected and used to generate protein lysates for Western Blotting analysis. Lysates were run on 10% Sodium Dodecyl Sulphate-Polyacrylamide Gel (SDS-PAGE) and transferred to polyvinylidene (PVDF) membrane. PVDF membrane was blocked in 5% milk for 1 hour at room temperature, incubated overnight in primary antibody (ASK1, pP38, IkBα, pERK), washed 3 times in 1X TBST and incubate for 1 hour in 1:2000 secondary antibody. Protein signal was enhanced by chemiluminescence and visualised using autoradiography. Blots were stripped and re-probed for GAPDH as the loading control.

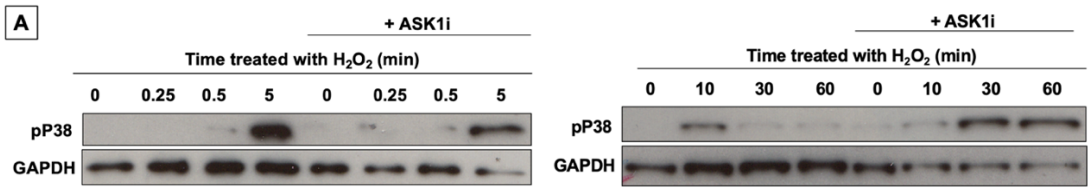

Figure 4.3.2: p38 MAPK regulation upon H_2O_2 treatment in chondrocytes with an ASK1 inhibitor

(A) Porcine metacarpophalangeal (MCP) joints were disinfected in 2% Virkon for 10 minutes. MCP joints were opened and cartilage was explanted. Explanted cartilage was incubated in DMEM containing 1m/ml Collagenase A overnight at 37°C. Collagenase digest was washed by centrifugation at 25200 RCF for 5 minutes three times. Pellets were resuspended in DMEM containing 4.5 g/L of glucose and L-Glutamine and were supplemented with 20 % fetal bovine serum (FBS), 1 % penicillin, streptomycin and amphotericin B. Primary chondrocytes were plated at a density of 2 million per well in each well of a 6-well plate in DMEM containing 20% FBS for 24 hours at 37°C, 5% CO_2. Primary chondrocytes were then serum starved by incubating for 24 hours in serum-free DMEM and then stimulated with either 100uM H_2O_2 or serum-free media as the 0 minute timepoint. For the ASK1i group, cells were treated with 10uM ASK1i for 30 minutes after serum starvation but prior to H_2O_2 treatment. After stimulation, primary chondrocytes were gently washed with 1X sterile PBS and incubated with ice-cold 1X RIPA Buffer for 45 minutes, 4°C. Chondrocytes were harvested using a cell scraper and centrifuged at 18900 RCF, 4°C. Supernatant was collected and used to generate protein lysates for Western Blotting analysis. Lysates were run on 10% Sodium Dodecyl Sulphate-Polyacrylamide Gel (SDS-PAGE) and transferred to polyvinylidene (PVDF) membrane. PVDF membrane was blocked in 5% milk for 1 hour at room temperature, incubated overnight in primary antibody (pP38), washed 3 times in 1X TBST and incubate for 1 hour in 1:2000 secondary antibody. Protein signal was enhanced by chemiluminescence and visualised using autoradiography. Blots were stripped and re-probed for GAPDH as the loading control.

Discussion

In this chapter I first showed that TGFβ stimulation does indeed, rapidly and transiently activate MAPKs in primary porcine chondrocytes. The investigation of MAPKs upon direct stimulation of TGFβ has not been explored in chondrocytes, but has been reported in other cell systems such as cancer cells and fibroblasts (Wang W et al., 2014, Watanabe H et al., 2001). In these reports, TGFβ-induced MAPK activation can be driven by Smads as well as TAK1 MAP3K. The experimental framework I performed may also be extended to investigate Smad and TAK1 activation by TGFβ using phospho-Smad and phospho-TAK1 antibodies respectively. I didn't get round to doing this but this would be of interest to do in the future.
TGFβ is a growth factor present in the PCM, and has been reported to be a mechanosensitive mediator in cartilage (Neu C et al., 2007, Tang X et al., 2018). TGFβ is regarded as a chondroprotective agent in cartilage and chondrocytes, by promoting chondrogenesis in MSCs and inhibiting chondrocyte terminal differentiation (Yang X et al., 2001). TGFβ signaling occurs through phosphorylation of downstream Smad proteins. TAK1 is conventionally described as a downstream mediator of TGFβ, which consequently activates MAPKs and NF-kB pathways (Kim S et al., 2009).

The activation of MAPKs by TGFβ is well described in cancer, whereby growth factors like TGFβ have the MAPK pathway constantly switched on to promote proliferation, survival and differentiation of cancer cells. Chronic activation of MAPKs in cancers is malignant, as cancers can acquire metastatic potential and endless proliferation through MAPK signalling (Chapnick D et al., 2011).

Our group has previously shown that CTGF was required for sequestration of latent TGFβ in the matrix (Tang X et al., 2018). They proposed that CTGF is covalently bound (via disulfide bonds) to latent TGFβ in the endoplasmic reticulum of chondrocytes. This latent complex is sequestered in the chondrocyte PCM via binding to heparin sulfate chains of perlecan. Upon mechanical compression of cartilage, the latent complex is released from perlecan and interacts with TGFβR3 on the chondrocyte cell surface in a CTGF-dependent manner, and TGFβ signaling is initiated via Smad2/3 phosphorylation. Others have reported that TGFβ plays a dual role in cartilage maintenance, depending on which downstream Smad signals are activated (Blaney Davidson E et al., 2009). It has been reported Smad2/3 promotes reparative responses while Smad1/5/8 triggers hypertrophic responses in chondrocytes (Blaney Davidson E et al., 2009). TGFβ has also been reported to signal through the Rho-like GTPase and PI3K/AKT pathways in multiple other systems (Wang W et al., 2014). However, the extent which TGFβ plays a role for these pathways in cartilage is unknown.

In the second part to this chapter, I investigated the chondrocyte response to IL1. I showed that IL1 stimulation onto chondrocytes induces transient activation patterns of MAPKs and NF-κB signaling (Figure 4.2.1). Additionally, I observed accumulation of ASK1 protein that increased with time stimulated with IL1 (Figure 4.2.1). The ASK1 accumulation pattern observed here resembles that seen in the porcine cartilage injury model, where ASK1 protein accumulated upon cartilage injury (Chapter 3). This could indicate that IL1-stimulated ASK1 is phosphorylated and thus stabilized in a similar manner to ASK1 in injured cartilage. It should also therefore be proteosome dependent although this wasn't tested.

IL1 induction of MAPKs ERK (Wang X et al., 2011) and p38 (Radons J et al., 2006) produce catabolic responses in chondrocytes and cartilage. Activation of these two MAPKs promotes the matrix-degrading collagenases and aggrecanases such as MMP1, MMP3, MMP13 and ADAMTS4 (Jenei-Lanzl Z et al., 2019). *Adamts5* is not much regulated by IL1 on a mRNA level in most species tested (Vincent T., 2019). ERK or p38 activation by IL1 stimulates the production of inflammatory and chemo-attractive molecules PGE2, NO, IL6, LIF and iNOS, which inhibits matrix synthesis processes and induce chondrocyte apoptosis (Wang X et al., 2010). IL1-mediated NF-κB is also well described and shares many similarities to the MAPK cascade in terms of inflammatory mediator production. However, IL1-mediated NF-κB signaling differs from MAPK activation due to the fact that NF-κB has not yet been linked with aggrecan degradation (Jenei-Lanzl Z et al., 2019). IL1-induced activation of MAPK JNK in chondrocytes is also well described, although not performed in this work. Our group demonstrated that IL1 promotes the production of aggrecanase ADAMTS5 through the JNK2 pathway in human chondrocytes (Ismail H et al., 2015).

The activation of ASK1 by IL1 in chondrocytes has not been described yet but has been briefly described in a few other cell systems (Mochida Y et al., 2000; Zhang Q et al., 2016). In an OA-related study, stimulation of mouse embryonic fibroblasts (MEFs) with IL1β activated ASK1 by phosphorylation at the Thr838 site (Zhang Q et al., 2016). Knocking out ASK1 in MEFs reduced p38/JNK/NF-κB activation in response to IL1β compared to WT MEFs (Zhang Q et al., 2016). Moreover, IL1β-stimulated expression of chondrocyte hypertrophy markers *Colx*, *Mmp13*, and *Vegf* were inhibited in ASK1 KO MEFs compared to WT MEFs (Zhang Q et al., 2016). Together, these results suggest that in the presence of inflammatory cytokines, the absence or

inhibition of ASK1 prevents MAPK signaling and characteristics associated with chondrocyte catabolism or hypertrophy. The proposed mechanism of IL1-induced ASK1 activation is by receptor-proximal activation of TRAF6 upstream, as demonstrated by a few immunology-related studies (Dainichi T et al., 2019, Yen JH et al., 2022).

My findings on ASK1i treatment seem contradictory to the published literature. I did not observe inhibition of p38 activation when treating chondrocytes with IL1 in the presence of ASK1i (Figure 4.2.2). The ASK1i (serlonsertib), which had been used by our group prior to my project, suppressed MAPKs ERK and JNK completely upon cartilage injury (Figure 1.5B). Furthermore, we showed that the ASK1i suppressed upregulation of inflammatory genes upon cartilage injury (Figure 1.5C). It has been described in many in vivo and in vitro systems that the ASK1 MAP3K is a strong regulator of the MAPKs and NF-κB (Liu H et al., 2000). Serlonsertib had been shown to inhibit IL1-induced ASK1/p38/JNK activation in vitro (Meijles D et al., 2020; Yan J et al., 2021). These contradictory findings may have been due to unknown off-target effects of the ASK1i, such as the interference of other ASK1-independent pathways that also regulate MAPK and NF-κB. As my results were based on single experiments, despite attempts to repeat, it would be premature to read too much into these results and the role of ASK1 on IL1 activation, therefore, remains unknown.

In the final part to this chapter, I investigated the chondrocyte response to H_2O_2. I show that H_2O_2 stimulation of chondrocytes induces transient activation of MAPKs and NF-κB signaling (Figure 4.3.1). H_2O_2, and other oxygen radicals, can activate MAPKs through multiple mechanisms such as ligand-independent clustering and activation of growth factor receptors, such

as the receptor tyrosine kinases (Nakashima I et al., 2005). For example, it has been shown that H_2O_2 activates and phosphorylates epidermal growth factor receptor (Meves A et al., 2001). Activation of MAPKs by exogenous stimulation of H_2O_2 in vitro have been described before (Dabrowski A et al., 2000; Ruffels J et al., 2004). The mechanisms of ROS-induced MAPK activation is not well defined, as oxygen radicals can alter protein structure by reacting with critical amino acid residues of proteins (Son Y et al., 2011).

Conversely, ROS can also affect MAPK cascades by inactivating and degrading the MAPK phosphatases (MKPs) – also known as the MAPK signalling deactivators. Studies have reported that H_2O_2 accumulation can inactivate MKPs by oxidizing their catalytic cysteine residues, leading sustained MAPK signalling (Son Y et al., 2011). Furthermore, it has been reported that ROS can interfere with the mRNA stabilisation and translation of MKPs (Kuwano Y et al., 2008). The oxidative potentials of ROS can also be determined based on the site and kinetics of ROS production and the availability of antioxidants in the cell (Son Y et al., 2011). Thus, the disparity in the H_2O_2 response between the MAPKs may be due to the different sensitivities of their upstream MAP2Ks and MAP3Ks to ROS, as well as the different sensitivities of their respective deactivators (MKPs) to ROS.

ROS can also activate signalling cascades through the modification of intracellular kinases. The ASK1 MAP3K is known to be an oxidative stress sensor and transducer. ASK1 binds to the inhibitory thioredoxin (Trx) in a non-stressed state. Upon an increase in oxidative stress, Trx is oxidized and dissociates from ASK1, leading to oligomerization and autophosphorylation of ASK1, subsequent activation of ASK1 and its downstream pathways (Nagai H et al., 2007). Prior to this experiment, I hypothesized that ASK1 would be

activated by H_2O_2 stimulation, mimicking ROS stimulation. As mentioned in a previous chapter, I was not able to fully validate a phospho-ASK1 antibody to detect ASK1 activation by its phosphorylation state, which would have been useful in this experiment. I previously observed that ASK1 total protein accumulated upon cartilage injury, and that this was suppressed by an ASK1i inhibitor (serlonsertib) which specifically inhibits the catalytic kinase domain of ASK1 (the kinase domain associated with ASK1 activation). From that result, I inferred that ASK1 activation is also associated with its accumulation at the total protein level. In this chapter, H_2O_2 stimulation of chondrocytes did not induce noticeable regulation of ASK1 total protein, which did not coincide with my hypothesis.

There may be several reasons why I did not observe ASK1 total protein accumulation as hypothesised. First, the concentration of H_2O_2 I used in this experiment (100μM) may have been insufficient to switch on ASK1, while the other MAPKs were activated at this concentration (likely by other ROS-sensitive, ASK1-independent pathways). In literature, concentrations of H_2O_2 used to stimulate ASK1 in vitro are in the low millimolar (mM) range. For example, treatment of HepG2 human hepatoma cells with 1mM H_2O_2 activated ASK1 by Thr845 phosphorylation (Zhang N et al., 2016). Meanwhile, treatment of COS7 kidney cells with 1-5mM H_2O_2 induced ASK1 Ser967 dephosphorylation (the Ser967 site is associated with ASK1 inactivation), but ASK1 total protein expression was unchanged (Goldman E et al., 2004). Despite these reports, micromolar (μM) ranges of H_2O_2 stimulation is sufficient to stimulate cell responses in other cell systems. Various studies investigating the effect of H_2O_2 on chondrocytes in vitro observed dose-dependent responses in chondrocyte viability or apoptosis within the 5-800μM range (Asada S et al., 2001; Gao G et al., 2018; Martin G

et al., 2005). Physiological concentrations of oxygen radicals range from 10^{-11} to 10^{-8} M in mammalian cells (Chance B et al., 1979), so it would be safe to assume that concentrations of H_2O_2 used in my experiments are supra-physiological.

Another reason why ASK1 accumulation in vitro did not occur in my hands may be because of the different mechanisms of ASK1 activation upon cartilage injury (in previous chapter) versus H_2O_2 stimulation. I previously observed that an ASK1i (serlonsertib), which targets the catalytic kinase domain of ASK1, suppressed ASK1 accumulation upon cartilage injury. ASK1's activation site is reported to be at Thr838, within its kinase domain (aa 670-940) (Bunkoczi G et al., 2007). Thus, I inferred that mechanism of ASK1 accumulation was dependant on ASK1 Thr838 phosphorylation and activation. However, the ASK1 regulation mechanism may be more complex than just a single phosphorylation site. A recent study has reported a total of 5 dynamic phosphorylation sites in ASK1, and another 7 phospho-sites of ASK1 that have completely unknown functions (Betanzos C et al., 2016). Each of these phospho-sites need to be explored in greater detail to understand the mechanism of ASK1 activation in different systems. This kinase remains poorly understood.

The inevitable exposure of chondrocytes to an oxygenated environment in my chondrocyte cell culture model may have also rendered the cells resistant to external oxidative stress stimuli. As discussed in the Introduction, chondrocytes reside in a hypoxic environment (approximately 7% oxygen tension) within cartilage. However, explanting cartilage and culturing chondrocytes exposes the chondrocytes to atmospheric oxygen (16-21% oxygen). As a result, chondrocytes may already have switched on their

intrinsic antioxidant systems prior to H_2O_2 treatment in my experiments. These factors are usually not considered in the published literature but may be especially relevant in chondrocyte in vitro studies making interpretation difficult.

ASK1 inhibition with H_2O_2 stimulation also seemed to contradict studies published in other cells. For instance, serlonsertib had been shown to inhibit H_2O_2-induced ASK1/p38/JNK activation in cardiomyocytes in vitro (Meijles D et al., 2020). In my hands, p38 activation seemed unaffected by serlonsertib in H_2O_2-stimulated chondrocytes. Like my experience with IL1, these results cannot be considered definitive as I was unable to reproduce the result with good positive controls. However, there was increased phosphorylation of MAPKs in all of the H_2O_2 experiments when the ASK1 inhibitor was present suggesting that this result may yet be shown to be robust. It will be important for someone else in the lab to repeat this as it could be an important addition to the literature.

Recognising the potential limitations of studying these types of pathways in a normoxic (hyperoxic for chondrocytes) environment in vivo, my last chapter will describe two attempts to modulate mechanoflammation and OA in vivo.

CHAPTER 5: BIOLOGICAL CONSEQUENCES OF INHIBITING MECHANO-INFLAMMATORY PATHWAYS IN MURINE OA

Introduction

Over the years our group has defined many components of the mechano-inflammatory response in cartilage and their impact on disease in murine OA (unpublished data Kamalathevan et al.,; Vincent T., 2019; Vincent T., 2020). This is summarized in Figure 1.7. The pathways that have been targeted in vivo thus far are shown and include: TAK1 (mice died 48 hours after post-natal pan-tissue conditional knockout), JNK2 (mice protected from DMM-induced OA), atRA boosting using Talarozole (mice protected from OA) (Ismail H et al., 2016; Zhu L et al., 2022). This provided proof of concept that interfering with mechanoflammation in vivo was a potential therapeutic approach in OA. Work done in this thesis and by Kamalathevan previously has also identified three further pathways that can also be targeted Where commercial inhibitors of KO animals exist. These include cPLA2, 12/15 LOX, ASK1 and neutralization of ROS (Figure 5.1).

cPLA2 is an enzyme that catalyzes arachidonic acid formation from polyunsaturated fatty acids (PUFAs) in the lipid bilayer (Sun G et al., 2021), leading to the generation of, amongst other things, 12/15 LOX-derived metabolites that cause a reduction in atRA, thus influencing mechano-inflammatory gene regulation (unpublished data Kamalathevan et al, Vincent group). Inhibitors to both cPLA2 and 12/15 LOX have been used in in vivo. cPLA2-floxed mice are also available and are held as a live colony at the Kennedy. During my time in the Kennedy Institute, our group generated data showing that cPLA2 total KO mice displayed reduced OA scores after DMM

surgery, albeit not quite reaching statistical significance (unpublished data, Vincent group).

PUFAs in the cell membrane undergo non-enzymatic oxidation by ROS in a process known as lipid peroxidation. In this process, free oxygen radicals oxidise unsaturated lipids to form lipid hyperoxides (lipid peroxidation product) and a hydroxyl radical (Ayala A et al., 2014). The ability of cPLA2 to generate arachidonic acid from the cell membrane is dependent on an acyl group on PUFAs. A collaborator of ours, Dr Shchepinov, has generated a modified chow diet in which all PUFAs are resistant to lipid peroxidation and oxidative stress (Firsov A et al., 2022). This has been used in other in vivo models and in small scale clinical studies (Callaghan B et al., 2023; Liu Y et al., 2022; Shchepinov M., 2020). By feeding animals with the modified diet, they should be unable to generate lipid hyperoxide byproducts and pro-inflammatory lipid mediators.

Evidence from our group and from literature suggest that ASK1 is a mediator of mechanoflammation. I have shown that ASK1 drives downstream inflammatory signalling and is activated upon cartilage injury (Figure 3.2). Furthermore, the use of an ASK1 specific inhibitor (serlonsertib) suppressed inflammatory gene upregulation and ASK1 protein accumulation upon injury, as summarised by a previous student in Chapter 1.9 (Figure 1.6). So far, serlonsertib has only been implemented in one study concerning OA. Yan et al. reported that intra-articular injection of serlonsertib prevented cartilage damage in a rat OA model, as analysed by histological assessment and immunohistochemistry techniques (Yan J et al., 2021). Taken together, serlonsertib may be a candidate in OA therapy that attenuates cartilage damage and degradation.

In this chapter I explore these alternative targeting approaches by studying (1) mice fed with the oxidation-resistant modified chow diet (2) mice receiving the ASK1 inhibitor (daily by oral gavage). I hypothesize that both the modified diet and ASK1i models would be protective against murine OA as our group's work and others suggest a catabolic role for reactive oxygen species and a pro-inflammatory role for ASK1.

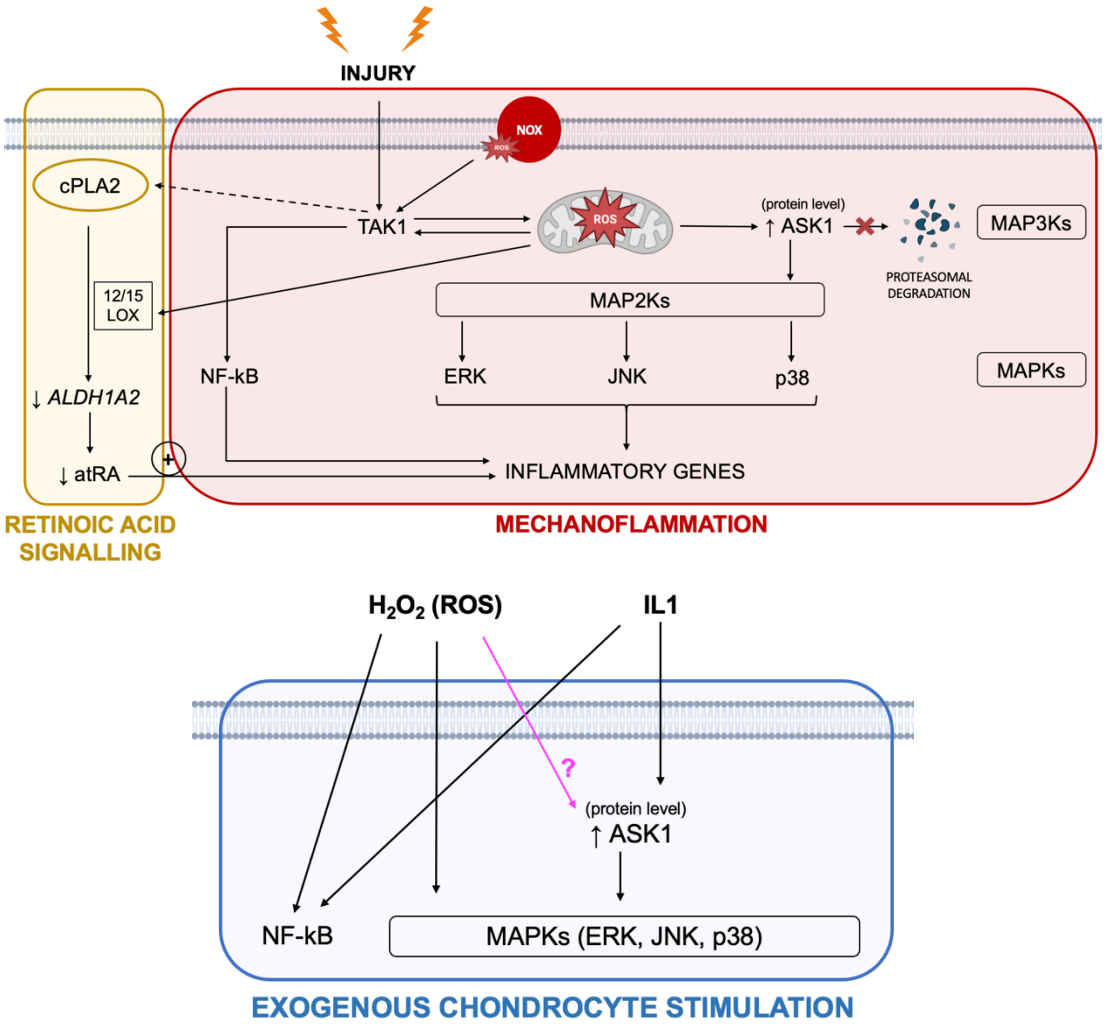

Figure 5.1 Revised schematic of mechanoflammation signalling in cartilage and in chondrocytes
Mechanoflammation activates Transforming growth factor beta-activated kinase 1 (TAK1) that drives mitochondrial production of reactive oxygen species (ROS). Apoptosis signal-regulating kinase 1 (ASK1) is activated by mitochondrial ROS that

drives phosphorylation of the mitogen activated protein kinases (MAPKs) (extracellular signal-regulated kinase (ERK), Jun N-terminal kinase (JNK) and p38) which subsequently increases inflammatory gene regulation. TAK1 also activates downstream Nuclear factor kappa B (NF-κB) signalling but it is not currently known whether this requires ASK1. Mechanical injury downregulates all-trans-retinoic acid (atRA)-dependent genes in both a reactive oxygen species (ROS)-dependent and cytosolic phospholipase A2 (cPLA2)-dependent manner. Transforming growth factor activated-beta kinase 1 (TAK1) is responsible for partially phosphorylating cPLA2 on cartilage injury. The phosphorylation of cPLA2 on cartilage injury is also NOX-dependent and likely mediated via TAK1. 12/15 LOX is also sensitive to ROS. In chondrocytes, interleukin-1 (IL1) hydrogen peroxide (H_2O_2) activates MAPKs and NF-κB. IL1 also activates ASK1 as observed by ASK1 total protein accumulation, but this was not the case for H_2O_2, despite being reported in literature (pink arrow). activates Block black line = direct, full activation. Dotted line = partial activation.

5.1 Effect of a deuterated diet in murine OA models

In this work, we designed a study to investigate whether feeding mice with modified diets consisting of deuterated arachidonic acid (compared to a normal diet of unaltered arachidonic acid) impacts cartilage degradation and inflammation in a murine post-traumatic OA model. Deuteration is the process of replacing hydrogen atoms (^{1}H) with the heavier isotope, deuterium (^{2}H). The deuteration of arachidonic acid renders it more resistant to oxidation, due to the higher energy required to dissociate the heavier isotopes from their bonds (Pestov N et al., 2011). The oxidation-resistant properties of deuteration have been described previously (Pestov N et al., 2011). Since my studies have shown the importance of reactive oxygen species and the oxidative stress response, we hypothesized that an oxidation-resistant diet may be protective against OA.

5.1.1 Validation of murine hip injury model with JNK2$^{-/-}$ mice

Before performing a long term in vivo experiment, I first determined whether feeding over relatively short periods could replace the native PUFAs in a sufficient way to change mechano-inflammatory gene regulation after injury using the murine hip injury model. To validate the hip injury model in my hands, I first attempted to reproduce results that had been obtained previously in the *JNK2*$^{-/-}$ mice (Ismail H et al., 2016). At 4-6 weeks of age, articular cartilage was avulsed from the hips of wildtype (n=8) and *JNK2*$^{-/-}$ mice (n=8). Cartilage was immediately injured (cut once) and snap frozen

immediately or cultured in serum-free media for 4 hours post injury before being snap frozen. mRNA was extracted from hips and a panel of genes measured by microfluidic TaqMan gene expression array, listed in Table 2.2. Gene expression from wildtype and *JNK2*$^{-/-}$ mice 4 hours after hip avulsion was compared to respective 0 hour baseline gene expression. None of the atRA-responsive genes were regulated in *JNK2*$^{-/-}$ or wildtype mice at any time point. For inflammatory genes, up-regulation of a number of genes was observed at 4h (although this was only statistical for CCL2) and this regulation was similar for *JNK2*$^{-/-}$ and wildtype hips. (Figure 5.2). This aligned with previous observations from the group that *JNK2*$^{-/-}$ mice did not show mechano-inflammatory gene regulation (Ismail H et al., 2015).

5.1.2 Hips from mice fed a deuterated diet appear to mount a less inflammatory response upon avulsion injury

I examined the modified diet on the hip injury response in mice that had been fed modified or control diet for 3 weeks from weaning (3-4 weeks old) until the experimental endpoint (6 weeks of age). I performed gene expression analysis on murine hip cartilage to assess the effect of diet modification on cartilage injury-induced gene regulation. At 6 weeks of age, articular cartilage was avulsed from the hips of control diet (n=8) and modified diet mice (n=7). Cartilage was injured (cut once) and snap frozen immediately or cultured in serum-free media for 4 h post injury before being snap frozen. mRNA was extracted from hips. 15 genes were measured by microfluidic TaqMan gene expression array, listed in Table 2.2. Gene expression of control diet and

modified diet mice at 4 hours after hip avulsion with injury was compared to respective 0 hour baseline gene expression. A number of atRA-responsive genes, including Hoxa4 and Rarb showed a trend to suppression upon hip injury but none of the results reached statistical significance. Of the inflammatory genes, a number showed some evidence of up-regulation upon injury of wildtype hips (as previously demonstrated by our group). A few of these such as Mmp3, Il6 and Ptgs2, reached statistical significance. Although there was only one gene that was significantly suppressed by the modified diet (Mmp3, suppressed by 47%, $p<0.01$) (Figure 5.3), most of the others showed a strong trend towards suppression. These results provided some confidence that even a 3 week feeding period could change the response to ex vivo cartilage injury, making reasonably likely that we might see something over a longer in vivo study.

5.1.3 The effect of modified diet on the course of murine OA induced by PMX

For this experiment mice were switched onto the modified or control diet from 3-4 weeks, at the time of weaning, and OA was induced by surgical partial medial meniscectomy (PMX) at 10 weeks of age. Feeding continued according to chow group over the course of the experiment. Mice were culled at 10 weeks and joints sectioned for histological assessment. Contrary to what we might have expected, the modified diet group showed a statistically significant increase in OARSI score compared to the control diet group ($p<0.05$) (Figure 5.4A). Representative images are shown in Figure 5.4B.

There was not difference between osteophyte size or maturity between the two groups (Figure 5.4C,D).

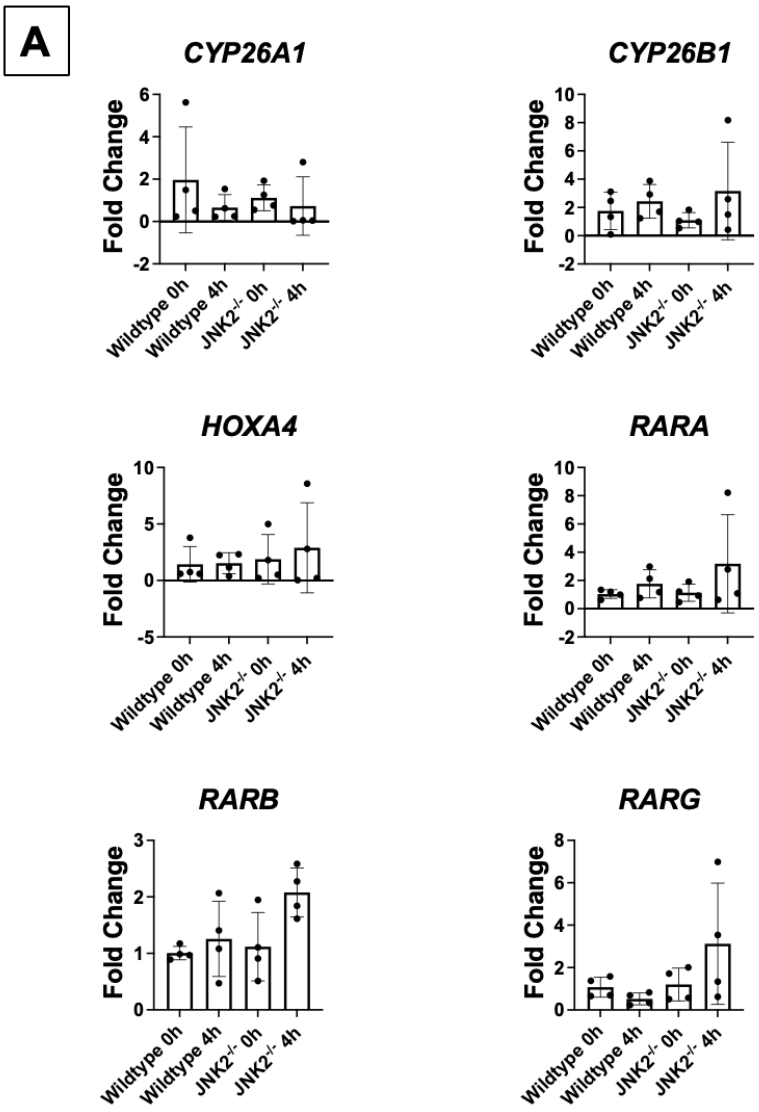

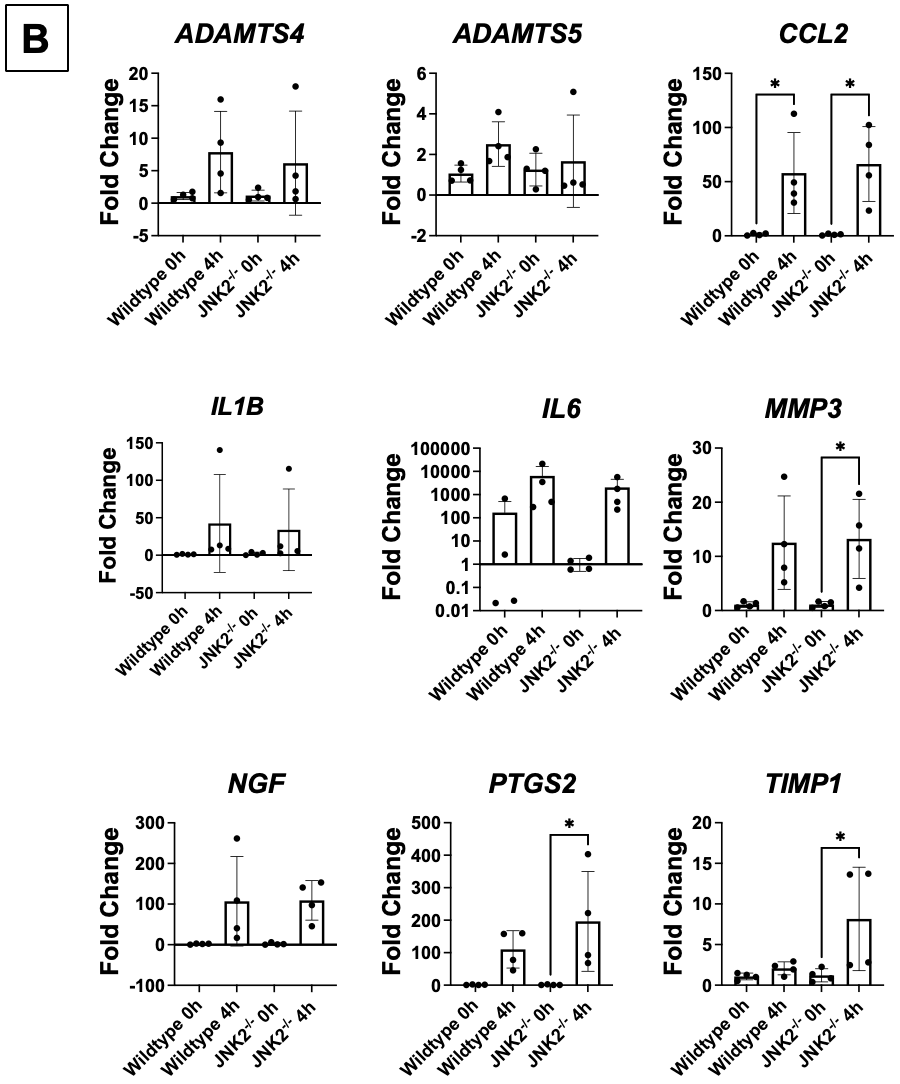

Figure 5.2: Comparison of inflammatory and atRA-responsive gene expression in JNK2$^{-/-}$ and wildtype mice

Mice were culled by CO_2, and the acetabulofemoral (hip) joints were exposed by blunt dissection. The cartilaginous femoral cap was avulsed using forceps. Murine hip cartilage was avulsed directly into serum-free DMEM and incubated for 4 hours at 37°C, then snap frozen at -80°C. RNA was subsequently extracted from the tissue and used in a microfluidic gene expression array to measure a panel of (A) atRA-response genes and (B) inflammatory genes. 18S was used as the housekeeping gene. Statistical significance of comparison between treatment groups was conducted using a two-way ANOVA, with post-hoc multiple comparisons corrected using Tukey's tests. Bars shows the mean ± SEM of 4 independent experiments (n= 4 separate mice). * = p<0.05; ** = p<0.01; *** = p<0.001. ADAMTS4 = ADAM metallopeptidase with thrombospondin type 1 motif 4, ADAMTS5 = ADAM metallopeptidase with thrombospondin type 1 motif 5, CCL2 = C-C motif chemokine ligand 2, CYP26A1 = Cytochrome P450 Family 26 Subfamily A Member 1, CYP26B1 = Cytochrome P450 Family 26 Subfamily B Member 1, HOXA4 = homeobox A4, IL1B = interleukin 1 beta, IL6 = interleukin 6, MMP3 = matrix metallopeptidase 3, NGF = nerve growth factor, PTGS2 = prostaglandin-

endoperoxide synthase 2, RARA = Retinoic Acid Receptor Alpha, RARB = Retinoic Acid Receptor Beta, RARG = Retinoic Acid Receptor Gamma, TIMP1 = TIMP metallopeptidase inhibitor 1.

A

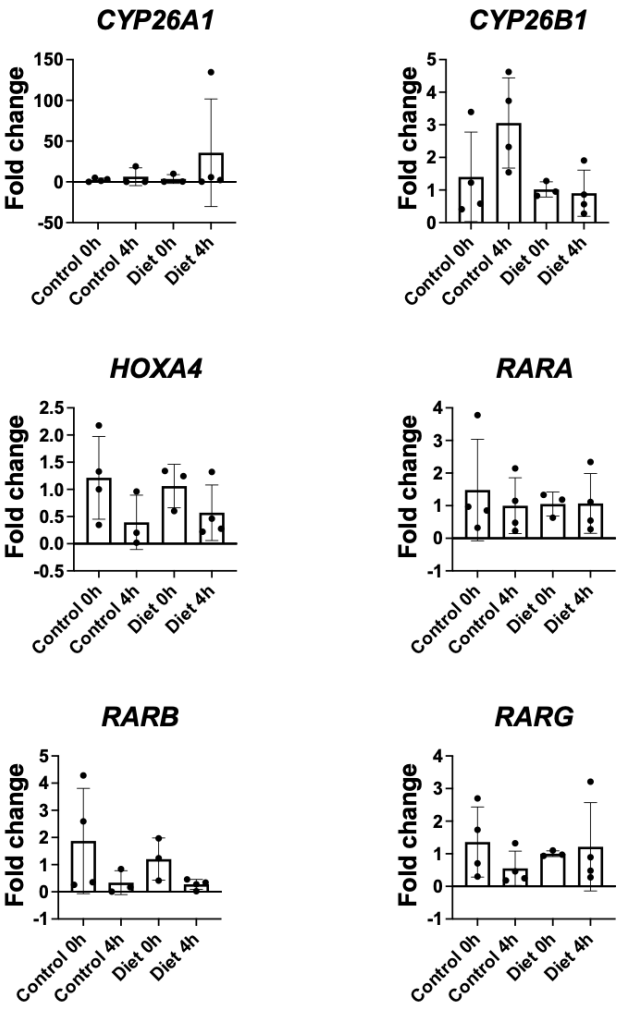
CYP26A1
Fold change
150
100
50
0
-50
Control 0h
Control 4h
Diet 0h
Diet 4h
CYP26B1
Fold change
5
4
3
2
1
0
Control 0h
Control 4h
Diet 0h
Diet 4h
HOXA4
Fold change
2.5
2.0
1.5
1.0
0.5
0.0
-0.5
Control 0h
Control 4h
Diet 0h
Diet 4h
RARA
Fold change
4
3
2
1
0
-1
Control 0h
Control 4h
Diet 0h
Diet 4h
RARB
Fold change
5
4
3
2
1
0
-1
Control 0h
Control 4h
Diet 0h
Diet 4h
RARG
Fold change
4
3
2
1
0
-1
Control 0h
Control 4h
Diet 0h
Diet 4h

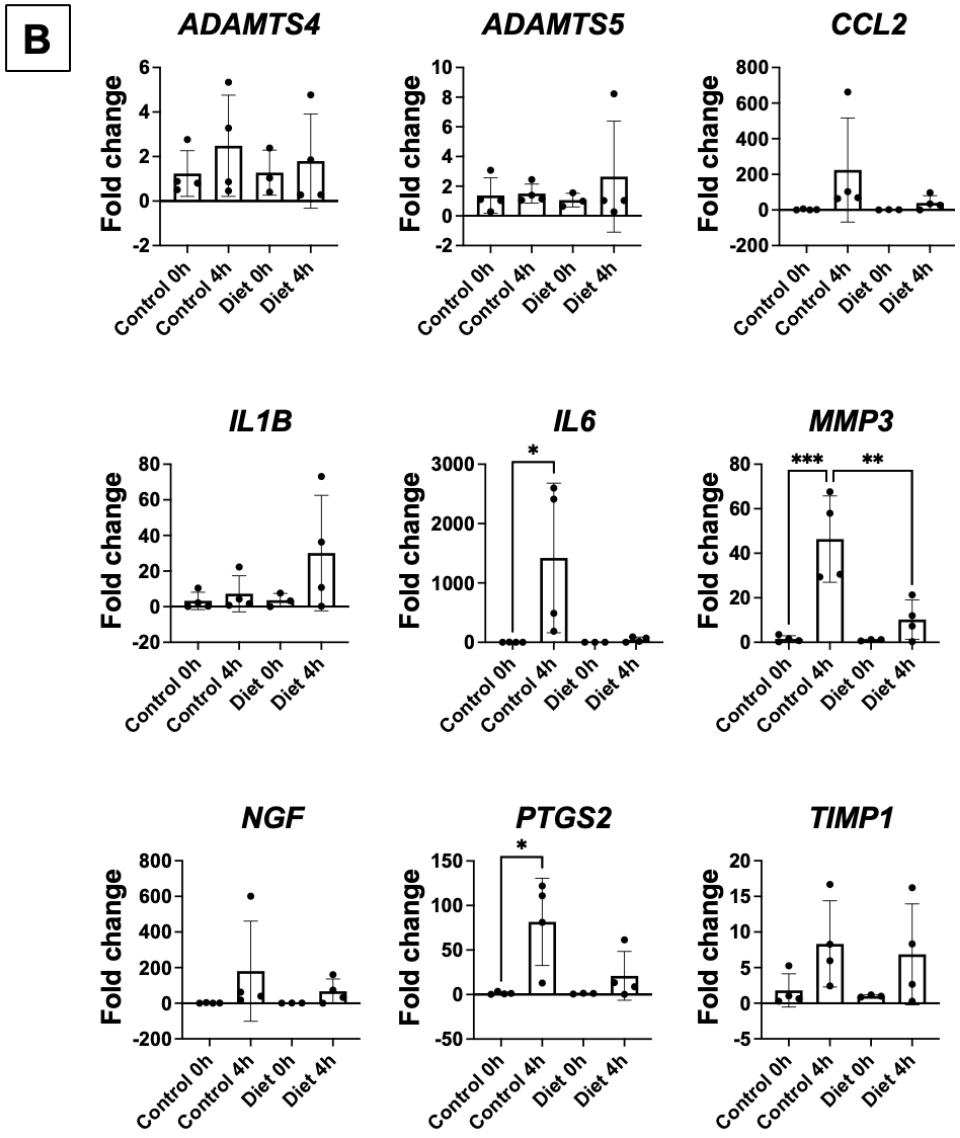

Figure 5.3: Comparison of inflammatory and atRA-responsive gene expression in normal diet (Control) vs modified diet (Diet) mice
Mice were culled by CO_2, and the acetabulofemoral (hip) joints were exposed by blunt dissection. The cartilaginous femoral cap was avulsed using forceps. Murine hip cartilage was avulsed directly into serum-free DMEM and incubated for 4 hours at 37°C, then snap frozen at -80°C. RNA was subsequently extracted from the tissue and used in a microfluidic gene expression array to measure a panel of (A) atRA-response genes and (B) inflammatory genes. 18S was used as the housekeeping gene. Statistical significance of comparison between treatment groups was conducted using a two-way ANOVA, with post-hoc multiple comparisons corrected using Tukey's tests. Bars shows the mean ± SEM of at least 3 independent experiments. * = $p<0.05$; ** = $p<0.01$; *** = $p<0.001$. ADAMTS4 = ADAM metallopeptidase with thrombospondin type 1 motif 4, ADAMTS5 = ADAM metallopeptidase with thrombospondin type 1 motif 5, CCL2 = C-C motif chemokine ligand 2, CYP26A1 = Cytochrome P450 Family 26 Subfamily A Member 1, CYP26B1 = Cytochrome P450 Family 26 Subfamily B Member 1, HOXA4 =

homeobox A4, IL1B = interleukin 1 beta, IL6 = interleukin 6, MMP3 = matrix metallopeptidase 3, NGF = nerve growth factor, PTGS2 = prostaglandin-endoperoxide synthase 2, RARA = Retinoic Acid Receptor Alpha, RARB = Retinoic Acid Receptor Beta, RARG = Retinoic Acid Receptor Gamma, TIMP1 = TIMP metallopeptidase inhibitor 1.

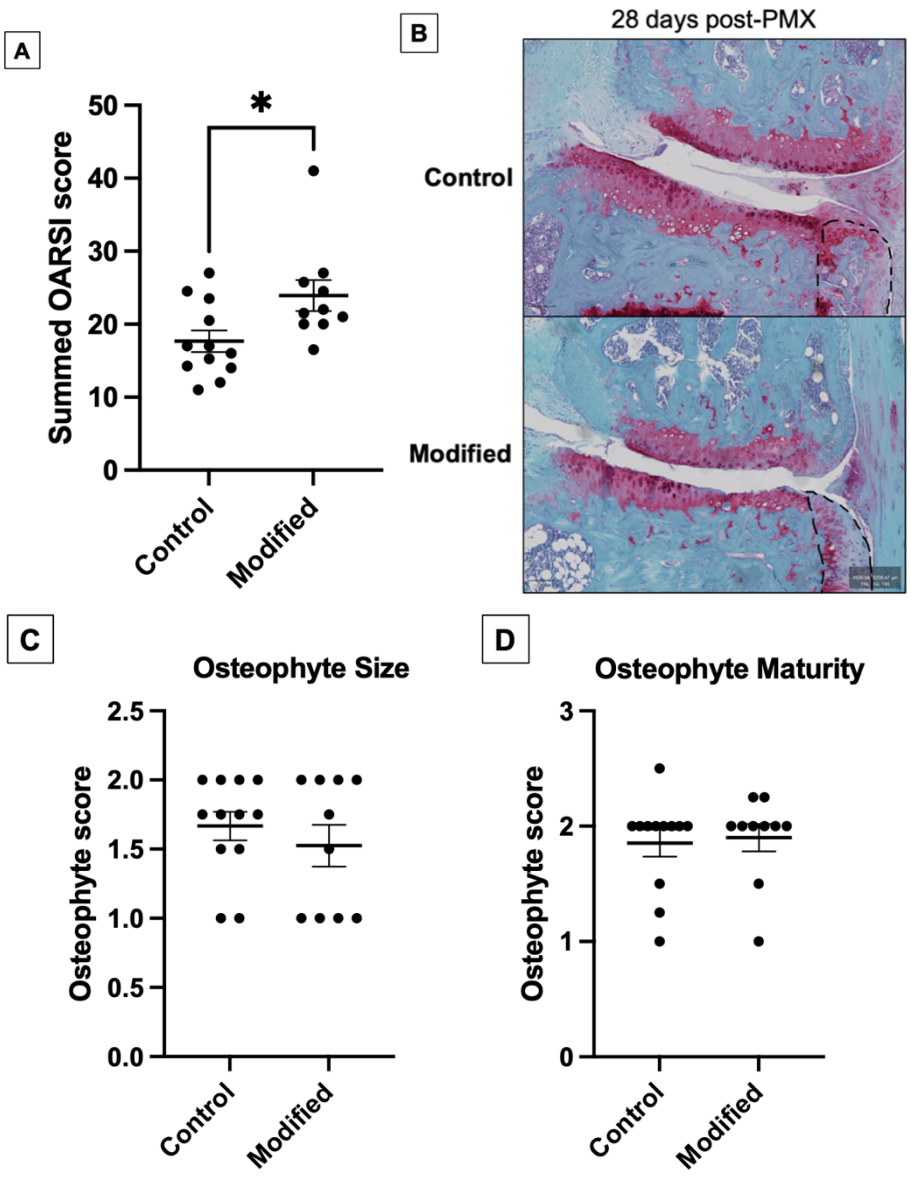

Figure 5.4: Mice fed with modified diet show increased cartilage damage after PMX surgery.
Partial removal of the medial meniscus (PMX) surgery was conducted in 15 week old male C57BL/6 mice, culled 28 days post-surgery for histological analysis (A) Modified OARSI scores (mean ± SEM) of Control (normal diet) (n=12) or Modified (Modified diet) (n=10). Statistical significance of comparison between treatment groups was conducted using an unpaired, non-parametric t-test. (B) Representative Safranin O stained images of Control (normal diet) or Modified (Modified diet) mouse medial joint sections (cartilage, red).Osteophyte scores of control diet (n=12) or modified diet mice (n=10), based on (C) size or (D) maturity. Osteophyte regions are outlined in black dotted line. Statistical significance of comparison between treatment groups was conducted using an unpaired, non-parametric t-test. Bars shows the mean ± SEM of at least 3 independent experiments. * = $p<0.05$; ** = $p<0.01$; *** = $p<0.001$

Bars shows the mean ± SEM of at least 3 independent experiments. * = $p<0.05$; ** = $p<0.01$; *** = $p<0.001$

5.2 Oral administration of ASK1 inhibitor (serlonsertib) has no effect on the development of post-traumatic OA

To follow on directly from my previous mechanoflammation work in cartilage injury responses, I also tested whether oral administration of serlonsertib could modify in vivo cartilage injury after surgical destabilisation of the joint (by partial meniscectomy). Due to a delay in delivery of serlonsertib, post-traumatic OA was induced in 15-week old C57BL/6 male mice (5 weeks later than our usual protocol) by partial medial meniscectomy (PMX). Mice received ASK1i or vehicle control by gavage daily for 28 days after PMX surgery. Joints were harvested and osteoarthritis severity was assessed by histology; OARSI scoring and osteophyte scoring are presented in Figure 5.5.

A small, non-statistically significant reduction in histological cartilage degradation was seen in the ASK1i group (p=0.5922) (Figure 5.5A) with represented histology shown in Figure 5.5B. Two very high outliers in the ASK1i group may have skewed the score. There was not difference between osteophyte size or maturity between the two groups (Figure 5.4C,D). Overall, no significant differences in cartilage damage or osteophyte severity can seen.

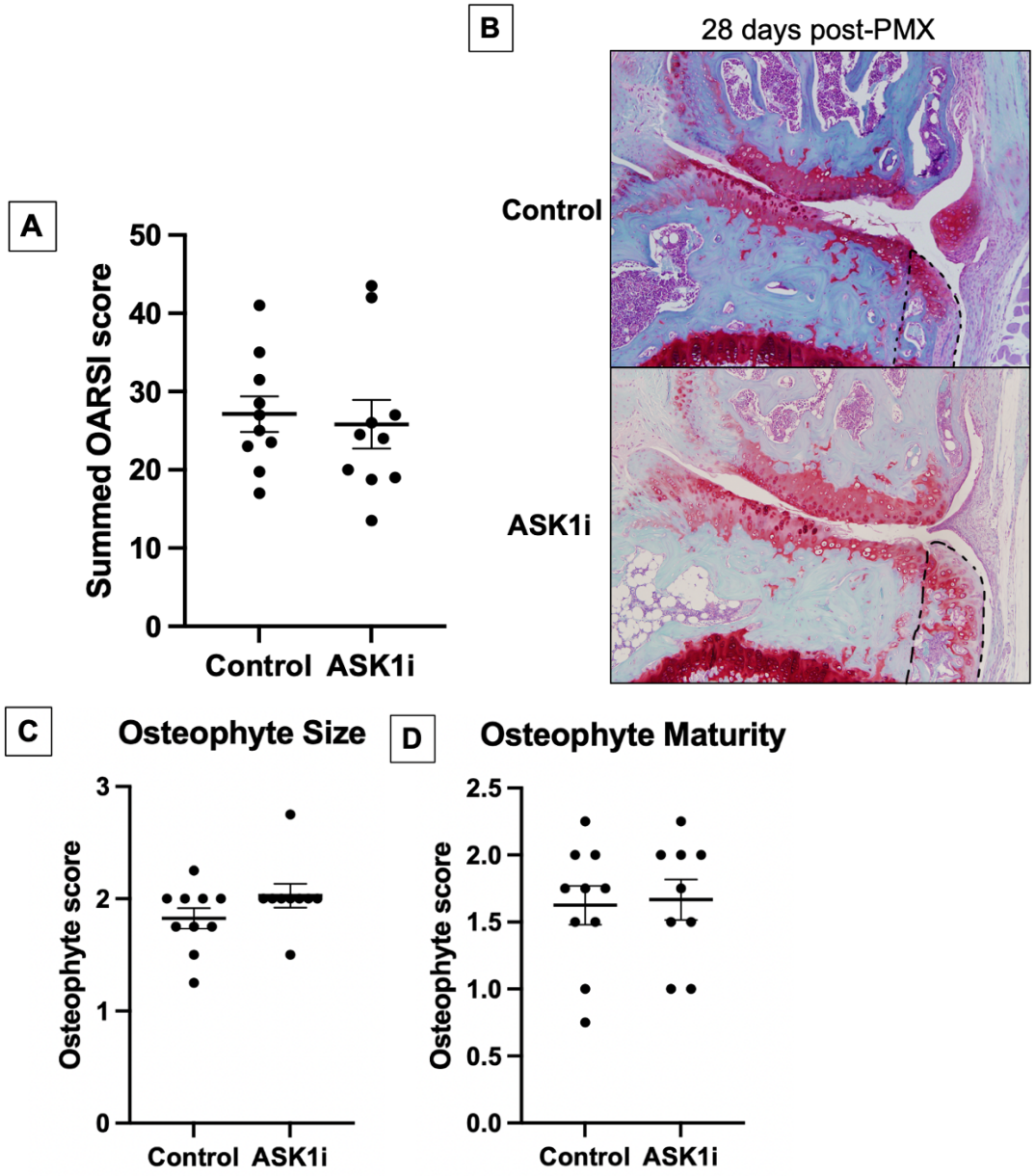

Figure 5.5: Mice administrated with ASK1i did not affect cartilage damage or osteophyte development after PMX surgery.
Partial removal of the medial meniscus (PMX) surgery was conducted in 15 week old male C57BL/6 mice, culled 28 days post-surgery for histological analysis (A) Representative Safranin O stained images of Control or ASK1i mouse medial joint sections (cartilage, red). (B) Modified OARSI scores (mean ± SEM) of control and ASK1i mice (n=10). Osteophyte scores of control (n=10) and ASK1i mice (n=9), based on (C) size or (D) maturity. Osteophyte regions are outlined in black dotted line. Statistical significance of comparison between treatment groups was conducted using an unpaired, non-parametric t-test. Bars shows the mean ± SEM of at least 3 independent experiments. * = $p<0.05$; ** = $p<0.01$; *** = $p<0.001$

Discussion

In this chapter I attempted to examine pathways relevant to mechanoflammation in vivo. I first validated whether I could test the regulation of mechano-inflammatory genes upon injury. I used the JNK2$^{-/-}$ mouse which was available in our unit and where the observed response to hip injury was already known. I observed a response to hip injury in both wildtype and JNK2$^{-/-}$ hips that was similar, as expected, to wildtype. Even though JNK2$^{-/-}$ mice were significantly protected from surgically induced OA, JNK2 does not appear to have a direct role in induction of mechano-inflammatory genes (Ismail H et al., 2016). Rather, it seems that JNK2 influences Complex 1 of the mitochondria by changing several of the genes involved in the electron transport chain (Ismail et al, unpublished data).

I attempted to influence the mechano-inflammatory pathways in vivo using two approaches. Firstly by modifying the PUFAs in the cell membrane to test whether oxidative stress on these was driving a sizeable part of the mechano-inflammatory response, and secondly, by in vivo ASK1 inhibition using serlonsertib. I observed that incorporating a oxidative-resistant diet to mice for just 3 weeks appeared to suppress some of the inflammatory genes regulated by hip avulsion, but 6 week pre-feeding was unable to suppress cartilage damage after partial meniscectomy. Indeed, I actually observed a significant increase in cartilage damage by histology assessment. This conflicted with my expectations as I hypothesised less ROS/oxidation-induced adverse effects on cartilage in the modified diet group. There are several possible explanations for this. It could be that there were inadequate amounts of deuterated PUFA incorporated into the membrane of articular chondrocytes due to low incorporation of knee articular chondrocytes as

these cells are probably not turning over during the treatment window (chondrocyte turnover is extremely low post-natally). We would need to measure phospholipids from the chondrocyte membranes by mass spectrometry to establish this which was beyond the scope of my project. I could have perhaps also used labelled deuterated compounds to track the deuterated compounds in joint tissue. The mechanism of PUFA incorporation into chondrocytes is not known, but there are previous reports that a change in dietary fat content can accelerate OA development (Harasymowicz N et al., 2019). These studies report that the elevated fat content induces pro-inflammatory signals, such as HIF-1a, VEGF and interleukins (Harasymowicz N et al., 2019). The deuterated compound in the modified diet for this experiment is arachidonic acid. Prostaglandins, the derivatives of arachidonic acid, have been implicated in OA. Prostaglandins have been reported to inhibit chondrocyte differentiation through activation of protein kinase A/C pathways (Li T et al., 2004). Prostaglandin E synthases (PGESs) and cyclooxygenase-2 (COX2) catalyse arachidonic acid into prostaglandins and mediates pro-inflammatory processes in OA (Kojima F et al., 2004). An anti-inflammatory effect has been demonstrated in animal models whereby altering dietary PUFA intake resolved inflammatory response to a number of inflammatory and immune diseases (Calder P et al., 2002). Inflammation can be aggravated with the intake of some dietary fatty acids that are incorporated into the synthesis of membrane phospholipids (Raphael W et al., 2013). There has been a wide range of evidence suggesting that PUFA abundance and intake is directly associated with inflammatory-based pathologies such as cancer, rheumatoid arthritis, atherosclerosis, and obesity (Raphael W et al., 2013). Suppression of arachidonic acid in this experiment was expected to alleviate the inflammatory response due to alteration of pro-inflammatory prostanoid signals.

However, dietary intake of certain PUFAs can impact the biosynthesis of phospholipid-derived lipid mediators that can have pro- as well as anti-inflammatory effects (Calder P et al., 2002). Prostaglandins, leukotrienes, lipoxins and other lipid metabolites not only possess pro-inflammatory roles but also take part in resolution of inflammation (Sugimoto M et al., 2016). These pro-resolving lipids are called ‘resolvins’, aid the resolving phase of inflammation to initiate tissue repair (Loynes C et al., 2018). Resolving pathways target the clearance of inflammatory stimuli and mediators, to dampen any active pro-inflammatory signals (Fullerton J et al., 2016). It is also likely that the alteration of arachidonic acid by deuteration in this experiment hindered the synthesis arachidonic acid-derived resolvins, thereby inhibiting the resolving effects that arachidonic acid and its downstream metabolites provide. Because of the key roles that arachidonic acid plays in pro- and anti-inflammation, inhibiting or modifying it may be a double-edged sword. Indeed, in this case, inhibiting the pathway at the top appears to have caused worsening of disease rather than improvement.

The deuterated diet in this experiment didn’t fully inhibit inflammatory gene regulation on cartilage injury. Only *Mmp3* expression was significantly inhibited in the modified diet group, while *Il6* and *Ptgs* also showed an encouraging anti-inflammatory trend in the modified diet group, albeit non-statistically significant. In the control diet group, most atRA-response genes did decrease upon injury, but diet did not seem to change the trend. It has been reported that a high-fat diet rich in omega-3 fatty acids reduced OA in a guinea pig model, including the suppression of the *Adamts’* and *Mmp3* mRNA (Curtis C et al., 2000). Arachidonic acid is upstream of lipoxygenases as well as cyclooxygenases and it is the former, specifically 12/15 LOX, that

controls the levels of atRA and hence regulation of inflammatory genes (Kamalathevan et al., unpublished data). It is possible, therefore, that inhibition of mechanoflammation in vivo may be more easily realised by moving further down the pathway below the level of arachidonic acid.

The concept of deuterating PUFA compounds has been performed before, in the context of neurodegenerative diseases. PUFAs are essential in the maintenance of the lipids, especially in the nervous system where oxidative stress to PUFAs can lead to the pathological development of several neuronal diseases (Shchepinov M., 2020). Callaghan et al. demonstrated that deuteration of PUFAs provided protection against oxidative stress in ocular fibroblasts derived from glaucoma tissue (Callaghan B et al., 2023). A different study showed that deuteration of docosahexaenoic acid protected against iron-induced oxidative stress in atrophy-like retinal degeneration (Liu Y et al., 2022). In fact, one group currently have a phase 3 clinical trial underway that involves the use of a deuterated linethyl ester-incorporated diet to treat Friedreich ataxia (Shchepinov M., 2020). The use of deuteration as a technique to reduce ROS-induced effects in OA or cartilage has never been performed before.

I also focused on the role of an ASK1i (serlonsertib) on cartilage damage and osteophyte severity in this chapter. Oral administration serlonsertib did not protect against cartilage damage and osteophyte development after partial meniscectomy. This observation did not align with our hypothesis, as we expected that inhibition of ASK1, a driver of mechanoflammation, would suppress mechanoflammation and reduce cartilage damage in the murine PMX model. As introduced earlier in Yan et al., intra-articular injection of serlonsertib prevented cartilage destruction in rats following anterior cruciate

ligament transection and partial medial meniscectomy (Yan J et al., 2021). They observed a significantly lower OARSI score in the serlonsertib group (PMX surgery + intra-articular injection of 25μM serlonsertib once a week) compared to the OA group (PMX surgery + intra-articular injection of equal volume of sterile saline once a week), and immunohistochemistry showed a decrease in COX2, MMP13 and caspase-3 expression in cartilage tissue with serlonsertib treatment. Our current study was somewhat complicated by the fact that the mice we performed this on were already 15 weeks old at the time of surgery. Despite running the model for only four weeks, the mice had very severe disease. It is possible that a therapeutic response might more easily be seen in a slower progressing model.

The disparities in the biological effects of serlonsertib on cartilage between the Yan study and my one may be due to differences in administration, although it is unclear whether administration routes actually affect drug concentrations cartilage. Administration doses in my experiments were also similar to Yan et al.'s study. To address whether oral dosing does get into the cartilage, it might be worth doing the hip avulsion model in mice that have been dosed with serlonsertib for a few days prior to injury. This would at least tell us that serlonsertib penetrates cartilage and can affect mechano-inflammatory gene regulation ex vivo. Even if it is successful, however, there is also the possibility that chondrocytes of the articular cartilage are harder to reach than the majority of chondrocytes that make up the hip (largely hypertrophic chondrocytes of the future 2nd ossification centre, and growth plate chondrocytes, with a few articular chondrocytes).

CHAPTER 6: FINAL DISCUSSION

The work of this thesis builds on previous discoveries of the Vincent laboratory that inflammatory signaling cascades are activated upon cartilage injury (a process termed mechanoflammation). We revealed that MAPKs and NF-κB signals are activated, led by the upstream MAP3K TAK1 (Vincent T et al., 2019). The activation of mechanoflammation results in the induction of a host of inflammatory genes, that promote the production of matrix-degrading enzymes and inflammatory mediators. The consequence of this is cartilage degradation and pain in the joint. The upstream activator to injury is not known but it is believed to be neither soluble nor secreted upon cartilage injury (Ismail H et al., 2017). Prior to the start of my MSc(Res), our group showed that ASK1 MAP3K was a driver of MAPKs (JNK and ERK) and inflammatory genes on cartilage injury (Figure 1.7). In our system and in other OA-related reports, ASK1 is highly ROS-dependant (Zhang Q et al., 2016). Between ASK1 and TAK1, TAK1 is important in many physiological functions, given that constitutive knockout of TAK1 is embryonic lethal. Thus, ASK1 might represent a more refined target for pharmaceutical intervention of OA especially as pharmacological agents have already been tested in phase III clinical trials (for liver disease).

To further build upon our group's findings on ASK1, it became my primary objective for this MSc(Res) to investigate the role of ASK1 in cartilage injury. ASK1 is known to be a mechanotransducer, although its mechano-sensing properties had yet to be studied in cartilage (Matsui H et al., 2014; Tang R et al., 2022). I showed that ASK1 is activated and phosphorylated upon injury. This observation was associated ASK1's accumulation on the total protein level. Furthermore, I showed that ASK1's accumulation occurred in a

proteasome-dependant manner. Together, these findings were supportive of other studies which reported that ASK1 activation causes stabilisation of the protein, becoming more resistant to proteasomal degradation (Nagai H et al., 2009).

I also investigated the effect of IL1 or ROS stimulation on signaling in chondrocytes in vitro. Both IL1 and ROS have been highly implicated in OA, by driving degradative, apoptotic and inflammatory responses (Dinarello C., 2011; Drevet S et al., 2018; Li D et al., 2012). Many IL1 and ROS-induced pathways overlap, such as the MAPKs, which were studied in this work in chondrocytes (Meves A et al., 2001). I showed that IL1 or H_2O_2 treatment of chondrocytes activated MAPKs and NF-κB in a transient manner. Surprisingly, I observed that only IL1 but not H_2O_2 stimulation caused ASK1 accumulation. Since I previously associated ASK1's activation to its accumulation, I expected ASK1 activation by oxidative stress to also induce ASK1 protein accumulation. Furthermore, it had been widely reported in many cell systems (including chondrocytes) that ASK1 is activated by oxidative stress and ROS (Zhang Q et al., 2016). Further repeats or higher concentrations of H_2O_2 may be required to see a statistically significant effect. It may be the case that my chondrocyte cell culture model is flawed for examining oxidative stress stimulation because exposure of isolated chondrocytes to atmospheric oxygen levels in culture may alter endogenous antioxidant systems and oxygen sensitivity. The ASK1 inhibitory protein, Trx, is also an antioxidant and is likely altered by partial oxygen fluctuations. It is perhaps also important to note that the injury response observed by our group also occurs when injury is performed under hypoxic conditions, and it is not the exposure to atmospheric oxygen for the first time that leads to ROS-dependent inflammatory signalling (Kamalathevan et al., unpublished

data). Upon the addition of an ASK1 inhibitor (serlonsertib) to the IL1- or H_2O_2-induced chondrocyte cultures, I expected MAPKs to be inhibited, as ASK1 has been shown to mediate these pathways in other systems (Eaton G et al., 2013). However, my observations were not consistent with this. Addition of serlonsertib had no apparent effect on p38 MAPK activation in either IL1- or H_2O_2-induced chondrocyte cultures. The reason for this observation is difficult to explain, but it may be due to unknown off-target effects of serlonsertib on the MAPKs. A number of ASK1 inhibitors have been developed, but serlonsertib was chosen for current and past work in our group since it is the most extensively studied and most used in research (Ogier J et al., 2020). Serlonsertib is the only known ASK1 inhibitor that has progressed to clinical trials. The mechanism of action for serlonsertib has been reported to inhibit the catalytic kinase domain of ASK1 (Bunkoczi G et al., 2007). Currently, 12 phospho-sites of ASK1 have been identified, of which 2 are functionally characterised (Betanzos C et al., 2016). The involvement of unknown phospho-sites for ASK1 in this work is definitely a possibility.

In this thesis, I used serlonsertib in in vivo, ex vivo and in vitro models. Serlonsertib injection into the ex vivo porcine cartilage injury model did suppress ASK1 accumulation as expected, but its usage in mice and chondrocytes did not follow expectations. The role of ASK1 in OA has been studied. ASK1 total KO mice are viable, and show no growth or developmental abnormalities (Ogier J et al., 2020). ASK1 total KO mice were protected from developing OA in a joint destabilisation (DMM) or partial meniscectomy (PMX) model, as reflected by cartilage damage and osteophyte volume assessment (Zhang Q et al., 2016). In this work, strong statistical significance ($p<0.01$) was achieved in both PMX and DMM ($n=13$ for both) ASK1 total KO models, which was reassuring (Zhang Q et al.,

2016). In my work I investigated the effect of oral administration of an ASK1 inhibitor (serlonsertib) on the development of post-traumatic OA in mice. Based on assessment of cartilage damage and osteophyte severity, treatment of serlonsertib had no effect on OA development. This observation was not in line with a previous report that intra-articular injection of serlonsertib alleviates rat OA (Yan J et al., 2021). Serlonsertib has been used in non-OA related clinical trials, with the most recent one being a phase 3 trial for treatment of non-alcoholic steatohepatitis (NASH), a fibrotic liver disease (Harrison S et al., 2020). In that trial, serlonsertib led to dose-dependent reductions in hepatic p38 activation, which was indicative of target engagement (Harrison S et al., 2020). Unfortunately, serlonsertib had no significant effect on liver biochemistry, cirrhosis progression and adjudicated clinical events. Side effects of serlonsertib were similar between treatment and placebo groups (Harrison S et al., 2020). Overall, I was unable to demonstrate therapeutic efficacy of serlonsertib. In view of the benefits already demonstrated by ASK1 inhibition by others and the strong in vitro data that support its use in OA, it may be worth considering slightly different approaches to drug delivery and assessment. This might include putting the drug into chow so that the mice receive a more continuous dose, or using the inhibitor is a slightly less aggressive model in which more subtle changes may be more easy to demonstrate.

While chronic mechanoflammation is considered deleterious in cartilage injury, it is important to appreciate that there is likely to be a benefit to the acute inflammatory response. Tissue injury generally incites inflammation prior to repair. This may help to ensure that the wound is sterile before repair occurs, but it is also likely to be important to drawing the correct repair-promoting cells into the joint and to help remodel the damaged tissue before

repair occurs. The incorporation of the modified to mice from weaning at 3-4 weeks prior to PMX surgery may have incited an early protective response which affected the natural injurious response at the time of PMX surgery. This may have rendered the protectiveness of the diet less effective compared to feeding the mice the modified diet immediately post-surgery. Thus, it is worth repeating this experiment by feeding the modified diet to mice post-surgery, to attain a better picture of the modified diet's ability to alter the acute inflammatory response and subsequent OA development phase. As with the ASK1i in vivo experiment, the mice were administered the ASK1i post-surgery up till culling, thus it could be hypothesised that the ASK1i is important in the acute post-surgery phase to aid cartilage homeostasis and may suggest a rationale whereby the diet showed a worse outcome due to early inhibition.

Cartilage injury also leads to the release of sequestered growth factors and regulatory molecules in the PCM, such as FGF2, TGFβ, HDGF and CTGF (Tang X et al., 2018, Vincent T et al. 2007). Both FGF and TGFβ, considered pro-regenerative growth factors, are deemed as good clinical predictors when measured in synovial fluid over the course of a joint distraction suggesting their importance in the joint when the cartilage is repairing (Watt F et al., 2020). Prior to this thesis, our group speculated that TGFβ may be one of the drivers responsible for TAK1 activation upon injury, as TAK1 has been historically described as a downstream target of TGFβ signaling. In this thesis, I saw that stimulation of chondrocytes with TGFβ activated inflammatory MAPKs in a transient manner indicating that it likely contributes to the mechano-inflammatory response. It would be interesting to use the TGFβ inhibitor to measure what the relative contribution of TGFβ is to the mechano-inflammatory response after cartilage explantation. My work also

showed that YAP is stimulated upon cartilage injury. Previous work from our lab has shown that YAP mRNA induction occurs in a highly FGF2-dependent fashion, indicating that the YAP pathway is activated upon release of pericellular FGF2 in the acute injury response (unpublished data, Vincent group). YAP has been reported to facilitate chondrocyte differentiation but inhibit chondrocyte maturation (Zarka M et al., 2021). Importantly, YAP has been reported to reciprocally inhibit TAK1 to modulate downstream NF-kB signaling in chondrocytes (Deng Y et al., 2018), thus suggesting the potential for targeting YAP to indirectly modulate mechanoflammation. How these chondroprotective responses interact with mechanoflammation at the intracellular level is not known, but it appears that they act synergistically and in a coordinated fashion when the tissue is injured. Whilst it may have beneficial effects in the acute scenario, we presume that chronic mechanoflammation, which occurs in OA, is detrimental and it is this that needs to be inhibited if we are to slow disease.

Our group previously investigated the effect that lipid peroxidation of PUFAs play in mechanoflammation. ROS-induced lipid peroxidation products, such as 4-Hydroxynonenal (4-HNE) were implicated OA (Vaillancourt F et al., 2008) and were shown by Kamalathevan to cause a reduction in atRA, as had previously been demonstrated by others. Our group identified cPLA2, the enzyme responsible for the liberation of arachidonic acid from PUFAs in the lipid bilayer to drive mechanoflammation (Kamalathevan et al., unpublished data). This was supported by findings that anti-oxidative agents can reduce mechanoflammation pathways and gene expression (Figure 1.5). In this thesis, I investigated the effect of a oxidation-resistant deuterated diet on murine OA. Interestingly, cartilage damage by histological assessment was higher in the modified diet groups than control groups. Low deuteration of

compounds, even water, give antioxidant effects, but excessive deuteration can also promote cell damage and cell death (Zhang X et al., 2020). For example, the deuterium/hydrogen ratio in cancer cells has been reported to regulate entry into cell cycle phases (Somlyai G et al., 2010). Modification of arachidonic acid may have also altered the anti-inflammatory (pro-resolving) effects of arachidonic acid and its derivatives, thus leading to impaired resolution of inflammation. Thus, it may be possible that the amount of deuteration in the modified diet caused more adverse than protective effects upon incorporation into cartilage. As a next step, it would be helpful to measure whether ROS molecules or lipid peroxidation metabolites can regulate by mechanical injury by reporter assay or mass spectroscopy.

Taken together my data have added to a large body of data that has arisen from our lab that mechanoflammation is an important driver of OA. I have added novel insights on the activation and stabilisation of ASK1 in cartilage, described for the first time the phosphorylation of YAP on injury, and tested new mechano-inflammatory pathway inhibition in vivo. Future work will continue to refine our understanding and define the most promising targets for future clinical studies.

7: REFERENCES

Ahmad R, Sylvester J, Zafarullah M. MyD88, IRAK1 and TRAF6 knockdown in human chondrocytes inhibits interleukin-1-induced matrix metalloproteinase-13 gene expression and promoter activity by impairing MAP kinase activation. Cell Signal. 2007;19(12):2549-57.

Akkiraju H, Nohe A. Role of Chondrocytes in Cartilage Formation, Progression of Osteoarthritis and Cartilage Regeneration. J Dev Biol. 2015;3(4):177-92.

Altay MA, Erturk C, Bilge A, Yapti M, Levent A, Aksoy N. Evaluation of prolidase activity and oxidative status in patients with knee osteoarthritis: relationships with radiographic severity and clinical parameters. Rheumatol Int. 2015;35(10):1725-31.

Altindag O, Erel O, Aksoy N, Selek S, Celik H, Karaoglanoglu M. Increased oxidative stress and its relation with collagen metabolism in knee osteoarthritis. Rheumatol Int. 2007;27(4):339-44.

Aragon E, Goerner N, Xi Q, Gomes T, Gao S, Massague J, et al. Structural basis for the versatile interactions of Smad7 with regulator WW domains in TGF-beta Pathways. Structure. 2012;20(10):1726-36.

Archer CW, Francis-West P. The chondrocyte. The international journal of biochemistry & cell biology. 2003;35(4):401-4.

Asada S, Fukuda K, Nishisaka F, Matsukawa M, Hamanisi C. Hydrogen peroxide induces apoptosis of chondrocytes; involvement of calcium ion and extracellular signal-regulated protein kinase. Inflamm Res. 2001;50(1):19-23.

Ayala A, Munoz MF, Arguelles S. Lipid peroxidation: production, metabolism, and signaling mechanisms of malondialdehyde and 4-hydroxy-2-nonenal. Oxid Med Cell Longev. 2014;2014:360438.

Bashir A, Gray ML, Boutin RD, Burstein D. Glycosaminoglycan in articular cartilage: in vivo assessment with delayed Gd(DTPA)(2-)-enhanced MR imaging. Radiology. 1997;205(2):551-8.

Bedard K, Krause KH. The NOX family of ROS-generating NADPH oxidases: physiology and pathophysiology. Physiol Rev. 2007;87(1):245-313.

Beecher BR, Martin JA, Pedersen DR, Heiner AD, Buckwalter JA. Antioxidants block cyclic loading induced chondrocyte death. Iowa Orthop J. 2007;27:1-8.

Berenbaum F, Eymard F, Houard X. Osteoarthritis, inflammation and obesity. Current opinion in rheumatology. 2013 Jan 1;25(1):114-8.

Blaney Davidson EN, Remst DF, Vitters EL, van Beuningen HM, Blom AB, Goumans MJ, et al. Increase in ALK1/ALK5 ratio as a cause for elevated MMP-13 expression in osteoarthritis in humans and mice. J Immunol. 2009;182(12):7937-45.

Boileau C, Martel-Pelletier J, Brunet J, Schrier D, Flory C, Boily M, et al. PD-0200347, an alpha2delta ligand of the voltage gated calcium channel, inhibits in vivo activation of the Erk1/2 pathway in osteoarthritic chondrocytes: a PKCalpha dependent effect. Ann Rheum Dis. 2006;65(5):573-80.

Borreguero-Munoz N, Fletcher GC, Aguilar-Aragon M, Elbediwy A, Vincent-Mistiaen ZI, Thompson BJ. The Hippo pathway integrates PI3K-Akt signals with mechanical and polarity cues to control tissue growth. PLoS Biol. 2019;17(10):e3000509.

Borrelli Jr J, Olson SA, Godbout C, Schemitsch EH, Stannard JP, Giannoudis PV. Understanding articular cartilage injury and potential treatments. Journal of orthopaedic trauma. 2019;33:S6-S12.

Bougault C, Gosset M, Houard X, Salvat C, Godmann L, Pap T, et al. Stress-induced cartilage degradation does not depend on the NLRP3 inflammasome in human osteoarthritis and mouse models. Arthritis Rheum. 2012;64(12):3972-81.

Boulton TG, Yancopoulos GD, Gregory JS, Slaughter C, Moomaw C, Hsu J, et al. An insulin-stimulated protein kinase similar to yeast kinases involved in cell cycle control. Science. 1990;249(4964):64-7.

Brown KK, Heitmeyer SA, Hookfin EB, Hsieh L, Buchalova M, Taiwo YO, et al. P38 MAP kinase inhibitors as potential therapeutics for the treatment of joint degeneration and pain associated with osteoarthritis. J Inflamm (Lond). 2008;5:22.

Buckwalter J, Mankin H. Articular cartilage: tissue design and chondrocyte-matrix interactions. Instructional course lectures. 1998;47:477-86.

Bunkoczi G, Salah E, Filippakopoulos P, Fedorov O, Muller S, Sobott F, et al. Structural and functional characterization of the human protein kinase ASK1. Structure. 2007;15(10):1215-26.

Burleigh A, Chanalaris A, Gardiner MD, Driscoll C, Boruc O, Saklatvala J, et al. Joint immobilization prevents murine osteoarthritis and reveals the highly mechanosensitive nature of protease expression in vivo. Arthritis Rheum. 2012;64(7):2278-88.

Calder PC, Grimble RF. Polyunsaturated fatty acids, inflammation and immunity. Eur J Clin Nutr. 2002;56 Suppl 3:S14-9.

Callaghan B, Vallabh NA, Willoughby CE. Deuterated polyunsaturated fatty acids provided protection against oxidative stress in ocular fibroblasts derived from glaucoma patients. Mechanisms of ageing and development. 2023;211:111778.

Cargnello M, Roux PP. Activation and function of the MAPKs and their substrates, the MAPK-activated protein kinases. Microbiol Mol Biol Rev. 2011;75(1):50-83.

Chance B, Sies H, Boveris A. Hydroperoxide metabolism in mammalian organs. Physiological reviews. 1979 Jul;59(3):527-605.

Chang L, Marston G, Martin A. Anatomy, Cartilage. StatPearls. StatPearls Publishing LLC.: Treasure Island, FL, USA; 2022.

Chapnick DA, Warner L, Bernet J, Rao T, Liu X. Partners in crime: the TGFbeta and MAPK pathways in cancer progression. Cell Biosci. 2011;1:42.

Chen A, Balogun-Lynch J, Aggarwal K, Dick E, Gupte CM. Should all elective knee radiographs requested by general practitioners be performed weight-bearing?. Springerplus. 2014 Dec;3(1):1-5.

Chen CT, Burton-Wurster N, Borden C, Hueffer K, Bloom SE, Lust G. Chondrocyte necrosis and apoptosis in impact damaged articular cartilage. J Orthop Res. 2001;19(4):703-11.

Chen LX, Lin L, Wang HJ, Wei XL, Fu X, Zhang JY, et al. Suppression of early experimental osteoarthritis by in vivo delivery of the adenoviral vector-mediated NF-kappaBp65-specific siRNA. Osteoarthritis Cartilage. 2008;16(2):174-84.

Cheng J, Hu X, Dai L, Zhang X, Ren B, Shi W, et al. Inhibition of transforming growth factor beta-activated kinase 1 prevents inflammation-related cartilage degradation in osteoarthritis. Sci Rep. 2016;6:34497.

Chertow GM, Pergola PE, Chen F, Kirby BJ, Sundy JS, Patel UD, et al. Effects of Selonsertib in Patients with Diabetic Kidney Disease. J Am Soc Nephrol. 2019;30(10):1980-90.

Chevalier X, Goupille P, Beaulieu AD, Burch FX, Bensen WG, Conrozier T, et al. Intraarticular injection of anakinra in osteoarthritis of the knee: a multicenter, randomized, double-blind, placebo-controlled study. Arthritis Rheum. 2009;61(3):344-52.

Chia SL, Sawaji Y, Burleigh A, McLean C, Inglis J, Saklatvala J, et al. Fibroblast growth factor 2 is an intrinsic chondroprotective agent that suppresses ADAMTS-5 and delays cartilage degradation in murine osteoarthritis. Arthritis Rheum. 2009;60(7):2019-27.

Choi MC, Jo J, Park J, Kang HK, Park Y. NF-kappaB Signaling Pathways in Osteoarthritic Cartilage Destruction. Cells. 2019;8(7).

Choi ME, Ding Y, Kim SI. TGF-beta signaling via TAK1 pathway: role in kidney fibrosis. Semin Nephrol. 2012;32(3):244-52.

Chong KW, Chanalaris A, Burleigh A, Jin H, Watt FE, Saklatvala J, et al. Fibroblast growth factor 2 drives changes in gene expression following injury to murine cartilage in vitro and in vivo. Arthritis Rheum. 2013;65(9):2346-55.

Chu M, Zhu X, Wang C, Rong J, Wang Y, Wang S, et al. The rs4238326 polymorphism in ALDH1A2 gene potentially associated with non-post traumatic knee osteoarthritis susceptibility: a two-stage population-based study. Osteoarthritis Cartilage. 2017;25(7):1062-7.

Clements KM, Price JS, Chambers MG, Visco DM, Poole AR, Mason RM. Gene deletion of either interleukin-1beta, interleukin-1beta-converting enzyme, inducible nitric oxide synthase, or stromelysin 1 accelerates the development of knee osteoarthritis in mice after surgical transection of the medial collateral ligament and partial medial meniscectomy. Arthritis Rheum. 2003;48(12):3452-63.

Cohen SB, Proudman S, Kivitz AJ, Burch FX, Donohue JP, Burstein D, et al. A randomized, double-blind study of AMG 108 (a fully human monoclonal antibody to IL-1R1) in patients with osteoarthritis of the knee. Arthritis Res Ther. 2011;13(4):R125.

Conde J, Scotece M, Abella V, Lois A, Lopez V, Garcia-Caballero T, et al. IL-36alpha: a novel cytokine involved in the catabolic and inflammatory response in chondrocytes. Sci Rep. 2015;5:16674.

Correa D, Lietman SA, editors. Articular cartilage repair: current needs, methods and research directions. Seminars in cell & developmental biology; 2017: Elsevier.

Culley KL, Lessard SG, Green JD, Quinn J, Chang J, Khilnani T, et al. Inducible knockout of CHUK/IKKα in adult chondrocytes reduces progression of cartilage degradation in a surgical model of osteoarthritis. Scientific Reports. 2019;9(1):8905.

Curtis CL, Hughes CE, Flannery CR, Little CB, Harwood JL, Caterson B. n-3 fatty acids specifically modulate catabolic factors involved in articular cartilage degradation. J Biol Chem. 2000;275(2):721-4.

D'Lima DD, Hashimoto S, Chen PC, Colwell CW, Jr., Lotz MK. Human chondrocyte apoptosis in response to mechanical injury. Osteoarthritis Cartilage. 2001;9(8):712-9.

Dabrowski A, Boguslowicz C, Dabrowska M, Tribillo I, Gabryelewicz A. Reactive oxygen species activate mitogen-activated protein kinases in pancreatic acinar cells. Pancreas. 2000;21(4):376-84.

De Fusco C, Messina A, Monda V, Viggiano E, Moscatelli F, Valenzano A, et al. Osteopontin: Relation between Adipose Tissue and Bone Homeostasis. Stem Cells Int. 2017;2017:4045238.

Decker RS, Koyama E, Pacifici M. Articular Cartilage: Structural and Developmental Intricacies and Questions. Curr Osteoporos Rep. 2015;13(6):407-14.

Deng Y, Wu A, Li P, Li G, Qin L, Song H, et al. Yap1 Regulates Multiple Steps of Chondrocyte Differentiation during Skeletal Development and Bone Repair. Cell Rep. 2016;14(9):2224-37.

Denoble AE, Huffman KM, Stabler TV, Kelly SJ, Hershfield MS, McDaniel GE, et al. Uric acid is a danger signal of increasing risk for osteoarthritis through inflammasome activation. Proc Natl Acad Sci U S A. 2011;108(5):2088-93.

Di-Luoffo M, Ben-Meriem Z, Lefebvre P, Delarue M, Guillermet-Guibert J. PI3K functions as a hub in mechanotransduction. Trends Biochem Sci. 2021;46(11):878-88.

Dinarello CA. Interleukin-1 and interleukin-1 antagonism. Blood. 1991;77(8):1627-52.

Dinarello CA. Immunological and inflammatory functions of the interleukin-1 family. Annu Rev Immunol. 2009;27:519-50.

Dinarello CA. Interleukin-1 in the pathogenesis and treatment of inflammatory diseases. Blood. 2011;117(14):3720-32.

Dingle JT, Page Thomas DP, King B, Bard DR. In vivo studies of articular tissue damage mediated by catabolin/interleukin 1. Ann Rheum Dis. 1987;46(7):527-33.

Dossumbekova A, Anghelina M, Madhavan S, He L, Quan N, Knobloch T, et al. Biomechanical signals inhibit IKK activity to attenuate NF-kappaB transcription activity in inflamed chondrocytes. Arthritis Rheum. 2007;56(10):3284-96.

Dreier R. Hypertrophic differentiation of chondrocytes in osteoarthritis: the developmental aspect of degenerative joint disorders. Arthritis Res Ther. 2010;12(5):216.

Drevet S, Gavazzi G, Grange L, Dupuy C, Lardy B. Reactive oxygen species and NADPH oxidase 4 involvement in osteoarthritis. Exp Gerontol. 2018;111:107-17.

Drexler S, Wann A, Vincent TL. Are cellular mechanosensors potential therapeutic targets in osteoarthritis? International Journal of Clinical Rheumatology. 2014;9(2):155.

Dupont S, Morsut L, Aragona M, Enzo E, Giulitti S, Cordenonsi M, et al. Role of YAP/TAZ in mechanotransduction. Nature. 2011;474(7350):179-83.

Eaton G, Diallo C, Freeman T. Oxidative stress activates apoptosis signal-regulated kinase (ASK1) in articular chondrocytes. Osteoarthritis and Cartilage. 2013;21:S131-S2.

Eaton GJ, Zhang QS, Diallo C, Matsuzawa A, Ichijo H, Steinbeck MJ, et al. Inhibition of apoptosis signal-regulating kinase 1 enhances endochondral bone formation by increasing chondrocyte survival. Cell Death Dis. 2014;5(11):e1522.

Eyre DR, Weis MA, Wu JJ. Articular cartilage collagen: an irreplaceable framework? Eur Cell Mater. 2006;12:57-63.

Falchuk KH, Goetzl EJ, Kulka JP. Respiratory gases of synovial fluids. An approach to synovial tissue circulatory-metabolic imbalance in rheumatoid arthritis. Am J Med. 1970;49(2):223-31.

Fan Z, Soder S, Oehler S, Fundel K, Aigner T. Activation of interleukin-1 signaling cascades in normal and osteoarthritic articular cartilage. Am J Pathol. 2007;171(3):938-46.

Fanning PJ, Emkey G, Smith RJ, Grodzinsky AJ, Szasz N, Trippel SB. Mechanical regulation of mitogen-activated protein kinase signaling in articular cartilage. J Biol Chem. 2003;278(51):50940-8.

Farnaghi S, Prasadam I, Cai G, Friis T, Du Z, Crawford R, et al. Protective effects of mitochondria-targeted antioxidants and statins on cholesterolinduced osteoarthritis. The FASEB Journal. 2017;31(1):356-67.

Fermor B, Christensen SE, Youn I, Cernanec JM, Davies CM, Weinberg JB. Oxygen, nitric oxide and articular cartilage. Eur Cell Mater. 2007;13:56-65; discussion

Fermor B, Youn I, Christensen S, Guilak F, editors. The influence of oxygen tension on matrix turnover and physical properties of articular cartilage. Proc 50th Annual Meeting, Orthopaedic Research Society, San Francisco, CA, abstract; 2004.

Fernández-Moreno M, Rego I, Carreira-Garcia V, Blanco FJ. Genetics in osteoarthritis. Current genomics. 2008 Dec 1;9(8):542-7.

Firsov AM, Franco MSF, Chistyakov DV, Goriainov SV, Sergeeva MG, Kotova EA, et al. Deuterated polyunsaturated fatty acids inhibit photoirradiation-induced lipid peroxidation in lipid bilayers. J Photochem Photobiol B. 2022;229:112425.

Fleischmann RM, Bliddal H, Blanco FJ, Schnitzer TJ, Peterfy C, Chen S, et al. A Phase II Trial of Lutikizumab, an Anti-Interleukin-1alpha/beta Dual Variable Domain Immunoglobulin, in Knee Osteoarthritis Patients With Synovitis. Arthritis Rheumatol. 2019;71(7):1056-69.

Forstermann U, Sessa WC. Nitric oxide synthases: regulation and function. Eur Heart J. 2012;33(7):829-37, 37a-37d.

Fu L, Hu Y, Song M, Liu Z, Zhang W, Yu FX, et al. Up-regulation of FOXD1 by YAP alleviates senescence and osteoarthritis. PLoS Biol. 2019;17(4):e3000201.

Fujino G, Noguchi T, Matsuzawa A, Yamauchi S, Saitoh M, Takeda K, et al. Thioredoxin and TRAF family proteins regulate reactive oxygen species-dependent activation of ASK1 through reciprocal modulation of the N-terminal homophilic interaction of ASK1. Mol Cell Biol. 2007;27(23):8152-63.

Fukai A, Kamekura S, Chikazu D, Nakagawa T, Hirata M, Saito T, et al. Lack of a chondroprotective effect of cyclooxygenase 2 inhibition in a surgically induced model of osteoarthritis in mice. Arthritis Rheum. 2012;64(1):198-203.

Fullerton JN, Gilroy DW. Resolution of inflammation: a new therapeutic frontier. Nature reviews Drug discovery. 2016;15(8):551-67.

Gao G, Ding H, Zhuang C, Fan W. Effects of Hesperidin on H(2)O(2)-Treated Chondrocytes and Cartilage in a Rat Osteoarthritis Model. Med Sci Monit. 2018;24:9177-86.

Gao SG, Li KH, Zeng KB, Tu M, Xu M, Lei GH. Elevated osteopontin level of synovial fluid and articular cartilage is associated with disease severity in knee osteoarthritis patients. Osteoarthritis Cartilage. 2010;18(1):82-7.

Gao ST, Lv ZT, Sheng WB. The association between rs12901499 polymorphism in SMAD3 gene and risk of osteoarthritis: a meta-analysis. Therapeutics and clinical risk management. 2018 May 15:929-36.

Ge HX, Zou FM, Li Y, Liu AM, Tu M. JNK pathway in osteoarthritis: pathological and therapeutic aspects. J Recept Signal Transduct Res. 2017;37(5):431-6.

Gelse K, Soder S, Eger W, Diemtar T, Aigner T. Osteophyte development--molecular characterization of differentiation stages. Osteoarthritis Cartilage. 2003;11(2):141-8.

Gery I, Gershon RK, Waksman BH. Potentiation of the T-lymphocyte response to mitogens. I. The responding cell. J Exp Med. 1972;136(1):128-42.

Glasson SS. In vivo osteoarthritis target validation utilizing genetically-modified mice. Curr Drug Targets. 2007;8(2):367-76.

Goldman EH, Chen L, Fu H. Activation of apoptosis signal-regulating kinase 1 by reactive oxygen species through dephosphorylation at serine 967 and 14-3-3 dissociation. Journal of Biological Chemistry. 2004;279(11):10442-9.

Goldring MB. Articular cartilage degradation in osteoarthritis. HSS J. 2012;8(1):7-9.

Goldring SR, Goldring MB. The role of cytokines in cartilage matrix degeneration in osteoarthritis. Clin Orthop Relat Res. 2004(427 Suppl):S27-36.

Gong Y, Li SJ, Liu R, Zhan JF, Tan C, Fang YF, et al. Inhibition of YAP with siRNA prevents cartilage degradation and ameliorates osteoarthritis development. J Mol Med (Berl). 2019;97(1):103-14.

Grange L, Nguyen MV, Lardy B, Derouazi M, Campion Y, Trocme C, et al. NAD(P)H oxidase activity of Nox4 in chondrocytes is both inducible and involved in collagenase expression. Antioxid Redox Signal. 2006;8(9-10):1485-96.

Gross O, Thomas CJ, Guarda G, Tschopp J. The inflammasome: an integrated view. Immunol Rev. 2011;243(1):136-51.

Gruber J, Vincent TL, Hermansson M, Bolton M, Wait R, Saklatvala J. Induction of interleukin-1 in articular cartilage by explantation and cutting. Arthritis Rheum. 2004;50(8):2539-46.

Guilak F, Nims RJ, Dicks A, Wu CL, Meulenbelt I. Osteoarthritis as a disease of the cartilage pericellular matrix. Matrix Biol. 2018;71-72:40-50.

Guingamp C, Gegout-Pottie P, Philippe L, Terlain B, Netter P, Gillet P. Mono-iodoacetate-induced experimental osteoarthritis: a dose-response study of loss of mobility, morphology, and biochemistry. Arthritis Rheum. 1997;40(9):1670-9.

Halder G, Dupont S, Piccolo S. Transduction of mechanical and cytoskeletal cues by YAP and TAZ. Nat Rev Mol Cell Biol. 2012;13(9):591-600.

Hame SL, Alexander RA. Knee osteoarthritis in women. Current reviews in musculoskeletal medicine. 2013 Jun;6:182-7.

Harasymowicz NS, Dicks A, Wu CL, Guilak F. Physiologic and pathologic effects of dietary free fatty acids on cells of the joint. Annals of the New York Academy of Sciences. 2019;1440(1):36-53.

Harrison SA, Wong VW, Okanoue T, Bzowej N, Vuppalanchi R, Younes Z, et al. Selonsertib for patients with bridging fibrosis or compensated cirrhosis due to NASH: Results from randomized phase III STELLAR trials. J Hepatol. 2020;73(1):26-39.

Hashimoto S, Takahashi K, Amiel D, Coutts RD, Lotz M. Chondrocyte apoptosis and nitric oxide production during experimentally induced osteoarthritis. Arthritis Rheum. 1998;41(7):1266-74.

Hayakawa R, Hayakawa T, Takeda K, Ichijo H. Therapeutic targets in the ASK1-dependent stress signaling pathways. Proc Jpn Acad Ser B Phys Biol Sci. 2012;88(8):434-53.

Hedbom E, Heinegard D. Binding of fibromodulin and decorin to separate sites on fibrillar collagens. J Biol Chem. 1993;268(36):27307-12.

Heidari B. Knee osteoarthritis prevalence, risk factors, pathogenesis and features: Part I. Caspian journal of internal medicine. 2011;2(2):205.

Henrotin Y, Deby-Dupont G, Deby C, De Bruyn M, Lamy M, Franchimont P. Production of active oxygen species by isolated human chondrocytes. Br J Rheumatol. 1993;32(7):562-7.

Henrotin Y, Kurz B, Aigner T. Oxygen and reactive oxygen species in cartilage degradation: friends or foes? Osteoarthritis and cartilage. 2005;13(8):643-54.

Hermansson MA. Application of proteomics to analysis of chondrocyte gene expression. 2003.

Hiran TS, Moulton PJ, Hancock JT. Detection of superoxide and NADPH oxidase in porcine articular chondrocytes. Free Radic Biol Med. 1997;23(5):736-43.

Hunter DJ, Schofield D, Callander E. The individual and socioeconomic impact of osteoarthritis. Nat Rev Rheumatol. 2014;10(7):437-41.

Ismail HM, Didangelos A, Vincent TL, Saklatvala J. Rapid Activation of Transforming Growth Factor beta-Activated Kinase 1 in Chondrocytes by Phosphorylation and K(63) -Linked Polyubiquitination Upon Injury to Animal Articular Cartilage. Arthritis Rheumatol. 2017;69(3):565-75.

Ismail HM, Miotla-Zarebska J, Troeberg L, Tang X, Stott B, Yamamoto K, et al. Brief Report: JNK-2 Controls Aggrecan Degradation in Murine Articular Cartilage and the Development of Experimental Osteoarthritis. Arthritis Rheumatol. 2016;68(5):1165-71.

Ismail HM, Yamamoto K, Vincent TL, Nagase H, Troeberg L, Saklatvala J. Interleukin-1 acts via the JNK-2 signaling pathway to induce aggrecan degradation by human chondrocytes. Arthritis & rheumatology. 2015;67(7):1826-36.

Israel A. The IKK complex, a central regulator of NF-kappaB activation. Cold Spring Harb Perspect Biol. 2010;2(3):a000158.

Jenei-Lanzl Z, Meurer A, Zaucke F. Interleukin-1beta signaling in osteoarthritis - chondrocytes in focus. Cell Signal. 2019;53:212-23.

Jeong JW, Lee HH, Choi EO, Lee KW, Kim KY, Kim SG, et al. Schisandrae Fructus Inhibits IL-1beta-Induced Matrix Metalloproteinases and Inflammatory Mediators Production in SW1353 Human Chondrocytes by Suppressing NF-kappaB and MAPK Activation. Drug Dev Res. 2015;76(8):474-83.

Johnson K, Jung A, Murphy A, Andreyev A, Dykens J, Terkeltaub R. Mitochondrial oxidative phosphorylation is a downstream regulator of nitric oxide effects on chondrocyte matrix synthesis and mineralization. Arthritis Rheum. 2000;43(7):1560-70.

Joosten LA, Smeets RL, Koenders MI, van den Bersselaar LA, Helsen MM, Oppers-Walgreen B, et al. Interleukin-18 promotes joint inflammation and induces interleukin-1-driven cartilage destruction. Am J Pathol. 2004;165(3):959-67.

Kania K, Colella F, Riemen AHK, Wang H, Howard KA, Aigner T, et al. Regulation of Gdf5 expression in joint remodelling, repair and osteoarthritis. Sci Rep. 2020;10(1):157.

Karystinou A, Roelofs AJ, Neve A, Cantatore FP, Wackerhage H, De Bari C. Yes-associated protein (YAP) is a negative regulator of chondrogenesis in mesenchymal stem cells. Arthritis Res Ther. 2015;17(1):147.

Kim H, Seo J, Lee Y, Park K, Perry TA, Arden NK, et al. The current state of the osteoarthritis drug development pipeline: a comprehensive narrative review of the present challenges and future opportunities. Ther Adv Musculoskelet Dis. 2022;14:1759720X221085952.

Kim SI, Kwak JH, Na HJ, Kim JK, Ding Y, Choi ME. Transforming growth factor-beta (TGF-beta1) activates TAK1 via TAB1-mediated autophosphorylation, independent of TGF-beta receptor kinase activity in mesangial cells. J Biol Chem. 2009;284(33):22285-96.

Klatt AR, Klinger G, Neumuller O, Eidenmuller B, Wagner I, Achenbach T, et al. TAK1 downregulation reduces IL-1beta induced expression of MMP13, MMP1 and TNF-alpha. Biomed Pharmacother. 2006;60(2):55-61.

Klatt AR, Klinger G, Paul-Klausch B, Renno JH, Schmidt J, Malchau G, et al. TAK1 mediates the collagen-II-dependent induction of the COX-2 gene and PGE2 release in primary human chondrocytes. Connect Tissue Res. 2010;51(6):452-8.

Kloppenburg M, Peterfy C, Haugen IK, Kroon F, Chen S, Wang L, et al. Phase IIa, placebo-controlled, randomised study of lutikizumab, an anti-interleukin-1alpha and anti-interleukin-1beta dual variable domain immunoglobulin, in patients with erosive hand osteoarthritis. Ann Rheum Dis. 2019;78(3):413-20.

Kobayashi H, Hirata M, Saito T, Itoh S, Chung UI, Kawaguchi H. Transcriptional induction of ADAMTS5 protein by nuclear factor-kappaB (NF-kappaB) family member RelA/p65 in chondrocytes during osteoarthritis development. J Biol Chem. 2013;288(40):28620-9.

Kojima F, Naraba H, Miyamoto S, Beppu M, Aoki H, Kawai S. Membrane-associated prostaglandin E synthase-1 is upregulated by proinflammatory cytokines in chondrocytes from patients with osteoarthritis. Arthritis Res Ther. 2004;6(4):R355-65.

Kuwano Y, Gorospe M. Protecting the stress response, guarding the MKP-1 mRNA. Cell Cycle. 2008;7(17):2640-2.

Kyriakis JM, Avruch J. Mammalian mitogen-activated protein kinase signal transduction pathways activated by stress and inflammation. Physiol Rev. 2001;81(2):807-69.

Lamplot JD, Bansal A, Nguyen JT, Brophy RH. Risk of subsequent joint arthroplasty in contralateral or different joint after index shoulder, hip, or knee arthroplasty: association with index joint, demographics, and patient-specific factors. The Journal of Bone and Joint surgery. American Volume. 2018 Oct 10;100(20):1750.

Latourte A, Cherifi C, Maillet J, Ea HK, Bouaziz W, Funck-Brentano T, et al. Systemic inhibition of IL-6/Stat3 signalling protects against experimental osteoarthritis. Ann Rheum Dis. 2017;76(4):748-55.

Lee J, Hong YS, Jeong JH, Yang EJ, Jhun JY, Park MK, et al. Coenzyme Q10 ameliorates pain and cartilage degradation in a rat model of osteoarthritis by regulating nitric oxide and inflammatory cytokines. PLoS One. 2013;8(7):e69362.

Lee W, Leddy HA, Chen Y, Lee SH, Zelenski NA, McNulty AL, et al. Synergy between Piezo1 and Piezo2 channels confers high-strain mechanosensitivity to articular cartilage. Proc Natl Acad Sci U S A. 2014;111(47):E5114-22.

Lepetsos P, Papavassiliou AG. ROS/oxidative stress signaling in osteoarthritis. Biochim Biophys Acta. 2016;1862(4):576-91.

Li D, Xie G, Wang W. Reactive oxygen species: the 2-edged sword of osteoarthritis. Am J Med Sci. 2012;344(6):486-90.

Li G, Yin J, Gao J, Cheng TS, Pavlos NJ, Zhang C, et al. Subchondral bone in osteoarthritis: insight into risk factors and microstructural changes. Arthritis research & therapy. 2013;15:1-12.

Li J, Wang X, Ruan G, Zhu Z, Ding C. Sprifermin: a recombinant human fibroblast growth factor 18 for the treatment of knee osteoarthritis. Expert Opin Investig Drugs. 2021;30(9):923-30.

Li T, Chubinskaya S, Esposito A, Jin X, Tagliafierro L, Loeser R, et al. TGF-beta type 2 receptor-mediated modulation of the IL-36 family can be therapeutically targeted in osteoarthritis. Sci Transl Med. 2019;11(491).

Li T, Peng J, Li Q, Shu Y, Zhu P, Hao L. The Mechanism and Role of ADAMTS Protein Family in Osteoarthritis. Biomolecules. 2022;12(7).

Li TF, Zuscik MJ, Ionescu AM, Zhang X, Rosier RN, Schwarz EM, et al. PGE2 inhibits chondrocyte differentiation through PKA and PKC signaling. Exp Cell Res. 2004;300(1):159-69.

Li Y, Frank EH, Wang Y, Chubinskaya S, Huang HH, Grodzinsky AJ. Moderate dynamic compression inhibits pro-catabolic response of cartilage to mechanical injury, tumor necrosis factor-alpha and interleukin-6, but accentuates degradation above a strain threshold. Osteoarthritis Cartilage. 2013;21(12):1933-41.

Liacini A, Sylvester J, Li WQ, Zafarullah M. Inhibition of interleukin-1-stimulated MAP kinases, activating protein-1 (AP-1) and nuclear factor kappa B (NF-kappa B) transcription factors down-regulates matrix metalloproteinase gene expression in articular chondrocytes. Matrix Biol. 2002;21(3):251-62.

Lianxu C, Hongti J, Changlong Y. NF-kappaBp65-specific siRNA inhibits expression of genes of COX-2, NOS-2 and MMP-9 in rat IL-1beta-induced and TNF-alpha-induced chondrocytes. Osteoarthritis Cartilage. 2006;14(4):367-76.

Lin JH, Zhang JJ, Lin SL, Chertow GM. Design of a phase 2 clinical trial of an ASK1 inhibitor, GS-4997, in patients with diabetic kidney disease. Nephron. 2015;129(1):29-33.

Little CB, Barai A, Burkhardt D, Smith SM, Fosang AJ, Werb Z, et al. Matrix metalloproteinase 13-deficient mice are resistant to osteoarthritic cartilage erosion but not chondrocyte hypertrophy or osteophyte development. Arthritis Rheum. 2009;60(12):3723-33.

Liu SC, Lee HP, Hung CY, Tsai CH, Li TM, Tang CH. Berberine attenuates CCN2-induced IL-1beta expression and prevents cartilage degradation in a rat model of osteoarthritis. Toxicol Appl Pharmacol. 2015;289(1):20-9.

Liu T, Zhang L, Joo D, Sun SC. NF-kappaB signaling in inflammation. Signal Transduct Target Ther. 2017;2:17023-.

Liu Y, Bell BA, Song Y, Zhang K, Anderson B, Axelsen PH, et al. Deuterated docosahexaenoic acid protects against oxidative stress and geographic atrophy-like retinal degeneration in a mouse model with iron overload. Aging Cell. 2022;21(4):e13579.

Loomba R, Lawitz E, Mantry PS, Jayakumar S, Caldwell SH, Arnold H, et al. The ASK1 inhibitor selonsertib in patients with nonalcoholic steatohepatitis: A randomized, phase 2 trial. Hepatology. 2018;67(2):549-59.

Lou G, Li A, Cen Y, Yang Q, Zhang T, Qi J, et al. Selonsertib, a potential drug for liver failure therapy by rescuing the mitochondrial dysfunction of macrophage via ASK1–JNK–DRP1 pathway. Cell & bioscience. 2021;11(1):1-13.

Loynes CA, Lee JA, Robertson AL, Steel MJ, Ellett F, Feng Y, et al. PGE(2) production at sites of tissue injury promotes an anti-inflammatory neutrophil phenotype and determines the outcome of inflammation resolution in vivo. Sci Adv. 2018;4(9):eaar8320.

Lushchak VI. Glutathione homeostasis and functions: potential targets for medical interventions. J Amino Acids. 2012;2012:736837.

Ma B, Hottiger MO. Crosstalk between Wnt/beta-Catenin and NF-kappaB Signaling Pathway during Inflammation. Front Immunol. 2016;7:378.

Madhavan S, Anghelina M, Sjostrom D, Dossumbekova A, Guttridge DC, Agarwal S. Biomechanical signals suppress TAK1 activation to inhibit NF-kappaB transcriptional activation in fibrochondrocytes. J Immunol. 2007;179(9):6246-54.

Mao X, Fu P, Wang L, Xiang C. Mitochondria: Potential Targets for Osteoarthritis. Front Med (Lausanne). 2020;7:581402.

Martel-Pelletier J, Barr AJ, Cicuttini FM, Conaghan PG, Cooper C, Goldring MB, et al. Osteoarthritis. Nature Reviews Disease Primers. 2016;2(1):16072.

Martel-Pelletier J, Mineau F, Jovanovic D, Di Battista JA, Pelletier JP. Mitogen-activated protein kinase and nuclear factor kappaB together regulate interleukin-17-induced nitric oxide production in human osteoarthritic chondrocytes: possible role of transactivating factor mitogen-activated protein kinase-activated proten kinase (MAPKAPK). Arthritis Rheum. 1999;42(11):2399-409.

Martin G, Andriamanalijaona R, Mathy-Hartert M, Henrotin Y, Pujol JP. Comparative effects of IL-1beta and hydrogen peroxide (H2O2) on catabolic and anabolic gene expression in juvenile bovine chondrocytes. Osteoarthritis Cartilage. 2005;13(10):915-24.

Massam-Wu T, Chiu M, Choudhury R, Chaudhry SS, Baldwin AK, McGovern A, et al. Assembly of fibrillin microfibrils governs extracellular deposition of latent TGF beta. J Cell Sci. 2010;123(Pt 17):3006-18.

Mathy-Hartert M, Deby-Dupont GP, Reginster JY, Ayache N, Pujol JP, Henrotin YE. Regulation by reactive oxygen species of interleukin-1beta, nitric oxide and prostaglandin E(2) production by human chondrocytes. Osteoarthritis Cartilage. 2002;10(7):547-55.

Matsui H, Fukuno N, Kanda Y, Kantoh Y, Chida T, Nagaura Y, et al. The expression of Fn14 via mechanical stress-activated JNK contributes to apoptosis induction in osteoblasts. Journal of Biological Chemistry. 2014;289(10):6438-50.

Meijles DN, Cull JJ, Markou T, Cooper ST, Haines ZH, Fuller SJ, et al. Redox regulation of cardiac ASK1 (apoptosis signal-regulating kinase 1) controls p38-MAPK (mitogen-activated protein kinase) and orchestrates cardiac remodeling to hypertension. Hypertension. 2020;76(4):1208-18.

Mendes AF, Caramona MM, Carvalho AP, Lopes MC. Differential roles of hydrogen peroxide and superoxide in mediating IL-1-induced NF-kappa B activation and iNOS expression in bovine articular chondrocytes. J Cell Biochem. 2003;88(4):783-93.

Mendoza H, Campbell DG, Burness K, Hastie J, Ronkina N, Shim JH, et al. Roles for TAB1 in regulating the IL-1-dependent phosphorylation of the TAB3 regulatory subunit and activity of the TAK1 complex. Biochem J. 2008;409(3):711-22.

Meves A, Stock SN, Beyerle A, Pittelkow MR, Peus D. H(2)O(2) mediates oxidative stress-induced epidermal growth factor receptor phosphorylation. Toxicol Lett. 2001;122(3):205-14.

Minas T, Gomoll AH, Solhpour S, Rosenberger R, Probst C, Bryant T. Autologous chondrocyte implantation for joint preservation in patients with early osteoarthritis. Clinical Orthopaedics and Related Research®. 2010 Jan;468:147-57.

Minato M, Kubota S, Kawaki H, Nishida T, Miyauchi A, Hanagata H, et al. Module-specific antibodies against human connective tissue growth factor: utility for structural and functional analysis of the factor as related to chondrocytes. J Biochem. 2004;135(3):347-54.

Miranda FF, Thórólfsson M, Teigen K, Sanchez-Ruiz JM, Martínez A. Structural and stability effects of phosphorylation: Localized structural changes in phenylalanine hydroxylase. Protein science. 2004;13(5):1219-26.

Mo JS, Park HW, Guan KL. The Hippo signaling pathway in stem cell biology and cancer. EMBO Rep. 2014;15(6):642-56.

Mochida Y, Takeda K, Saitoh M, Nishitoh H, Amagasa T, Ninomiya-Tsuji J, et al. ASK1 inhibits interleukin-1-induced NF-kappa B activity through disruption of TRAF6-TAK1 interaction. J Biol Chem. 2000;275(42):32747-52.

Moldovan F, Pelletier JP, Jolicoeur FC, Cloutier JM, Martel-Pelletier J. Diacerhein and rhein reduce the ICE-induced IL-1beta and IL-18 activation in human osteoarthritic cartilage. Osteoarthritis Cartilage. 2000;8(3):186-96.

Monteagudo S, Cornelis FMF, Wang X, de Roover A, Peeters T, Quintiens J, et al. ANP32A represses Wnt signaling across tissues thereby protecting against osteoarthritis and heart disease. Osteoarthritis Cartilage. 2022;30(5):724-34.

Morales Betanzos C, Federspiel JD, Palubinsky AM, McLaughlin B, Liebler DC. Dynamic Phosphorylation of Apoptosis Signal Regulating Kinase 1 (ASK1) in Response to Oxidative and Electrophilic Stress. Chem Res Toxicol. 2016;29(12):2175-83.

Morrison DK. MAP kinase pathways. Cold Spring Harb Perspect Biol. 2012;4(11).

Muir H. The chondrocyte, architect of cartilage. Biomechanics, structure, function and molecular biology of cartilage matrix macromolecules. Bioessays. 1995;17(12):1039-48.

Murahashi Y, Yano F, Kobayashi H, Makii Y, Iba K, Yamashita T, et al. Intra-articular administration of IkappaBalpha kinase inhibitor suppresses mouse knee osteoarthritis via downregulation of the NF-kappaB/HIF-2alpha axis. Sci Rep. 2018;8(1):16475.

Murphy CL. What makes the permanent articular cartilage permanent? : Wiley Subscription Services, Inc., A Wiley Company Hoboken; 2011. p. 2564-6.

Murphy MP. How mitochondria produce reactive oxygen species. Biochem J. 2009;417(1):1-13.

Nagai H, Noguchi T, Homma K, Katagiri K, Takeda K, Matsuzawa A, et al. Ubiquitin-like sequence in ASK1 plays critical roles in the recognition and stabilization by USP9X and oxidative stress-induced cell death. Molecular cell. 2009;36(5):805-18.

Nagai H, Noguchi T, Takeda K, Ichijo H. Pathophysiological roles of ASK1-MAP kinase signaling pathways. J Biochem Mol Biol. 2007;40(1):1-6.

Nakashima I, Takeda K, Kawamoto Y, Okuno Y, Kato M, Suzuki H. Redox control of catalytic activities of membrane-associated protein tyrosine kinases. Arch Biochem Biophys. 2005;434(1):3-10.

Nam J, Aguda BD, Rath B, Agarwal S. Biomechanical thresholds regulate inflammation through the NF-kappaB pathway: experiments and modeling. PLoS One. 2009;4(4):e5262.

Napoli JL. Physiological insights into all-trans-retinoic acid biosynthesis. Biochim Biophys Acta. 2012;1821(1):152-67.

Nemirovskiy OV, Radabaugh MR, Aggarwal P, Funckes-Shippy CL, Mnich SJ, Meyer DM, et al. Plasma 3-nitrotyrosine is a biomarker in animal models of arthritis: Pharmacological dissection of iNOS' role in disease. Nitric Oxide. 2009;20(3):150-6.

Neu CP, Khalafi A, Komvopoulos K, Schmid TM, Reddi AH. Mechanotransduction of bovine articular cartilage superficial zone protein by transforming growth factor beta signaling. Arthritis Rheum. 2007;56(11):3706-14.

Nishi H, Hashimoto K, Panchenko AR. Phosphorylation in protein-protein binding: effect on stability and function. Structure. 2011;19(12):1807-15.

Nishida T, Kawaki H, Baxter RM, Deyoung RA, Takigawa M, Lyons KM. CCN2 (Connective Tissue Growth Factor) is essential for extracellular matrix production and integrin signaling in chondrocytes. J Cell Commun Signal. 2007;1(1):45-58.

Nishida T, Kubota S, Kojima S, Kuboki T, Nakao K, Kushibiki T, et al. Regeneration of defects in articular cartilage in rat knee joints by CCN2 (connective tissue growth factor). J Bone Miner Res. 2004;19(8):1308-19.

Noguchi T, Takeda K, Matsuzawa A, Saegusa K, Nakano H, Gohda J, et al. Recruitment of tumor necrosis factor receptor-associated factor family proteins to apoptosis signal-regulating kinase 1 signalosome is essential for oxidative stress-induced cell death. J Biol Chem. 2005;280(44):37033-40.

Notoya K, Jovanovic DV, Reboul P, Martel-Pelletier J, Mineau F, Pelletier JP. The induction of cell death in human osteoarthritis chondrocytes by nitric oxide is related to the production of prostaglandin E2 via the induction of cyclooxygenase-2. J Immunol. 2000;165(6):3402-10.

O'Conor CJ, Leddy HA, Benefield HC, Liedtke WB, Guilak F. TRPV4-mediated mechanotransduction regulates the metabolic response of chondrocytes to dynamic loading. Proc Natl Acad Sci U S A. 2014;111(4):1316-21.

Obsilova V, Honzejkova K, Obsil T. Structural insights support targeting ASK1 kinase for therapeutic interventions. International Journal of Molecular Sciences. 2021;22(24):13395.

Oeckinghaus A, Ghosh S. The NF-kappaB family of transcription factors and its regulation. Cold Spring Harb Perspect Biol. 2009;1(4):a000034.

Ogier JM, Nayagam BA, Lockhart PJ. ASK1 inhibition: a therapeutic strategy with multi-system benefits. J Mol Med (Berl). 2020;98(3):335-48.

Oh M, Fukuda K, Asada S, Yasuda Y, Tanaka S. Concurrent generation of nitric oxide and superoxide inhibits proteoglycan synthesis in bovine articular chondrocytes: involvement of peroxynitrite. J Rheumatol. 1998;25(11):2169-74.

Ostalowska A, Birkner E, Wiecha M, Kasperczyk S, Kasperczyk A, Kapolka D, et al. Lipid peroxidation and antioxidant enzymes in synovial fluid of patients with primary and secondary osteoarthritis of the knee joint. Osteoarthritis Cartilage. 2006;14(2):139-45.

Palmer RM, Hickery MS, Charles IG, Moncada S, Bayliss MT. Induction of nitric oxide synthase in human chondrocytes. Biochem Biophys Res Commun. 1993;193(1):398-405.

Pelletier JP, Fernandes JC, Brunet J, Moldovan F, Schrier D, Flory C, et al. In vivo selective inhibition of mitogen-activated protein kinase kinase 1/2 in rabbit experimental osteoarthritis is associated with a reduction in the development of structural changes. Arthritis Rheum. 2003;48(6):1582-93.

Pelletier JP, Jovanovic DV, Lascau-Coman V, Fernandes JC, Manning PT, Connor JR, et al. Selective inhibition of inducible nitric oxide synthase reduces progression of experimental osteoarthritis in vivo: possible link with the reduction in chondrocyte apoptosis and caspase 3 level. Arthritis Rheum. 2000;43(6):1290-9.

Pelletier JP, Martel-Pelletier J, Abramson SB. Osteoarthritis, an inflammatory disease: potential implication for the selection of new therapeutic targets. Arthritis Rheum. 2001;44(6):1237-47.

Pestov NB, Okkelman IA, Shmanai VV, Hurski AL, Giaccia AJ, Shchepinov MS. Control of lysyl oxidase activity through site-specific deuteration of lysine. Bioorg Med Chem Lett. 2011;21(1):255-8.

Petrvalska O, Kosek D, Kukacka Z, Tosner Z, Man P, Vecer J, et al. Structural Insight into the 14-3-3 Protein-dependent Inhibition of Protein Kinase ASK1 (Apoptosis Signal-regulating kinase 1). J Biol Chem. 2016;291(39):20753-65.

Qu R, Chen X, Wang W, Qiu C, Ban M, Guo L, et al. Ghrelin protects against osteoarthritis through interplay with Akt and NF-kappaB signaling pathways. FASEB J. 2018;32(2):1044-58.

Radons J, Bosserhoff AK, Grässel S, Falk W, Schubert TE. p38MAPK mediates IL-1-induced down-regulation of aggrecan gene expression in human chondrocytes. International journal of molecular medicine. 2006;17(4):661-8.

Raphael W, Sordillo LM. Dietary polyunsaturated fatty acids and inflammation: the role of phospholipid biosynthesis. Int J Mol Sci. 2013;14(10):21167-88.

Rashad S, Hemingway A, Rainsford K, Revell P, Low F, Walker F. Effect of non-steroidal anti-inflammatory drugs on the course of osteoarthritis. The Lancet. 1989 Sep 2;334(8662):519-22.

Rettig, L.A., Hastings II, H. and Feinberg, J.R., 2008. Primary osteoarthritis of the elbow: lack of radiographic evidence for morphologic predisposition, results of operative debridement at intermediate follow-up, and basis for a new radiographic classification system. *Journal of Shoulder and Elbow Surgery*, *17*(1), pp.97-105.

Roelofs AJ, Zupan J, Riemen AH, Kania K, Ansboro S, White N, Clark SM, De Bari C. Joint morphogenetic cells in the adult mammalian synovium. Nature communications. 2017 May 16;8(1):15040.

Ross TD, Coon BG, Yun S, Baeyens N, Tanaka K, Ouyang M, et al. Integrins in mechanotransduction. Curr Opin Cell Biol. 2013;25(5):613-8.

Roy Davis Altman MD. Early management of osteoarthritis. Am J Manag Care. 2010;16:S41-7.

Roughley PJ, Mort JS. The role of aggrecan in normal and osteoarthritic cartilage. Journal of experimental orthopaedics. 2014;1(1):1-11.

Ruffels J, Griffin M, Dickenson JM. Activation of ERK1/2, JNK and PKB by hydrogen peroxide in human SH-SY5Y neuroblastoma cells: role of ERK1/2 in H2O2-induced cell death. Eur J Pharmacol. 2004;483(2-3):163-73.

Saha N, Moldovan F, Tardif G, Pelletier JP, Cloutier JM, Martel-Pelletier J. Interleukin-1beta-converting enzyme/caspase-1 in human osteoarthritic tissues: localization and role in the maturation of interleukin-1beta and interleukin-18. Arthritis Rheum. 1999;42(8):1577-87.

Saito T, Fukai A, Mabuchi A, Ikeda T, Yano F, Ohba S, et al. Transcriptional regulation of endochondral ossification by HIF-2alpha during skeletal growth and osteoarthritis development. Nat Med. 2010;16(6):678-86.

Saitoh M, Nishitoh H, Fujii M, Takeda K, Tobiume K, Sawada Y, et al. Mammalian thioredoxin is a direct inhibitor of apoptosis signal-regulating kinase (ASK) 1. EMBO J. 1998;17(9):2596-606.

Saklatvala J, Bird T. A common class of receptors for the two types of porcine interleukin-1 on articular chondrocytes. Lymphokine Res. 1986;5 Suppl 1:S99-104.

Saklatvala J, Dingle JT. Identification of catabolin, a protein fro synovium which induces degradation of cartilage in organ culture. Biochem Biophys Res Commun. 1980;96(3):1225-31.

Sakurai H, Kohsaka H, Liu MF, Higashiyama H, Hirata Y, Kanno K, et al. Nitric oxide production and inducible nitric oxide synthase expression in inflammatory arthritides. J Clin Invest. 1995;96(5):2357-63.

Sawaji Y, Hynes J, Vincent T, Saklatvala J. Fibroblast growth factor 2 inhibits induction of aggrecanase activity in human articular cartilage. Arthritis Rheum. 2008;58(11):3498-509.

Schneider JR, Lodolce JP, Boone DL. An Ubiquitin-like Motif in ASK1 Mediates its Association with and Inhibition of the Proteasome. J Biochem Pharmacol Res. 2013;1(3):161-7.

Scott JL, Gabrielides C, Davidson RK, Swingler TE, Clark IM, Wallis GA, et al. Superoxide dismutase downregulation in osteoarthritis progression and end-stage disease. Ann Rheum Dis. 2010;69(8):1502-10.

Shchepinov MS. Polyunsaturated fatty acid deuteration against neurodegeneration. Trends in pharmacological sciences. 2020;41(4):236-48.

Shepherd C, Zhu D, Skelton AJ, Combe J, Threadgold H, Zhu L, et al. Functional Characterization of the Osteoarthritis Genetic Risk Residing at ALDH1A2 Identifies rs12915901 as a Key Target Variant. Arthritis Rheumatol. 2018;70(10):1577-87.

Shi-Wen X, Leask A, Abraham D. Regulation and function of connective tissue growth factor/CCN2 in tissue repair, scarring and fibrosis. Cytokine Growth Factor Rev. 2008;19(2):133-44.

Shiizaki S, Naguro I, Ichijo H. Activation mechanisms of ASK1 in response to various stresses and its significance in intracellular signaling. Adv Biol Regul. 2013;53(1):135-44.

Shim JH, Greenblatt MB, Xie M, Schneider MD, Zou W, Zhai B, et al. TAK1 is an essential regulator of BMP signalling in cartilage. EMBO J. 2009;28(14):2028-41.

Shim JH, Xiao C, Paschal AE, Bailey ST, Rao P, Hayden MS, et al. TAK1, but not TAB1 or TAB2, plays an essential role in multiple signaling pathways in vivo. Genes Dev. 2005;19(22):2668-81.

Silver FH, Bradica G, Tria A. Elastic energy storage in human articular cartilage: estimation of the elastic modulus for type II collagen and changes associated with osteoarthritis. Matrix Biol. 2002;21(2):129-37.

Sokolove J, Lepus CM. Role of inflammation in the pathogenesis of osteoarthritis: latest findings and interpretations. Ther Adv Musculoskelet Dis. 2013;5(2):77-94.

Somlyai G, Molnár M, Laskay G, Szabó M, Berkényi T, Guller I, et al. Biological significance of naturally occurring deuterium: the antitumor effect of deuterium depletion. Orvosi Hetilap. 2010;151(36):1455-60.

Son Y, Cheong YK, Kim NH, Chung HT, Kang DG, Pae HO. Mitogen-Activated Protein Kinases and Reactive Oxygen Species: How Can ROS Activate MAPK Pathways? J Signal Transduct. 2011;2011:792639.

Sophia Fox AJ, Bedi A, Rodeo SA. The basic science of articular cartilage: structure, composition, and function. Sports Health. 2009;1(6):461-8.

Starkman BG, Cravero JD, Delcarlo M, Loeser RF. IGF-I stimulation of proteoglycan synthesis by chondrocytes requires activation of the PI 3-kinase pathway but not ERK MAPK. Biochem J. 2005;389(Pt 3):723-9.

Steinberg J, Brooks RA, Southam L, Bhatnagar S, Roumeliotis TI, Hatzikotoulas K, et al. Widespread epigenomic, transcriptomic and proteomic differences between hip osteophytic and articular chondrocytes in osteoarthritis. Rheumatology (Oxford). 2018;57(8):1481-9.

Styrkarsdottir U, Thorleifsson G, Helgadottir HT, Bomer N, Metrustry S, Bierma-Zeinstra S, et al. Severe osteoarthritis of the hand associates with common variants within the ALDH1A2 gene and with rare variants at 1p31. Nat Genet. 2014;46(5):498-502.

Sugimoto MA, Sousa LP, Pinho V, Perretti M, Teixeira MM. Resolution of inflammation: what controls its onset? Frontiers in immunology. 2016;7:160.

Sun GY, Geng X, Teng T, Yang B, Appenteng MK, Greenlief CM, et al. Dynamic Role of Phospholipases A2 in Health and Diseases in the Central Nervous System. Cells. 2021;10(11).

Sun HY, Hu KZ, Yin ZS. Inhibition of the p38-MAPK signaling pathway suppresses the apoptosis and expression of proinflammatory cytokines in human osteoarthritis chondrocytes. Cytokine. 2017;90:135-43.

Sun SC. The noncanonical NF-kappaB pathway. Immunol Rev. 2012;246(1):125-40.

Sun SC, Ganchi PA, Ballard DW, Greene WC. NF-kappa B controls expression of inhibitor I kappa B alpha: evidence for an inducible autoregulatory pathway. Science. 1993;259(5103):1912-5.

Suzuki M, Asai Y, Kagi T, Noguchi T, Yamada M, Hirata Y, et al. TAK1 Mediates ROS Generation Triggered by the Specific Cephalosporins through Noncanonical Mechanisms. Int J Mol Sci. 2020;21(24).

Swagerty Jr DL, Hellinger D. Radiographic assessment of osteoarthritis. American Family Physician. 2001 Jul 15;64(2):279-87.

Sylvain-Prevost S, Ear T, Simard FA, Fortin CF, Dubois CM, Flamand N, et al. Activation of TAK1 by Chemotactic and Growth Factors, and Its Impact on Human Neutrophil Signaling and Functional Responses. J Immunol. 2015;195(11):5393-403.

Tanaka K. The proteasome: overview of structure and functions. Proc Jpn Acad Ser B Phys Biol Sci. 2009;85(1):12-36.

Tang R, Mei S, Xu Q, Feng J, Zhou Y, Xing S, et al. ASK1-ER stress pathway-mediated fibrotic-EV release contributes to the interaction of alveolar epithelial cells and lung fibroblasts to promote mechanical ventilation-induced pulmonary fibrosis. Exp Mol Med. 2022;54(12):2162-74.

Tang X, Muhammad H, McLean C, Miotla-Zarebska J, Fleming J, Didangelos A, et al. Connective tissue growth factor contributes to joint homeostasis and osteoarthritis severity by controlling the matrix sequestration and activation of latent TGFbeta. Ann Rheum Dis. 2018;77(9):1372-80.

Tao R, Xu X, Sun C, Wang Y, Wang S, Liu Z, et al. KPNA2 interacts with P65 to modulate catabolic events in osteoarthritis. Exp Mol Pathol. 2015;99(2):245-52.

Tobiume K, Matsuzawa A, Takahashi T, Nishitoh H, Morita K, Takeda K, et al. ASK1 is required for sustained activations of JNK/p38 MAP kinases and apoptosis. EMBO Rep. 2001;2(3):222-8.

Tobiume K, Saitoh M, Ichijo H. Activation of apoptosis signal-regulating kinase 1 by the stress-induced activating phosphorylation of pre-formed oligomer. J Cell Physiol. 2002;191(1):95-104.

Toh ML, Yang Y, Leech M, Santos L, Morand EF. Expression of mitogen-activated protein kinase phosphatase 1, a negative regulator of the mitogen-activated protein kinases, in rheumatoid arthritis: up-regulation by interleukin-1beta and glucocorticoids. Arthritis Rheum. 2004;50(10):3118-28.

Tomida T, Takekawa M, Saito H. Oscillation of p38 activity controls efficient pro-inflammatory gene expression. Nat Commun. 2015;6:8350.

Towle CA, Hung HH, Bonassar LJ, Treadwell BV, Mangham DC. Detection of interleukin-1 in the cartilage of patients with osteoarthritis: a possible autocrine/paracrine role in pathogenesis. Osteoarthritis Cartilage. 1997;5(5):293-300.

Trachootham D, Lu W, Ogasawara MA, Nilsa RD, Huang P. Redox regulation of cell survival. Antioxid Redox Signal. 2008;10(8):1343-74.

Tu M, Yao Y, Qiao FH, Wang L. The pathogenic role of connective tissue growth factor in osteoarthritis. Biosci Rep. 2019;39(7).

Tudorachi NB, Totu EE, Fifere A, Ardeleanu V, Mocanu V, Mircea C, et al. The Implication of Reactive Oxygen Species and Antioxidants in Knee Osteoarthritis. Antioxidants (Basel). 2021;10(6).

Turrens JF. Mitochondrial formation of reactive oxygen species. J Physiol. 2003;552(Pt 2):335-44.

Tyler JA. Articular cartilage cultured with catabolin (pig interleukin 1) synthesizes a decreased number of normal proteoglycan molecules. Biochem J. 1985;227(3):869-78.

Um JW, Im E, Park J, Oh Y, Min B, Lee HJ, et al. ASK1 negatively regulates the 26 S proteasome. J Biol Chem. 2010;285(47):36434-46.

Vaamonde-Garcia C, Riveiro-Naveira RR, Valcarcel-Ares MN, Hermida-Carballo L, Blanco FJ, Lopez-Armada MJ. Mitochondrial dysfunction increases inflammatory responsiveness to cytokines in normal human chondrocytes. Arthritis Rheum. 2012;64(9):2927-36.

Vaillancourt F, Fahmi H, Shi Q, Lavigne P, Ranger P, Fernandes JC, et al. 4-Hydroxynonenal induces apoptosis in human osteoarthritic chondrocytes: the protective role of glutathione-S-transferase. Arthritis Res Ther. 2008;10(5):R107.

Valverde-Franco G, Binette JS, Li W, Wang H, Chai S, Laflamme F, et al. Defects in articular cartilage metabolism and early arthritis in fibroblast growth factor receptor 3 deficient mice. Hum Mol Genet. 2006;15(11):1783-92.

van Dalen S, Blom A, Slöetjes A, Helsen M, Roth J, Vogl T, et al. Interleukin-1 is not involved in synovial inflammation and cartilage destruction in collagenase-induced osteoarthritis. Osteoarthritis and cartilage. 2017;25(3):385-96.

van de Laar IM, Oldenburg RA, Pals G, Roos-Hesselink JW, de Graaf BM, Verhagen JM, et al. Mutations in SMAD3 cause a syndromic form of aortic aneurysms and dissections with early-onset osteoarthritis. Nat Genet. 2011;43(2):121-6.

van der Kraan PM, Goumans MJ, Blaney Davidson E, ten Dijke P. Age-dependent alteration of TGF-beta signalling in osteoarthritis. Cell Tissue Res. 2012;347(1):257-65.

van der Kraan PM, van den Berg WB. Chondrocyte hypertrophy and osteoarthritis: role in initiation and progression of cartilage degeneration? Osteoarthritis Cartilage. 2012;20(3):223-32.

Verstak B, Nagpal K, Bottomley SP, Golenbock DT, Hertzog PJ, Mansell A. MyD88 adapter-like (Mal)/TIRAP interaction with TRAF6 is critical for TLR2-and TLR4-mediated NF-κB proinflammatory responses. Journal of Biological Chemistry. 2009 Sep 4;284(36):24192-203.

Vincent T, Hermansson M, Bolton M, Wait R, Saklatvala J. Basic FGF mediates an immediate response of articular cartilage to mechanical injury. Proc Natl Acad Sci U S A. 2002;99(12):8259-64.

Vincent T, Saklatvala J. Basic fibroblast growth factor: an extracellular mechanotransducer in articular cartilage? Biochem Soc Trans. 2006;34(Pt 3):456-7.

Vincent TL. Fibroblast growth factor 2: good or bad guy in the joint? Arthritis Res Ther. 2011;13(5):127.

Vincent TL. Targeting mechanotransduction pathways in osteoarthritis: a focus on the pericellular matrix. Curr Opin Pharmacol. 2013;13(3):449-54.

Vincent TL. Mechanoflammation in osteoarthritis pathogenesis. Semin Arthritis Rheum. 2019;49(3s):S36-s8.

Vincent TL. IL-1 in osteoarthritis: time for a critical review of the literature. F1000Res. 2019;8.

Vincent TL. Of mice and men: converging on a common molecular understanding of osteoarthritis. The Lancet Rheumatology. 2020;2(10):e633-e45.

Vincent TL. 2021: The Year We Rewrite the Osteoarthritis Textbooks? Function (Oxf). 2021;2(1):zqaa043.

Vincent TL, McLean CJ, Full LE, Peston D, Saklatvala J. FGF-2 is bound to perlecan in the pericellular matrix of articular cartilage, where it acts as a chondrocyte mechanotransducer. Osteoarthritis Cartilage. 2007;15(7):752-63.

Vincent TL, Saklatvala J. Is the response of cartilage to injury relevant to osteoarthritis? Arthritis Rheum. 2008;58(5):1207-10.

Vincent TL, Wann AKT. Mechanoadaptation: articular cartilage through thick and thin. J Physiol. 2019;597(5):1271-81.

Vincenti MP, Coon CI, Brinckerhoff CE. Nuclear factor kappaB/p50 activates an element in the distal matrix metalloproteinase 1 promoter in interleukin-1beta-stimulated synovial fibroblasts. Arthritis Rheum. 1998;41(11):1987-94.

Wada K, Itoga K, Okano T, Yonemura S, Sasaki H. Hippo pathway regulation by cell morphology and stress fibers. Development. 2011;138(18):3907-14.

Wada Y, Shimada K, Sugimoto K, Kimura T, Ushiyama S. Novel p38 mitogen-activated protein kinase inhibitor R-130823 protects cartilage by down-regulating matrix metalloproteinase-1,-13 and prostaglandin E2 production in human chondrocytes. Int Immunopharmacol. 2006;6(2):144-55.

Wang K, Degerny C, Xu M, Yang XJ. YAP, TAZ, and Yorkie: a conserved family of signal-responsive transcriptional coregulators in animal development and human disease. Biochem Cell Biol. 2009;87(1):77-91.

Wang QG, El Haj AJ, Kuiper NJ. Glycosaminoglycans in the pericellular matrix of chondrons and chondrocytes. J Anat. 2008;213(3):266-73.

Wang W, Rigueur D, Lyons KM. TGFbeta signaling in cartilage development and maintenance. Birth Defects Res C Embryo Today. 2014;102(1):37-51.

Wang X, Dong C, Li N, Ma Q, Yun Z, Cai C, et al. Modulation of TGF-beta activity by latent TGF-beta-binding protein 1 in human osteoarthritis fibroblast-like synoviocytes. Mol Med Rep. 2018;17(1):1893-900.

Wang X, Li F, Fan C, Wang C, Ruan H. Analysis of isoform specific ERK signaling on the effects of interleukin-1β on COX-2 expression and PGE2 production in human chondrocytes. Biochemical and biophysical research communications. 2010;402(1):23-9.

Wang Z, Qiu Y, Lu J, Wu N. Connective tissue growth factor promotes interleukin-1beta-mediated synovial inflammation in knee osteoarthritis. Mol Med Rep. 2013;8(3):877-82.

Wann AK, Zuo N, Haycraft CJ, Jensen CG, Poole CA, McGlashan SR, et al. Primary cilia mediate mechanotransduction through control of ATP-induced Ca2+ signaling in compressed chondrocytes. FASEB J. 2012;26(4):1663-71.

Watanabe H, de Caestecker MP, Yamada Y. Transcriptional cross-talk between Smad, ERK1/2, and p38 mitogen-activated protein kinase pathways regulates transforming growth factor-beta-induced aggrecan gene expression in chondrogenic ATDC5 cells. J Biol Chem. 2001;276(17):14466-73.

Watt FE, Hamid B, Garriga C, Judge A, Hrusecka R, Custers RJH, et al. The molecular profile of synovial fluid changes upon joint distraction and is associated with clinical response in knee osteoarthritis. Osteoarthritis Cartilage. 2020;28(3):324-33.

Watt FE, Ismail HM, Didangelos A, Peirce M, Vincent TL, Wait R, et al. Src and fibroblast growth factor 2 independently regulate signaling and gene expression induced by experimental injury to intact articular cartilage. Arthritis Rheum. 2013;65(2):397-407.

Watt FE, Paterson E, Freidin A, Kenny M, Judge A, Saklatvala J, et al. Acute Molecular Changes in Synovial Fluid Following Human Knee Injury: Association With Early Clinical Outcomes. Arthritis Rheumatol. 2016;68(9):2129-40.

Weber A, Wasiliew P, Kracht M. Interleukin-1 (IL-1) pathway. Sci Signal. 2010;3(105):cm1.

Wegner AM, Campos NR, Robbins MA, Haddad AF, Cunningham HC, Yik JHN, et al. Acute Changes in NADPH Oxidase 4 in Early Post-Traumatic Osteoarthritis. J Orthop Res. 2019;37(11):2429-36.

Weng T, Yi L, Huang J, Luo F, Wen X, Du X, et al. Genetic inhibition of fibroblast growth factor receptor 1 in knee cartilage attenuates the degeneration of articular cartilage in adult mice. Arthritis Rheum. 2012;64(12):3982-92.

Wilusz RE, Sanchez-Adams J, Guilak F. The structure and function of the pericellular matrix of articular cartilage. Matrix Biol. 2014;39:25-32.

Wojdasiewicz P, Poniatowski LA, Szukiewicz D. The role of inflammatory and anti-inflammatory cytokines in the pathogenesis of osteoarthritis. Mediators Inflamm. 2014;2014:561459.

Wolff KJ, Ramakrishnan PS, Brouillette MJ, Journot BJ, McKinley TO, Buckwalter JA, et al. Mechanical stress and ATP synthesis are coupled by mitochondrial oxidants in articular cartilage. J Orthop Res. 2013;31(2):191-6.

Xia B, Di C, Zhang J, Hu S, Jin H, Tong P. Osteoarthritis pathogenesis: a review of molecular mechanisms. Calcif Tissue Int. 2014;95(6):495-505.

Xie Y, Zinkle A, Chen L, Mohammadi M. Fibroblast growth factor signalling in osteoarthritis and cartilage repair. Nat Rev Rheumatol. 2020;16(10):547-64.

Xu L, Peng H, Glasson S, Lee PL, Hu K, Ijiri K, et al. Increased expression of the collagen receptor discoidin domain receptor 2 in articular cartilage as a key event in the pathogenesis of osteoarthritis. Arthritis Rheum. 2007;56(8):2663-73.

Xu L, Sun C, Zhang S, Xu X, Zhai L, Wang Y, et al. Sam68 Promotes NF-kappaB Activation and Apoptosis Signaling in Articular Chondrocytes during Osteoarthritis. Inflamm Res. 2015;64(11):895-902.

Xu YR, Lei CQ. TAK1-TABs Complex: A Central Signalosome in Inflammatory Responses. Front Immunol. 2020;11:608976.

Yamaguchi K, Shirakabe K, Shibuya H, Irie K, Oishi I, Ueno N, et al. Identification of a member of the MAPKKK family as a potential mediator of TGF-beta signal transduction. Science. 1995;270(5244):2008-11.

Yan D, Chen D, Cool SM, van Wijnen AJ, Mikecz K, Murphy G, et al. Fibroblast growth factor receptor 1 is principally responsible for fibroblast growth factor 2-induced catabolic activities in human articular chondrocytes. Arthritis Res Ther. 2011;13(4):R130.

Yan J, Zhang Y, Sheng G, Ni B, Xiao Y, Wang S, et al. Selonsertib Alleviates the Progression of Rat Osteoarthritis: An in vitro and in vivo Study. Front Pharmacol. 2021;12:687033.

Yang P, Tan J, Yuan Z, Meng G, Bi L, Liu J. Expression profile of cytokines and chemokines in osteoarthritis patients: Proinflammatory roles for CXCL8 and CXCL11 to chondrocytes. Int Immunopharmacol. 2016;40:16-23.

Yang X, Chen L, Xu X, Li C, Huang C, Deng CX. TGF-beta/Smad3 signals repress chondrocyte hypertrophic differentiation and are required for maintaining articular cartilage. J Cell Biol. 2001;153(1):35-46.

Yao X, Zhang J, Jing X, Ye Y, Guo J, Sun K, et al. Fibroblast growth factor 18 exerts anti-osteoarthritic effects through PI3K-AKT signaling and mitochondrial fusion and fission. Pharmacol Res. 2019;139:314-24.

Yen J-H, Huang W-C, Lin S-C, Huang Y-W, Chio W-T, Tsay GJ, et al. Metabolic remodeling in tumor-associated macrophages contributing to antitumor activity of cryptotanshinone by regulating TRAF6-ASK1 axis. Molecular Therapy-Oncolytics. 2022;26:158-74.

Yen YM, Cascio B, O'BRIEN LU, Stalzer S, Millett PJ, Steadman JR. Treatment of osteoarthritis of the knee with microfracture and rehabilitation. Medicine & Science in Sports & Exercise. 2008 Feb 1;40(2):200-5.

Yin W, Park JI, Loeser RF. Oxidative stress inhibits insulin-like growth factor-I induction of chondrocyte proteoglycan synthesis through differential regulation of phosphatidylinositol 3-Kinase-Akt and MEK-ERK MAPK signaling pathways. J Biol Chem. 2009;284(46):31972-81.

Ying W, Yuan F, He P, Ji P. Inhibition of Notch1 protects against IL-1β-induced inflammation and cartilage destruction in temporomandibular chondrocytes. Molecular Medicine Reports. 2017;15(6):4391-7.

Yoon YC, Fang Z, Lee JE, Park JH, Ryu JK, Jung KH, et al. Selonsertib Inhibits Liver Fibrosis via Downregulation of ASK1/ MAPK Pathway of Hepatic Stellate Cells. Biomol Ther (Seoul). 2020;28(6):527-36.

Zahan OM, Serban O, Gherman C, Fodor D. The evaluation of oxidative stress in osteoarthritis. Med Pharm Rep. 2020;93(1):12-22.

Zarka M, Hay E, Cohen-Solal M. YAP/TAZ in Bone and Cartilage Biology. Front Cell Dev Biol. 2021;9:788773.

Zhang H, Sun SC. NF-kappaB in inflammation and renal diseases. Cell Biosci. 2015;5:63.

Zhang L, Chen J, Fu H. Suppression of apoptosis signal-regulating kinase 1-induced cell death by 14-3-3 proteins. Proceedings of the National Academy of Sciences. 1999;96(15):8511-5.

Zhang N, Liu L, Dou Y, Song D, Deng H. Glycogen synthase kinase-3beta antagonizes ROS-induced hepatocellular carcinoma cell death through suppression of the apoptosis signal-regulating kinase 1. Med Oncol. 2016;33(7):60.

Zhang Q, Fang X, Zhao W, Liang Q. The transcriptional coactivator YAP1 is overexpressed in osteoarthritis and promotes its progression by interacting with Beclin-1. Gene. 2019;689:210-9.

Zhang QS, Eaton GJ, Diallo C, Freeman TA. Stress-Induced Activation of Apoptosis Signal-Regulating Kinase 1 Promotes Osteoarthritis. J Cell Physiol. 2016;231(4):944-53.

Zhang X, Cai D, Zhou F, Yu J, Wu X, Yu D, et al. Targeting downstream subcellular YAP activity as a function of matrix stiffness with Verteporfin-encapsulated chitosan microsphere attenuates osteoarthritis. Biomaterials. 2020;232:119724.

Zhang X, Wang J, Zubarev RA. Slight Deuterium Enrichment in Water Acts as an Antioxidant: Is Deuterium a Cell Growth Regulator? Mol Cell Proteomics. 2020;19(11):1790-804.

Zhao B, Li L, Wang L, Wang CY, Yu J, Guan KL. Cell detachment activates the Hippo pathway via cytoskeleton reorganization to induce anoikis. Genes Dev. 2012;26(1):54-68.

Zhong F, Lu J, Wang Y, Song H. Genetic variation of SMAD3 is associated with hip osteoarthritis in a Chinese Han population. J Int Med Res. 2018;46(3):1178-86.

Zhong W, Tian K, Zheng X, Li L, Zhang W, Wang S, et al. Mesenchymal stem cell and chondrocyte fates in a multishear microdevice are regulated by Yes-associated protein. Stem Cells Dev. 2013;22(14):2083-93.

Zhong W, Zhang W, Wang S, Qin J. Regulation of fibrochondrogenesis of mesenchymal stem cells in an integrated microfluidic platform embedded with biomimetic nanofibrous scaffolds. PLoS One. 2013;8(4):e61283.

Zhu L, Chanalaris A, Lympany S, Vincent T. Cartilage injury regulates inflammatory gene expression in part by suppressing cellular retinoic acid signaling. Osteoarthritis and Cartilage. 2017;25:S168.

Zhu L, Kamalathevan P, Koneva LA, Zarebska JM, Chanalaris A, Ismail H, et al. Variants in ALDH1A2 reveal an anti-inflammatory role for retinoic acid and a new class of disease-modifying drugs in osteoarthritis. Science Translational Medicine. 2022;14(676):eabm4054.